TOPOLOGICAL INTERPRETATION
OF
NON-LINEAR TRANSONIC AEROELASTIC PHENOMENA

by

John Anderson B.Sc., M.Sc.

Dissertation submitted to the Faculty of Engineering,
University of Glasgow, for the Degree of Doctor of Philosophy.

April 1993

ProQuest LLC.
789 East Eisenhower Parkway
P.O. Box 1346
Ann Arbor, MI 48106 – 1346

ABSTRACT

Recent computational studies based on numerical solutions of the unsteady Euler equations have revealed hitherto unanticipated transonic aeroelastic phenomena characterized by non-linear flutter and divergence and interactions between divergence and flutter. In the absence of extensive parametric searches, however, such quantitative studies provide little insight into the nature and extent of such bifurcational behaviour, particularly when multiple parameters are involved. Qualitative dynamical systems theory offers a complementary approach to the analysis of bifurcation problems. In the vicinity of bifurcation, the qualitative behaviour of complex dynamical systems can often be characterized by simple ordinary differential equation models. Of particular interest are the simplest models which exhibit complex interactions characteristic of those observed in non-linear aeroelastic systems. Such models offer scope for attaining greater insight into the nature of complex aeroelastic bifurcations and for systematically predicting qualitative changes resulting from parameter variations. The present work describes the elements of a qualitative, or *topological*, model identification strategy for a general class of aerodynamically non-linear *hereditary* aeroelastic systems. The methodology is motivated, principally, by a desire to circumvent the need for detailed knowledge of the unsteady aerodynamic environment. The approach employs a notional non-linear functional description of the aerodynamic force response free from any low-frequency or quasi-steady aerodynamic assumptions. Application of the scheme to the

transonic aeroelastic problem demonstrates the feasibility and limitations of qualitative techniques. Based on partial bifurcational information derived from published numerical solutions of the coupled aerodynamic and structural equations of motion, a simplified model is identified which captures the (local) bifurcational behaviour of a structurally linear typical section aerofoil in 2-D transonic flow. The model facilitates a new interpretation of divergence/flutter interaction phenomena in transonic flow, including the effects of structural asymmetry, and highlights some difficulties of definition and interpretation of non-linear flutter. Evidence is presented which suggests the existence of new transonic aeroelastic phenomena not previously encountered in computational studies.

ACKNOWLEDGEMENTS

A number of people have provided support and encouragement during the course of the research reported in this dissertation. In particular, I would like to express my appreciation to Prof. R.A.M. Galbraith who, as Head of the Department of Aerospace Engineering, has made available to me the time and resources to complete this research. Also, I would like to thank my colleague, Dr. Colin Goodchild, for his general advice and assistance and for his participation in numerous discussions. A final expression of appreciation is extended to my wife, Jo, for her practical support and encouragement over the years, and for her patience and understanding in the face of many a broken deadline.

J.A. April, 1993.

CONTENTS

GLOSSARY

CHAPTER ONE
INTRODUCTION

CHAPTER TWO
A CANONICAL AEROELASTIC MODEL

CHAPTER THREE

BIFURCATION AND GENERIC MODELS OF AEROELASTIC BEHAVIOUR

CHAPTER FOUR

A PROTOTYPE FOR DIVERGENCE/FLUTTER INTERACTION

CHAPTER FIVE

MODE INTERACTION PHENOMENA IN TRANSONIC FLOW

CHAPTER SIX

CONCLUSIONS AND RECOMMENDATIONS FOR FURTHER RESEARCH

APPENDIX ONE

ASYMMETRIC PERTURBATION OF THE PITCHFORK/HOPF BIFURCATION

REFERENCES

FIGURES

GLOSSARY

$\mathcal{A}$	Subset of physical parameter space.
B	Space of motion histories / B_L^0 .
BC	Space of bounded and continuous functions mapping $(-\infty,0]$ to $\mathbb{R}^n$.
B_L^0	Degenerate linearization of reduced equation set at bifurcation.
C	Structural generalized damping matrix.
C^k	Space of k times continuously (Fréchet) differentiable functions.
C_g	Space of continuous functions mapping $(-\infty,o]$ to $\mathbb{R}^n$ with norm $\|\cdot\|_g$.
D	Subspace of the state-history phase space / Jacobian operator.
F(t)	Generalized aerodynamic force response vector at time t.
$F^i(t)$	i'th generalized aerodynamic force response component at time t.
F_q	Approximate generalized indicial aerodynamic force response matrix.
F_q^*	Generalized aerodynamic deficiency matrix.
$\mathcal{F}(q_t)$	Generalized aerodynamic force response functional.
$\mathcal{F}_q(q_\tau,t,\tau)$	Generalized indicial aerodynamic force response matrix.
F_0	Degenerate vector field at bifurcation.
F_0^k	k'th-order truncation of Taylor expansion of F_0.
F_α	Perturbation of F_0.
f	Right-side operator in functional differential equation.
$\tilde{f}^k$	Component of F_0 consisting of terms of degree between 2 and k.
G	Right-side operator of normal form.
G_ε	First-order asymmetric perturbation of G.
$G_{\varepsilon,\beta,\gamma,\delta}$	General asymmetric perturbation of G.
G_μ^k	Universal unfolding of F_0.
G_0^k	Normal form equivalent of F_0^k.

g	Influence function in definition of $\|\cdot\|_g$.
$\tilde{g}^k$	Non-linear component of G_0^k.
$\mathcal{G}_k$	Complementary subspace in space of homogeneous polynomials of degree k.
$h, \hbar$	Non-linear component in functional differential equation.
I	Identity matrix.
K	Structural generalized stiffness matrix.
L_B^k	Mapping under Lie bracket operation.
$L(\alpha)$	Linearized aeroelastic functional parameterized by α.
$L(\alpha_0)$	Linearized aeroelastic functional at bifurcation.
M	Mach number / Structural generalized mass matrix.
M_f^α	Centre-manifold parameterized by α.
m, n	Parameters in normal form of reduced equation set.
m_f^α	Diffeomorphism relating state-history on centre-manifold and state-history projection on critical eigenspace.
N	Number of structural generalized co-ordinates.
n	Order of state-space model.
P_0	Subspace of phase space X invariant under the action of the dynamic T_L^0.
P_k	Homogeneous polynomial of degree k.
$\mathcal{P}_k$	Space of homogeneous polynomials of degree k.
Q_0	Complement of P_0 in X.
$q(t)$	Structural generalized displacement vector at time t.
$q^i(t)$	i'th component of $q(t)$.
q_t	Structural generalized displacement time-history vector.
S	Symmetry matrix.
$S_g(\gamma)$	Subspace of UC_g.
T_f^α	Non-linear state-history evolution operator.
T_L^0	Linearized state-history evolution operator at bifurcation.

t	Time variable.
UC_g	Admissible phase space.
$\bar{U}$	Reduced velocity.
u	Dependent variable in reduced equation set.
X	Phase space.
X_0	Matrix function on $(-\infty,0]$ with $X_0(\theta) = 0$, $\theta < 0$, $X_0(0) = I$.
$x(t)$	Structural state vector at time t.
x_t	Structural state time-history vector to time t.
x_0	Initial history.
x, r	Re-scaled steady-state and periodic amplitudes in normal form.
$\hat{x}$, $\hat{r}$, $\hat{\theta}$	Normal form variables in cylindrical co-ordinates.
$\hat{x}$, $\hat{y}$, $\hat{z}$	Normal form variables in Cartesian co-ordinates.
α	Physical parameter set.
α_0	Physical parameter set at bifurcation / Structural pre-twist.
$\varepsilon,\beta,\gamma,\delta$	Asymmetric unfolding parameters.
ε_i	Coefficients in prototype normal form.
Φ	Normal form transformation / Φ^0_L .
Φ^0_L	Matrix of critical initial eigenhistories of linearized aeroelastic operator.
γ	Element of symmetry group Γ.
Γ	Symmetry group.
Ψ^0_L , Ψ_0	Matrix of adjoint critical initial eigenhistories of linearized aeroelastic operator.
$\Lambda(\alpha_0)$	Set of (critical) eigenvalues of $L(\alpha_0)$ on imaginary axis.
$\lambda_i(\alpha_0)$	i'th eigenvalue of $L(\alpha_0)$.
λ, μ, σ	Unfolding parameters.
λ_x , λ_r	Values of λ at secondary x- and r-mode bifurcations.

$\pi(\alpha_0)$	Projection operator in X.
$\pi^{\perp}(\alpha_0)$	Complementary projection operator in X.
τ	Delay variable.
φ , ψ	Elements of the phase space X.
ω	Critical frequency of periodic mode at bifurcation.
$\xi(\alpha_0)$	Eigenvector of linearized aeroelastic operator at bifurcation.

$\mathbb{C}^n$	Complex n-dimensional vector space.
$\mathbb{R}^n$	Real n-dimensional vector space.
det	Matrix determinant.
tr	Matrix trace.
$\lvert\cdot\rvert$	Norm in $\mathbb{R}^n$.
$\lVert\cdot\rVert_X$	Norm in X.
$\lVert\cdot\rVert_g$	Norm in C_g.
sup	Supremum.

CHAPTER ONE

INTRODUCTION

1.1 NON-LINEAR FLUTTER AND DIVERGENCE IN TRANSONIC FLOW

Interest in non-linear transonic aeroelastic phenomena has paralleled recent developments in numerical integration procedures for the unsteady Euler equations. The attendant relaxation of shock strength and motion amplitude limitations, inherent in transonic small-disturbance theory, has exposed a range of new aeroelastic phenomena (for example, limit cycle behaviour, multiple steady-states, divergence/flutter interactions) influenced, predominantly, by aerodynamic non-linearities (Kousen [1989], Bendiksen [1989]). These phenomena differ substantially from the classical (linear) notions of divergence and flutter in that the post-critical behaviour depends intimately on the finite-amplitude nature of the response and not simply on the initial mode of instability. Parametric studies have revealed Mach number and reduced velocity ranges in which the post-critical behaviour displays sensitive dependence to variations in these parameters resulting in subtle secondary instabilities and transitions from one type of qualitative behaviour to another. More complex behaviour is observed upon variation of other parameters such as sweep and pre-twist. Reconciliation of such behaviour is made difficult by the need for extensive parametric searches. Consequently, the effect of parameter variations on the aeroelastic response, and the range of possible

aeroelastic behaviour, is difficult to predict and assess.

Attempts to rationalize anomalous aeroelastic behaviour in the transonic regime have, traditionally, focused on the role of shocks as sources of aerodynamic non-linearity and non-uniform delay (Ashley [1980], Tijdeman & Seebass [1980], Mabey [1989]). However, the subtle interplay between structural motion history, shock evolution and aerodynamic response makes identification of the detailed physical mechanisms responsible for a given pattern of behaviour difficult, in general. Moreover, explanations of the effects of parameter variations are not easily discernible from the governing aeroelastic equations - the coupled aerodynamic and structural equations of motion governing finite-amplitude transonic aeroelastic phenomena provide little insight into the interior mechanisms that connect the freestream and structural parameters to the aeroelastic response. While some effort has been made to embody the dominant physical characteristics of unsteady transonic flow in more tractable models of the transonic aeroelastic problem (Kerlick & Nixon [1982], Chyu & Schiff [1983], Ueda & Dowell [1984], Hui & Tobak [1985]), the underlying non-linear and hereditary nature of the aerodynamic response in unsteady transonic flow places severe restrictions on the range of applicability of such models. Paradoxically, *qualitative* models which circumvent the need for prescription of the aerodynamic response offer the potential for attaining greater insight into the nature of complex aeroelastic phenomena than conventional analytical and numerical models afford and for systematically predicting qualitative changes resulting from parameter variations.

1.2 TOPOLOGICAL MODELS OF LOCAL BIFURCATIONAL BEHAVIOUR

Transitions in qualitative behaviour which accompany loss of stability of stationary states of complex evolutionary processes are invariably linked to the influence of parameters and to the variation of parameters over certain critical values. The basic techniques for analyzing transitions in qualitative behaviour are those of bifurcation theory. However, the intractability of many complex processes often precludes formal bifurcation analysis. Nevertheless, patterns of behaviour observed under parametric perturbation can often be ascribed identifiable structures associated with the generic bifurcations of certain archetypal models. This analogy appears to work well where the evolution of the phenomenologically important process response variables can be identified, independently, with some underlying dynamical system. In the vicinity of bifurcation, many dynamical systems exhibit a strong two-time-scale structure. Stability and bifurcation characteristics of such systems (at least locally) are controlled by the slow dynamic on a limited region of the state space to which the fast (stable) dynamic converges. Essentially, the slow dynamic describes the evolution of system 'modes' that are close to marginal stability. If there exists only a finite number of marginally stable modes, then, locally, under reasonable conditions, the restricted system dynamic can be shown to be equivalent to that generated by some elemental dynamical system described by a finite-dimensional set of ordinary differential equations.

Bifurcation theory provides, to some degree, a classification of types of bifurcations and their generating equations (Guckenheimer & Holmes [1983], Golubitsky & Schaeffer [1985]). This classification can be utilized to identify a *minimal* system model which encapsulates the qualitative features of all possible asymptotic states of a process at different parameter values in the vicinity of bifurcation. The identification procedure is one of matching the patterns found in certain bifurcations with the macroscopic characteristics of the transitions observed in the process response. The goal of this 'inverse' approach is to characterize the simplest form of the generating equation displaying the requisite bifurcational behaviour. Not only is this approach capable of reproducing observed behaviour, locally in a region of parameter space, but it is also capable of predicting undetected transitions and yielding quasi-global information connecting apparently disparate behaviour in different regions of parameter space.

Importantly, the predictive capability outlined is achieved without explicit reference to the prevailing quantitative physical laws. Only bifurcations emanating from generating equations whose qualitative behaviour is preserved under permissible perturbations are assumed physically relevant. This assumption plays a fundamental role in the identification of the elemental system model which characterizes the persistent underlying structure of the observed behaviour. Candidate models are selected from within a class of qualitatively stable models. This restriction reflects the robustness property attributable to all observable physical

processes. Essentially, the description of a process should not change if the process itself is varied slightly. For a given elemental structure, and any symmetries or other special properties assigned to a qualitative model, the pattern of qualitatively stable behaviour is determined only by the number of (essential) system parameters. Experimental observations are exploited in a complementary fashion. If partial information about a complex process, such as several qualitatively distinct numerical solutions, is available, the (physically relevant) information on the whole process can be completed by determining the qualitatively stable elemental model which contains the known solution behaviour.

The rationale behind this approach can be traced to the concepts of *organizing centre* and *universal unfolding* formulated by Thom [1975] as part of his Catastrophe Theory. Different bifurcations may belong to the same neighbourhood of a bifurcation point if they can be considered as perturbations of the same singular system about their respective local bifurcation points. The different phenomena are brought together into a unifying scenario by condensing all the singularities into one. Enumeration of the qualitatively distinct and persistent perturbations of the resulting highly singular configuration enables the original arrangement to be recovered as some section through the space of perturbation parameters. In addition, new singular arrangements can be found corresponding to different sections of parameter space. While such an approach is essentially local in character and entails no concept of scale, empirically, one finds that the patterns of behaviour detected by such methods often persist in a neighbourhood of physical parameter

space much larger than expected. For problems involving multiple parameters, the topological interpretation of local bifurcational behaviour which naturally emerges from this procedure imposes a structure on the physical parameter space that provides a basis for a comprehensive view that allows new predictions.

This strategy has formed the basis for descriptions of bifurcational phenomena in a diverse range of applications in the physical sciences (Holmes & Rand [1975], Berry [1976], Armbruster [1983], Langford [1988], Barkley [1990]). Details of implementation differ, however, according to the form of the (notional) physical process model and the nature of the transitional behaviour. In general, these factors determine the most appropriate methods for establishing the existence and form of a suitable elemental model. Sufficient conditions permitting a reduced-dimensional characterization of the local bifurcational behaviour of general autonomous dynamical systems are embodied in the results of centre-manifold theory (Marsden & McCracken [1976], Carr [1980], Hale [1977]). For problems where the bifurcating states may be viewed as steady-states, Liapunov-Schmidt reduction can be employed instead (Chow & Hale [1982]). Associated with each category of problem is a natural equivalence concept which defines when two elemental models and their solution sets are qualitatively similar. Elemental models are identified from within an equivalence class of models. It is important to distinguish between equivalence classes which preserve the full system dynamics and those which preserve steady-state and periodic branches of equilibria but not, necessarily, stability. These differences pertaining to problem

category and equivalence type have culminated in a hierarchy of methods for the construction and classification of generating equations associated with specific model structures. The most general of these, and least systematic, derive from dynamical systems theory (Takens [1974a,b], Arnol'd [1972], Guckenheimer & Holmes [1983]). For steady-state problems, the techniques of singularity theory (Golubitsky & Schaeffer [1985]) are more appropriate and generalize many of the concepts originally embraced by catastrophe theory.

1.3 IDENTIFICATION OF AEROELASTIC BEHAVIOUR BY GENERIC MODELLING

The recognition that many complex processes possess well-defined geometrical structures in the neighbourhood of bifurcation motivates an attempt to reconcile the apparently disparate non-linear behaviour observed in the transonic aeroelastic response studies of Bendiksen [1989] and Kousen [1989]. It is possible that the transitions in qualitative behaviour, observed in these studies, can be described, locally, by the bifurcations of some elemental dynamical system which is not, necessarily, a rational derivation of the governing aeroelastic equations of motion. Phenomenologically, the important aeroelastic response variables are those associated with the structural states. Description of the observed aeroelastic behaviour in terms of these variables permits a succinct account of the macroscopic characteristics of the aeroelastic response. In the absence of *aerodynamic* bifurcations, one can conceive of a notional aeroelastic model, describing the evolution of the structural

states, whose underlying dynamic is qualitatively equivalent to that generated by the elemental system describing the observed transitional behaviour. Specifically, there exists a class of *hereditary* dynamical system models, possessing properties compatible with the gross physical features of the aerodynamic force response in transonic flow, whose local bifurcational characteristics are described by a finite-dimensional set of parameterized *ordinary* differential equations. The 'ordinary' nature of the bifurcation model, which arises from the restriction of the state(-history) dynamic onto a finite-dimensional manifold in the state-space (the centre-manifold), is distinguished from that of aeroelastic models which adopt quasi-steady, low-frequency, or rational transfer function aerodynamic approximations in their formulation. This distinction is significant in that it enables one to utilize, without approximation, the underlying rich theory of ordinary differential equations to carry out a qualitative analysis of hereditary aeroelastic phenomena aimed at exploring the various behaviour patterns that may be exhibited (although not all potential patterns are necessarily realizable (Hale [1985])). Appeal to the concepts of genericity, organizing centre and universal unfoldings, and consideration of the numerically observed behaviour, results in a topological 'picture' in parameter space of the qualitative characteristics of the aeroelastic response. In essence, one has the foundations of a geometrical, or qualitative, theory of non-linear hereditary aeroelastic systems from which one can synthesize a coherent understanding of the nature and extent of possible aeroelastic behaviour - importantly, without explicit knowledge of the unsteady aerodynamic environment.

In the present study, attention is focused on the divergence/ flutter interaction phenomena reported by Bendiksen and Kousen. This form of mode coupling in non-linear autonomous systems may arise when conditions for divergence and flutter occur simultaneously at a certain critical combination of the system parameters. In the proximity of a coincident divergence and flutter point, bifurcating steady-state and periodic solutions can interact non-linearly to generate interesting and subtle post-critical behaviour (Langford [1979], [1983], Holmes [1981], Armbruster *et al* [1985], Yu & Huseyin [1988]). In the spirit of earlier studies by Holmes & Rand [1975], Holmes [1977], and Holmes & Marsden [1978a], the aim of the present investigation, which extends and generalizes the work of Anderson [1991], is to ascertain, within a bifurcation-theoretic framework, whether the behaviour observed in the cited aeroelastic response studies in some sense conforms to the qualitatively stable unfoldings of a class of dynamical systems which arise, generically, in the vicinity of a coincident divergence and flutter point and, in so doing, make specific, and verifiable, qualitative predictions. The analysis presented precludes the possibility of chaotic motions. The system under study, however, does have the potential for other very complicated motions involving steady-state, periodic and quasi-periodic behaviour. Also, it should be noted at the outset that many of the arguments in support of the proposed methodology rely on assumptions that are *probably* true, yet are extremely difficult to verify directly. The supposition that the simplest explanation consistent with bifurcation theory is correct is adopted throughout. The ultimate test of the inferred results resides with future numerical studies of the coupled aeroelastic equations of motion.

1.4 ORGANIZATION OF THE DISSERTATION

The basic premise of the present study is that, locally in a region of physical parameter space, there exists an equivalence between the transitions in qualitative behaviour which characterize certain types of non-linear transonic aeroelastic phenomena and the local bifurcations of elemental dynamical systems described by finite-dimensional sets of parameterized ordinary differential equations. Moreover, the analogy lies with observations of behaviour of the structural states. Chapters Two and Three illustrate how such an equivalence arises for a representative class of hereditary aeroelastic models. In Chapter Four, the generic structure of a class of elemental dynamical systems exhibiting steady-state and periodic mode interactions is presented in association with a classification of persistent solution types. In Chapter Five, this classification is used in conjunction with partial bifurcational information derived from the numerical simulations of Bendiksen and Kousen to evaluate the qualitative characteristics of the divergence /flutter interaction phenomena observed in these simulations.

An hereditary structure for the aerodynamic response in unsteady transonic flow is proposed in Chapter Two. Heuristic arguments in support of the candidate structure are derived from an examination of the physical origins of time-history effects and delays in unsteady transonic flow. A natural representation of the aerodynamic force response as a non-linear functional of the structural state history leads to the definition of a canonical aeroelastic model in the form of an infinite-delay functional differential equation.

Properties assigned to the aerodynamic functional, compatible with certain empirical hypotheses, are used to define an appropriate function space setting for the aeroelastic initial-value problem thereby enabling a number of consequences of the model form to be deduced from standard results for functional differential equations.

In Chapter Three, the geometrical structure in the neighbourhood of bifurcation of a representative class of parameterized functional differential equations is described. The central concept permitting the reduction of the essentially infinite-dimensional problem to a finite-dimensional one is the existence of a local invariant manifold in the vicinity of bifurcation in the state-history ~ parameter space - the *centre-manifold*. The nature of the state-history dynamic on the centre-manifold and the equivalence of the qualitative behaviour of the restricted dynamic to that of a finite-dimensional set of ordinary differential equations are formally established for the class of functional differential equations under consideration. Properties of the aerodynamic functional which guarantee satisfaction of certain pre-requisites for the existence of a finite-dimensional centre-manifold provide an important link between the asymptotic behaviour of the state-history and that of the state. Specifically, the equivalence between the behaviour of the elemental system model in the neighbourhood of bifurcation and that of the state-history can be extended to that of the state. This equivalence is essential if elemental system models describing the qualitative behaviour of hereditary aeroelastic systems are to be identified on the basis of observations of states rather than state-histories. The qualitative characteristics of the

dynamic on the centre-manifold are identified with the *generic* bifurcations of vector fields. Local models of aeroelastic behaviour are derived from the universal unfoldings of degenerate vector fields and their associated normal forms. *A priori* knowledge of the model structure at bifurcation enables one to postulate a hypothetical degenerate form and thereby establish, via a notional equivalence transformation, the qualitative characteristics of the perturbed aeroelastic model in the vicinity of bifurcation. This association forms the basis of a qualitative model identification strategy for a general class of hereditary aeroelastic systems. Identification of an appropriate bifurcation model derives from an examination of the aeroelastic response and from assertions on the spectral characteristics of the linearized aeroelastic operator in the parameter range of interest.

A model structure appropriate to divergence/flutter interaction is presented in Chapter Four. The simplest degeneracy exhibiting steady-state and periodic mode interactions in the presence of a reflectional symmetry in the steady-state mode is the *pitchfork/ Hopf* degeneracy. The persistent bifurcations associated with this degeneracy are formed from the qualitatively distinct solution sets of a class of two-parameter unfoldings. Classification of all possible solution types reveals the range of behaviour associated with perturbations of the degeneracy. Generic unfoldings exhibiting secondary bifurcations of the primary steady-state and periodic solution branches are possible which involve coupled steady-state and periodic behaviour. Additionally, tertiary bifurcations to tori can occur leading to complicated quasi-periodic behaviour.

Analysis of the divergence/flutter interaction phenomena observed in the aeroelastic response studies of Bendiksen and Kousen is described in Chapter Five. Compatibility of the observed bifurcational phenomena with the existence of a coincident divergence and flutter point is examined by reviewing the qualitatively distinct and persistent bifurcations of an appropriate class of non-linear ordinary differential equations which arise, generically, in the neighbourhood of a steady-state and periodic bifurcation point. Correlation between observed and generic behaviour not only establishes consistency with the proposed underlying structure of the observed transitions but also facilitates a new interpretation of the observed phenomena and highlights some difficulties of definition and interpretation of non-linear flutter. The influence of symmetry and symmetry-breaking on divergence/flutter interaction phenomena is examined, empirically, in an attempt to understand the topological mechanisms responsible for some of the more unusual aeroelastic behaviour observed in the numerical simulations. The chapter concludes with the presentation of evidence for the existence of new transonic aeroelastic phenomena. The nature of the conjectured aeroelastic phenomena is discussed in relation to the generic behaviour of the identified bifurcation model.

CHAPTER TWO

A CANONICAL AEROELASTIC MODEL

2.1 INTRODUCTION

Mathematical models of (aerodynamically non-linear) autonomous aeroelastic systems are generally based on coupled aerodynamic and structural equations derived from the relevant physical conservation laws of mass, momentum and energy. Conventionally, the fluid and structure are modelled separately and coupled via the boundary conditions at the fluid-structure interface. The unsteady aerodynamic behaviour is modelled, typically, by the Euler or Navier-Stokes equations for an ideal gas while the elastic and inertial behaviour of the structure is modelled, in physical co-ordinates, by a system of discrete or finite (structural) elements or, alternatively, in the case of linear structural systems, by computationally or experimentally derived modes in modal co-ordinates. The resulting coupled evolution equations, in conjunction with an appropriate specification of initial and boundary conditions, represent an essentially exact mathematical model of the aeroelastic initial-value problem.

While such models are entirely appropriate as a basis for numerically computed response studies, their suitability for analytical bifurcation studies is questionable, particularly in the case of compressible flows exhibiting spatially discontinuous

flowfield behaviour. In such cases, the coupled aerodynamic and structural state evolution must be interpreted in a weak sense and questions of existence and uniqueness of solution, and smoothness of the evolution operator, must be posed in a subtle manner. Spatial discretization of the aerodynamic equations casts the problem in a more tractable setting. However, typical discretization schemes generally result in coupled evolution operators which lack smoothness with respect to the (spatially discrete) state vector. Consequently, the coupled aerodynamic and structural equations approach to modelling *transonic* aeroelastic systems is incompatible with the requirements of formal bifurcation analysis which demands a certain degree of differentiability of the evolution operator.

Phenomenologically, the state components of interest are those associated with the structural generalized displacements and velocities. For many aeroelastic configurations, time-evolution of the structural state components is inherently smooth. It is natural, therefore, to seek an interpretation of the aeroelastic initial-value problem in terms of the structural state alone. Such an interpretation is possible if the aerodynamic force response can be expressed as a (unique) *functional* of the structural state time-history. In classical (linear) aeroelasticity, and in applications admitting a local linearization of the aerodynamic force response, it is implicitly assumed that this is the case (see, for example, Woodcock [1981], Ballhaus & Goorjian [1978]). Empirical evidence suggests that a functional description of the aerodynamic force response is also justified for aeroelastic applications involving *finite-amplitude* motions in certain *non-linear* flow

regimes (Tobak & Chapman [1985]). Although explicit representation of the aerodynamic force response functional is generally unavailable for such applications, its notional existence permits a succinct mathematical description of the aeroelastic initial-value problem in the form of a functional differential equation in the structural state. This model form enables a close association to be maintained with the physical characteristics of the aeroelastic system. Characteristics of the aerodynamic force response observed in numerical studies of the coupled aerodynamic and structural equations, along with inherent physical symmetries, can be easily embodied in the properties of the aerodynamic functional.

The present chapter describes the development of a canonical functional differential equation model representative of a class of structurally linear aeroelastic systems operating in an inviscid transonic flow. The model is assigned properties compatible with the general characteristics of the aerodynamic force response identified for transonic flows. These properties enable the aeroelastic initial-value problem to be considered in a more formal mathematical setting in which further attributes of the model form can be deduced from standard results for functional differential equations.

2.2 FUNCTIONAL APPROXIMATION OF THE AERODYNAMIC FORCE RESPONSE

The existence of a *unique non-linear* aerodynamic force response functional appropriate to a particular flow regime is, necessarily, inferential. Non-uniqueness of the aerodynamic force response is

generally associated with certain types of degenerate flowfield behaviour. In particular, aerodynamic hysteresis, flow instability and bifurcation have been identified as key elements in the breakdown of unique, single-valued behaviour of the aerodynamic force response. In the transonic regime, flows admitting shocks, and entropy and vorticity production offer a potentially rich source of mechanisms for the realization of such phenomena. However, evidence derived from computational experiments suggests that, for certain classes of transonic flows, unique, single-valued behaviour of the aerodynamic force response is observed over the transonic parameter range.

2.2.1 Hereditary Structure of the Aerodynamic Force Response

A restrained aeroelastic system with N structural degrees-of-freedom is considered. The structural generalized displacement vector at time t referred to an appropriate basis is denoted by $q(t) \in \mathbb{R}^N$. Here $\mathbb{R}^N$ is a real N-dimensional vector space with norm $|q(t)|$. The structural displacement time-history over the interval $(-\infty,t]$ is denoted by q_t : $q_t(s) = q(t+s)$, $-\infty < s \leq 0$. It is assumed that all physical variables and parameters are suitably non-dimensionalized.

The generalized aerodynamic force response vector, $F(t) \in \mathbb{R}^N$, is assumed to depend on all past values of the structural generalized displacement vector. If $B((-\infty,0],\mathbb{R}^N)$ denotes an appropriate class of generalized displacement histories, then the aerodynamic force response may be interpreted as a mapping $\mathcal{F} : B \rightarrow \mathbb{R}^N$ and represented

by the (generally non-linear) functional relation

$$F(t) = \mathcal{F}(q_t) \quad . \tag{2.1}$$

The basic properties of the aerodynamic functional, $\mathcal{F}$, depend on the nature of the flow regime with which it is associated and the class of admissible motion histories for which it is defined.

2.2.2 Generalized Indicial Response and Non-Linear Integral Form of the Aerodynamic Force Response

Following Tobak & Pearson [1964], one defines the generalized (or non-linear) indicial response as illustrated in Figure 2.1. As shown for the case of a step change in the component q^j, two motions are considered. At time τ, the first motion is constrained so that the motion variables q^k, $k = 1,\ldots,N$, are held constant thereafter. The second motion differs only in the step in q^j imposed at time τ. The difference between the aerodynamic force response components at time t for each of the two motions, $\Delta F^k(t)$, $k = 1,\ldots,N$, is divided by the magnitude of the step. The *generalized indicial aerodynamic response* in F^i at time t per unit step in q^j at time τ is defined as the limit of the ratio $\frac{\Delta F^i}{\Delta q^j}$ as the step size approaches zero. Denoting the resulting generalized indicial response by $\mathcal{F}_q^{ij}(q_\tau, t, \tau)$, this definition may be represented symbolically as

$$\mathcal{F}_q^{ij}(q_\tau, t, \tau) \triangleq \lim_{\Delta q^j \to 0} \frac{\Delta F^i}{\Delta q^j} \quad . \tag{2.2}$$

As indicated by the notation, the indicial response is dependent not only on the levels $q(\tau)$ at which the step occurs, but may also depend on the entire history q_τ. Thus, in general, the indicial response components may themselves be functionals.

Based on the fundamental assumptions that the indicial response components exist and are unique (indicating the absence of aerodynamic bifurcations), and that differential increments in the aerodynamic force response may be represented as linear functionals of differential increments in the displacement history, the time-histories of the motion variables q^k, $k = 1,\ldots,N$, can be represented as a continuum of infinitesimal step changes and the aerodynamic force response $F(t)$ evaluated as a summation of the incremental responses to each of the steps over the interval $-\infty < \tau \leq t$. This results in an *exact* integral form for the aerodynamic force response $F(t)$. Each component of $F(t)$ has the form

$$F^i(t) = F^i(-\infty) + \sum_{j=1}^{N} \int_{-\infty}^{t} \mathcal{F}_q^{ij}(q_\tau, t, \tau) \frac{dq^j(\tau)}{d\tau} \, d\tau \quad , \quad i = 1,\ldots,N, \tag{2.3a}$$

with $\mathcal{F}_q^{ij}(q_\tau, t, \tau)$ defined as in (2.2).

More concisely,

$$F(t) = F(-\infty) + \int_{-\infty}^{t} \mathcal{F}_q(q_\tau, t, \tau) \frac{dq(\tau)}{d\tau} \, d\tau \tag{2.3b}$$

where $\mathcal{F}_q(q_\tau, t, \tau) \in \mathbb{R}^{N \times N}$ is the generalized indicial response matrix.

2.2.3 Simplifying Assumptions

In the form (2.3a), the component indicial responses are themselves functionals, depending, in general, on the whole past history of the motion (this is in contrast to the linear case where the indicial responses are independent of the motion history). Physical reasoning suggests that the indicial response should depend mainly on *local* events just prior to the origin of the step (see Figure 2.2). Further, where the asymptotic freestream conditions are time-invariant, the dependence of the indicial response on local events suggests that the indicial response be independent of the time at which the step occurs. That is, the indicial response must be a function of *elapsed* time $t-\tau$ rather than of t and τ separately.

For the finite-amplitude, high-frequency motions of interest in the present study, these assumptions are manifest in the approximation

$$\mathcal{F}_q(q_\tau, t, \tau) \cong F_q(t-\tau, q(\tau), \dot{q}(\tau)) \tag{2.4}$$

where the approximate indicial response matrix, F_q, is now a non-linear *function* of the elapsed time and the generalized displacements and velocities at the origin of the step. If the motion is locally smooth prior to the step, the approximation (2.4) is indicative of the non-persistence of distant past events and of a dominant dependence of the indicial response on the *recent* past.

Further re-arrangement of (2.4) allows for a more convenient form of the indicial response. It is evident from physical considerations

that, for stable flows, each of the indicial response components will approach a steady-state value with increasing value of the argument $t-\tau$. If each indicial response component is assumed to possess a unique, single-valued steady-state, independent of $\dot{q}(\tau)$, then the following identity can be introduced

$$F_q(t-\tau,q(\tau),\dot{q}(\tau)) = F_q(\infty,q(\tau),0) - F_q^*(t-\tau,q(\tau),\dot{q}(\tau)) \qquad (2.5)$$

where F_q^* is termed the *deficiency* matrix. Each of the components of F_q^* tends to vanish with increasing value of the elapsed time $t-\tau$. The general nature of the component deficiency functions can be deduced from the physical characteristics of the indicial response (Tobak & Schiff [1981]). The principal elements of the indicial response function (Figure 2.3) are identified with circulatory and non-circulatory (impulsive) components of the aerodynamic response. The generic features of this model of the indicial response are evident in several computational studies (see, for example, Magnus & Yoshihara [1975]).

Substitution of (2.4) and (2.5) in (2.3) reveals that the terms involving the steady-states form a perfect differential which can be immediately integrated to produce the following approximation for the aerodynamic force response,

$$F(t) \cong F_\infty(q(t)) - \int_{-\infty}^{t} F_q^*(t-\tau,q(\tau),\dot{q}(\tau)) \frac{dq}{d\tau}(\tau)\, d\tau \qquad (2.6)$$

where $F_\infty(q(t))$ is the steady-state value of $F(t)$ at the instantaneous $q(t)$.

Equation (2.6) conforms to the most general model form in a hierarchical class of approximate aerodynamic force response models originally proposed by Tobak & Schiff [1976a]. This model form is believed to be sufficiently general to encompass a broad class of flow regimes and motion histories, including finite-amplitude, high frequency motions in unsteady transonic flow. An intrinsic property of the integral term in (2.6), which reflects the dissipative nature of the aerodynamic force response in stable flows, and which is a direct consequence of the properties ascribed to the deficiency matrix, is that of *(integral) fading memory*. Essentially, for motions contained within some pre-defined bound, there will exist a limited time-segment of the recent past, dependent on the amplitude of the bound, for which the contribution to the integral term is above a certain threshold. This property plays an important role in the qualitative theory of the aeroelastic initial-value problem.

2.3 THE AEROELASTIC INITIAL-VALUE PROBLEM

Adopting the aerodynamic force response model of §2.2.3 and assuming a linear, time-invariant structural model with generalized mass, damping and stiffness matrices, $M \in \mathbb{R}^{N\times N}$, $C \in \mathbb{R}^{N\times N}$, and $K \in \mathbb{R}^{N\times N}$, the aeroelastic initial-value problem can be represented by an autonomous non-linear integro-differential equation of the form

$$M\ddot{q}(t) + C\dot{q}(t) + Kq(t) = F_{\infty}(q(t)) - \int_{-\infty}^{t} F_{q}^{*}(t-\tau, q(\tau), \dot{q}(\tau)) \frac{dq}{d\tau}(\tau)\, d\tau \qquad t > 0$$

subject to the initial histories q_0 and $\dot{q}_0$. (2.7)

2.3.1 Representation as a Functional Differential Equation

The aeroelastic initial-value problem is described more formally by its state space representation,

$$\dot{x}(t) = H(x(t),\alpha) + \int_{-\infty}^{t} Q(t-\tau,x(\tau),\alpha)d\tau \quad t > 0 \qquad (2.8a)$$

subject to the initial condition

$$x_0 = \varphi \quad , \quad \varphi \in D \subset X \qquad . \qquad (2.8b)$$

Here $x(t) = (q(t),\dot{q}(t))^T \in \mathbb{R}^{n=2N}$ denotes the structural state vector at time t, $x_t : x_t(s) = x(t+s)$, $-\infty < s \leq 0$, denotes the structural state time-history over the interval $(-\infty,t]$ and $X \triangleq X((-\infty,0], \mathbb{R}^n)$ denotes an appropriate space of functions - the *phase space* - mapping the interval $(-\infty,0]$ into $\mathbb{R}^n$. In general, X is a Banach space and the norm of an element ψ in X is designated by $\|\psi\|_X$.

The function H is defined explicitly in terms of the structural generalized mass, damping and stiffness matrices, M, C, and K, and the aerodynamic operator F_∞ while the function Q is defined in terms of the product of the aerodynamic deficiency matrix F_q^* and the generalized velocity vector.

In equation (2.8), the dependence of the aeroelastic system on freestream and/or structural control parameters is represented by the explicit inclusion of the control parameter set $\alpha \in \mathbb{R}^m$ in the arguments of H and Q.

2.3.2 Definition of the Phase Space

One of the main concerns in dealing with functional differential equations such as (2.8) lies in obtaining an appropriate choice of phase space X for a given equation (for a general survey, see Corduneanu & Lakshmikantham [1980]). Several investigators (for example, Hale [1979] or Hale & Kato [1978]) have studied properties (or axioms) of *admissible* spaces for functional differential equations with infinite delay. The significance of such spaces is that one may apply standard existence/uniqueness/continuation/ continuous-dependence results to any functional differential equations defined on an admissible space.

In particular, if X is an admissible space with D an open subset of X and if $f : D \times \mathbb{R}^m \to \mathbb{R}^n$ is continuous on $D \times \mathcal{A}$, $\mathcal{A} \subset \mathbb{R}^m$, then for each $\alpha \in \mathcal{A}$, the initial-value problem

$$\dot{x}(t) = f(x_t, \alpha) \quad , \tag{2.9}$$

subject to $$x_0 = \varphi \in D \quad ,$$

has a solution defined on an interval $[0,\sigma)$ for some $0 < \sigma \leq \infty$. If, in addition, $f = f(.,\alpha)$ satisfies a local Lipschitz condition in its first argument, then the solution is unique. By a solution of (2.9) having initial function φ at time $t = 0$, is meant a function x mapping an interval $(-\infty,\sigma)$, $0 < \sigma \leq \infty$, into $\mathbb{R}^n$ such that $x_t \in D$ for all $t \in [0,\sigma)$; $x_0 = \varphi$; x has a derivative $\dot{x}(t)$ at each $t \in (0,\sigma)$; and x satisfies (2.9) on $(0,\sigma)$.

A certain class of admissible spaces - UC_g spaces - frequently arises in a natural way for many types of integro-differential equations of the form (2.8) (Atkinson & Haddock [1988]). Although phase spaces of this type exclude initial histories involving step or impulse functions (such spaces are considered in Coleman & Mizel [1966], [1968]), they are sufficiently general to embrace the range of initial histories encountered in the present study.

To define the class of phase spaces of interest, a function g is introduced satisfying

(g1) $g : (-\infty,0] \to [1,\infty)$ is a continuous non-increasing function on $(-\infty,0]$ such that $g(0) = 1$.

The space of continuous functions which map $(-\infty,0]$ into $\mathbb{R}^n$ such that $\sup_{s\le 0}|\psi(s)|/g(s) < \infty$ is denoted by C_g. Equipped with the norm $\|\psi\|_g = \sup_{s\le 0}|\psi(s)|/g(s)$, C_g is a Banach space.

The subspace $UC_g \triangleq \{\psi \text{ in } C_g : \psi/g \text{ is uniformly continuous on } (-\infty,0]\}$ is an admissible space (Haddock & Terjéki [1990]) if, in addition, g satisfies

(g2) $[g(s+u)/g(s)] \to 1$ uniformly on $(-\infty,0]$ as $u \to 0$.

In many cases, only bounded continuous initial functions need be considered. Any such function is in UC_g whenever

(g3) $g(s) \to \infty$ as $s \to -\infty$.

Under conditions where the integral term in (2.8) possesses an *integral fading memory* property, and both H and Q are continuous functions of their arguments, it can be shown that the right side of (2.8) is continuous on an open subset of a UC_g space where g satisfies the properties (g1), (g2) and (g3).

More formally, if BC denotes the space of bounded and continuous functions that map $(-\infty,0]$ into $\mathbb{R}^n$, with the norm of this space designated by $\|\psi\|_\infty = \sup_{s\le 0}|\psi(s)|$, and if $\mathcal{A}$ denotes an open neighbourhood of some α_0 in $\mathbb{R}^m$, then[1] $Q : [0,\infty) \times \mathbb{R}^n \times \mathbb{R}^m \to \mathbb{R}^n$ is said to have *integral fading memory* in $\mathcal{A}$ if, for each $\varepsilon > 0$ and each $\delta > 0$, there exists $\kappa > 0$ such that

$$\int_{-\infty}^{-\kappa} |Q(-s,\psi(s),\alpha)|\,ds < \varepsilon \qquad (2.10)$$

for all α in $\mathcal{A}$ and all ψ in BC with $\|\psi\|_\infty \le \delta$.

Following Atkinson & Haddock [1988], if $Q : [0,\infty) \times \mathbb{R}^n \times \mathbb{R}^m \to \mathbb{R}^n$ is continuous and has integral fading memory in $\mathcal{A}$, then, for each $\gamma > 0$, there exists a function g satisfying (g1), (g2) and (g3) such that the function $M = M(\psi,\alpha)$ defined by

$$M(\psi,\alpha) = \int_{-\infty}^{0} |Q(-s,\psi(s),\alpha)|\,ds \qquad (2.11)$$

is continuous on $S_g(\gamma) \times \mathcal{A}$ where $S_g(\gamma) = \{\psi \text{ in } C_g : \|\psi\|_g < \gamma\}$.

[1] The change of variable $t-\tau = -s$ is introduced.

Consequently, if H and Q are continuous and Q has integral fading memory in $\mathcal{A}$, and, for each $\alpha \in \mathcal{A}$,

$$f(\psi,\alpha) \triangleq H(\psi(0),\alpha) + \int_{-\infty}^{0} Q(-s,\psi(s),\alpha)ds \qquad (2.12)$$

satisfies a local Lipschitz condition in ψ, then the aeroelastic initial-value problem (2.8) possesses a unique local solution on a subset of $S_g(\gamma)$.

2.3.3 Smoothness Hypotheses

To facilitate discussion of the asymptotic properties of solutions of (2.8) which remain in $S_g(\gamma)$ on the interval $(-\infty,+\infty)$, it is convenient to introduce additional hypotheses on f in (2.12), assumed valid in $S_g(\gamma) \times \mathcal{A}$, which are compatible with the choice of UC_g as an admissible phase space.

It is assumed that for all $(\psi,\alpha) \in S_g(\gamma) \times \mathcal{A}$, f in (2.12) affords the expansion

$$f(x_t,\alpha) = L(\alpha)x_t + \hbar(x_t,\alpha) \qquad (2.13)$$

where $L(\alpha) = f'(0,\alpha)$ is a bounded linear operator in UC_g. By implication, $f(.,\alpha)$ is locally Lipschitz continuous. Furthermore, both L and $\hbar$ are assumed continuous in $(\psi,\alpha) \in S_g(\gamma) \times \mathcal{A}$ and, for $\alpha \in \mathcal{A}$ fixed, $\hbar(\psi,\alpha)$ is assumed to be k-1 times continuously Fréchet differentiable in ψ.

The consistency of the aforementioned smoothness hypotheses with the physical characteristics of the transonic aeroelastic initial-value problem is difficult to assess. The basic requirement for continuity derives from the integral fading memory condition (2.10) and hence from the hereditary characteristics of the aerodynamic force response functional. In the transonic regime, the principal sources of heredity are the vorticity shed into the wake at earlier instants of time and the downstream convection of shock-generated vorticity and entropy (Batina [1988]). Additionally, the presence of shocks introduces a non-uniform delay in the propagation of acoustic waves, thereby limiting the degree to which downstream (or past) events are able to influence (present) upstream conditions (Tijdeman & Seebass [1980]). These features are inherently non-linear in origin and are accentuated in large-amplitude motions where there is significant interaction between the motion of the aerodynamic surface and the strength, geometry and location of the shocks. The effect of these fundamental physical characteristics in stable transonic flow is manifest as a non-linear, state-dependent, dynamic relaxation of the aerodynamic force response. The integral fading memory condition (2.10) may be interpreted as the formal representation of this behaviour. Empirical evidence (Ballhaus & Goorjian [1978]) suggests that the implied assumption of C^1-continuity of the aerodynamic functional, and the corresponding existence of a linearized aerodynamic operator, is not an unreasonable one. To deduce further properties of the aerodynamic functional, however, requires intimate knowledge of the aerodynamic response. The nature of unsteady transonic flow is such that few general characteristics of the aerodynamic functional can be

established beyond existence and uniqueness. Shock motion, in particular, plays an important role in limiting the degree of smoothness of the aerodynamic functional. For certain transonic aeroelastic configurations, shock motion manifests itself as a discontinuity in the time-derivative of the aerodynamic force response, signalling loss of Fréchet differentiability of the aerodynamic force response functional. In the present application, the implied smoothness properties assigned to the aerodynamic functional are assumed valid in the parameter range of interest without compromise to the physical fidelity of the model.

2.4 SUMMARY

The non-smooth character of the coupled aerodynamic and structural equations governing the transonic aeroelastic initial-value problem precludes the direct use of these equations in analytical bifurcation studies. In the absence of aerodynamic bifurcation, the notional existence of a unique single-valued functional of the structural state time-history, which approximates the aerodynamic force response, permits an alternative and concise description of the aeroelastic initial-value problem as an infinite-delay functional differential equation. Intrinsic fading memory properties assigned to the aerodynamic force response functional lead, naturally, to the definition of an admissible class of motion histories for which continuity of the functional is assured. Subject to certain additional smoothness hypotheses, unique local solution behaviour of the aeroelastic initial-value problem can be inferred from standard results for functional differential equations.

CHAPTER THREE

BIFURCATION AND GENERIC MODELS OF AEROELASTIC BEHAVIOUR

3.1 INTRODUCTION

A dynamical system depending on a set of parameters $\alpha = \{\alpha_1, \alpha_2, \ldots\}$ is said to undergo a bifurcation at $\alpha = \alpha_0$ when a qualitative change in the dynamics takes place as α passes through α_0. Near a *local* bifurcation from an equilibrium, recognized by a change in number or stability of solution, the solution structure is often characterized by solution curves which locally decay or are weakly attracted or repelled in the proximity of the equilibrium. Geometrically, the phase space is composed of *local invariant manifolds* - a *stable* manifold representing the directions in phase space in which the equilibrium acts as an attractor and a *centre* manifold representing those directions where the attraction or repulsion is weak. In directions complementary to the centre-manifold, the local dynamical behaviour is relatively simple since it is controlled by the contracting elements of the solution curves on the stable manifold (Figure 3.1). Locally, behaviour on the stable manifold does not change qualitatively as α passes through its critical value α_0 (Palis & Takens [1977]) and therefore bifurcations are restricted to the centre-manifold (strictly, a family of invariant manifolds parameterized by α). The restriction of the system dynamic to the centre-manifold completely captures the bifurcational behaviour locally (Marsden & McCracken [1976]).

Typically, the dimension of the centre-manifold is *finite* and evolution of the system dynamic on the centre-manifold is described by a finite-dimensional set of *ordinary* differential equations. The construction of the reduced equation set requires that the number of eigenvalues of the linearized system on the imaginary axis at $\alpha = \alpha_0$ be finite with all remaining eigenvalues of the linearized system bounded away from the imaginary axis for a range of α in the neighbourhood of α_0. In systems depending on several parameters it is possible to arrange for several eigenvalues to lie on the imaginary axis simultaneously. For nearby parameter values, the resulting low-dimensional system then describes finite-dimensional but potentially complex dynamics of the original system.

The centre-manifold reduction permits a dramatic simplification in the description of the qualitative characteristics of a dynamical system in the vicinity of bifurcation. Formal reduction, however, is inherently model dependent, requiring explicit representation of the governing evolution equation. Nevertheless, from a knowledge of the *degenerate form* of the reduced equation set at bifurcation, one can seek a *qualitatively equivalent* family of parameterized vector fields, describing the dynamic on the centre-manifold, which satisfies a *structural stability* or *persistence* criterion. Such a family is called a *versal unfolding*. A versal unfolding depending on the minimum number of parameters is called *universal* and that minimum number the *codimension*. The higher the codimension, the more varied and complex are the ways in which a degeneracy can unfold in response to (parametric) perturbation. Classifications of *generic* bifurcations of vector fields, catalogueing the persistent ways in

which degenerate singularities of particular codimension can be generically unfolded locally, enable one to associate candidate degenerate forms of the reduced equation set with particular universal unfoldings and bifurcation structures. Analysis of these unfoldings reveals the range of dynamics associated with the bifurcations and also indicates which coefficients in their Taylor expansions distinguish between various types of behaviour.

Under quite general hypotheses, the qualitative characteristics of *hereditary* aeroelastic systems can be identified with the generic bifurcations of vector fields. The model reduction and equivalence concepts embodied in this association provide a natural framework for a *geometrical*, or *topological*, interpretation of local aeroelastic behaviour. This chapter describes the principal elements of a qualitative model identification strategy for a general class of hereditary aeroelastic systems representative of the local aeroelastic model defined in Chapter Two. Only the salient features of the procedure are presented here. Further details may be found in the cited references.

3.2 GEOMETRICAL CHARACTERISTICS OF THE AEROELASTIC INITIAL-VALUE PROBLEM IN THE NEIGHBOURHOOD OF BIFURCATION

To introduce the class of aeroelastic systems that is of interest in this section, it is pertinent to set some preliminary notation and to detail the primary assumptions which define the class of systems under consideration.

3.2.1 Preliminaries

A general class of hereditary aeroelastic systems is considered in which $X = X((-\infty,0], \mathbb{R}^n)$ is an admissible phase space (satisfying the same general qualitative properties as the space UC_g introduced in §2.4.2), $x_t \in D \subset X$, $\alpha \in \mathcal{A} \subset \mathbb{R}^m$, $f \in C^k(D \times \mathcal{A}, \mathbb{R}^n)$, $k \geq 2$, and

$$\dot{x}(t) = f(x_t,\alpha) \quad , \quad f(0,\alpha_0) = 0 \quad . \tag{3.1}$$

For each $\varphi \in D$, $\alpha \in \mathcal{A}$ fixed, it is assumed that there exists a unique solution $x = x(\varphi,\alpha)$ of (3.1) satisfying the initial-value problem $x_0 = \varphi$, $x(t)$ solves (3.1) for $t > 0$. Further, it is assumed that all solutions remain in D for all $t \geq 0$. By definition, the zero solution is an equilibrium at $\alpha = \alpha_0$.

Given a solution $x(\varphi,\alpha)$ through φ of (3.1) at α, it is possible to define a mapping

$$T_f^\alpha(t) : D \to D \quad , \quad T_f^\alpha(t)\varphi = x_t(\varphi,\alpha) \tag{3.2}$$

for $t \geq 0$. The family of mappings $\{T_f^\alpha(t), t \geq 0\}$ defines a *dynamical system* on D satisfying the following properties:

$$T_f^\alpha(t)\varphi \text{ is continuous in } (t,\varphi,\alpha) \ ,$$

$$T_f^\alpha(0)\varphi = \varphi \ ,$$

$$T_f^\alpha(t+s)\varphi = T_f^\alpha(t)T_f^\alpha(s)\varphi \ , \ t \geq 0, \ s \geq 0 \ .$$

The objective is to determine the nature of the system dynamic generated by (3.1) in a neighbourhood of $(0,\alpha_0) \in D \times \mathcal{A}$ under the hypothesis that the linear equation

$$\dot{x}(t) = L(\alpha)x_t \ , \tag{3.3}$$

with $L(\alpha) = f'(0,\alpha)$ a bounded linear operator in X whose eigensolution pairs depend smoothly on the parameters, has p eigenvalues $\{\lambda_i(\alpha_0),\ i = 1,\ldots,p\} \equiv \Lambda(\alpha_0)$ on the imaginary axis when $\alpha = \alpha_0$ and the remaining ones have negative real parts bounded away from the imaginary axis for all α in an open neighbourhood of α_0.

The consistency of this hypothesis with the definition of the phase space $X \equiv UC_g$ is assured if UC_g possesses a *strong fading memory* property (Haddock & Horner [1988]). In this case, for some $t > 0$, the point spectrum of the *infinitesimal generator* of $T_L^0(t)$ (which, roughly, corresponds to the eigenvalues of $L(\alpha_0)$) lies to the right of a line $Re\{z\} = \beta$, $\beta < 0$, $z \in \mathbb{C}$, with the remaining spectrum bounded away from this line in the complex left-half plane (Naito [1979]). Moreover, to the right of any line $Re\{z\} = \rho$, $\beta < \rho < 0$, there is, at most, a finite number of eigenvalues of $L(\alpha_0)$. That the space UC_g, with g satisfying (g1), (g2), (g3) as in §2.3.2, does, in fact, possess a strong fading memory property follows from the assumed boundedness of the solution $x(\varphi,\alpha)$ on the interval $(-\infty,+\infty)$ (Haddock & Terjéki [1990]). This property implies that the function g in §2.3.2 additionally satisfies

(g4) $$\lim_{u\to\infty} \sup_{s\le 0} [g(s)/g(s-u)] = 0 \quad .$$

3.2.2 Decomposition of the Phase Space

Corresponding to the p eigenvalues on the imaginary axis at $\alpha = \alpha_0$ are non-zero exponential solutions of (3.3) of the form $\xi(\alpha_0)\exp(\lambda(\alpha_0)(t+\theta))$, $\theta \le 0$, with $\xi(\alpha_0) \in \mathbb{C}^n$, $\lambda(\alpha_0) \in \mathbb{C}$. These solutions are determined by the non-trivial solutions of the system

$$[\lambda I - L(\alpha_0, e^{\lambda \cdot} I)]\xi = 0 \ . \tag{3.4}$$

One can show (Naito [1979]) that a basis for the real and imaginary parts of the initial (generalized) eigensolution histories, $\xi_i(\alpha_0)\exp(\lambda_i(\alpha_0)\theta)$, $\theta \le 0$, $i = 1,\ldots,p$, spans a subspace, P_0 of X, of dimension p, which is invariant under the action of the dynamic $T_L^0(t)$, $t \ge 0$ generated by (3.3) at $\alpha = \alpha_0$. Also, there is a complementary subspace, Q_0 of X, which is also invariant under $T_L^0(t)$, $t \ge 0$, such that X admits the direct sum decomposition $X = P_0 \oplus Q_0$.

Associated with each of the subspaces are the projection operators $\pi(\alpha_0)$ and $\pi^{\perp}(\alpha_0) = I - \pi(\alpha_0)$ such that any $\psi \in X$ has the representation $\psi = \psi^P + \psi^Q$, $\psi^P = \pi(\alpha_0)\psi$, $\psi^Q = \pi^{\perp}(\alpha_0)\psi$.

One can show that there are constants $K(\alpha_0)$, $\delta(\alpha_0) > 0$ such that

$$\|T_L^0(t)\pi^{\perp}(\alpha_0)\|_X \le K(\alpha_0)\exp(-\delta(\alpha_0)t) \quad , \quad t \ge 0 \ .$$

Loosely, the action of $T_L^0(t)$ in Q_0 is a contraction.

3.2.3 Decomposition of the Solution Operator

For any α in some open neighbourhood of α_0, (3.1) may be written as

$$\dot{x}(t) = L(\alpha_0)x_t + h(x_t,\alpha) \tag{3.5}$$

where $h(x_t,\alpha) = f(x_t,\alpha) - L(\alpha_0)x_t$.

From the variation of constants formula (Lima [1977]), a function x is a solution of (3.5) through φ if and only if, for each α,

$$x_t = T_L^0(t)\varphi + \int_0^t T_L^0(t-s)X_0 h(x_s,\alpha)ds \ , \qquad t \geq 0 \ , \tag{3.6}$$

where X_0 is the $n \times n$ matrix function on $(-\infty,0]$ with $X_0(\theta) = 0$ for $-\infty < \theta < 0$, $X_0(0) = I$, the identity.

If $x_t^P = \pi(\alpha_0)x_t$, $x_t^Q = \pi^\perp(\alpha_0)x_t$, $X_0^P = \pi(\alpha_0)X_0$, $X_0^Q = \pi^\perp(\alpha_0)X_0$, then it can be shown that (Lima [1977])

$$x_t^P = T_L^0(t)x_0^P + \int_0^t T_L^0(t-s)X_0^P h(x_s,\alpha)ds \ , \ t \geq 0 \tag{3.7a}$$

$$x_t^Q = T_L^0(t)x_0^Q + \int_0^t T_L^0(t-s)X_0^Q h(x_s,\alpha)ds \ , \ t \geq 0 \ , \tag{3.7b}$$

where $T_L^0(t)x_0^P$, $T_L^0(t-s)X_0^P$ are defined for $-\infty < t < \infty$.

Also, if $\Phi = \Phi_L^0 = \{\varphi_1,\ldots,\varphi_p\}$ is a basis for $\pi(\alpha_0)X$ then there is a $p \times p$ matrix $B = B_L^0$ (assumed Jordan block) whose spectrum is $\Lambda(\alpha_0)$

and a $p \times n$ matrix $\Psi_0 = \Psi_L^0(0)$ (where Ψ_L^0 forms a basis for the adjoint initial eigensolution histories of (3.3) associated with $\Lambda(\alpha_0)$) such that (*cf.* Lima [1977], Hale [1974])

$$T_L^0(t)\Phi = \Phi\exp(Bt), \qquad -\infty < t < \infty , \tag{3.8a}$$

$$T_L^0(t)X_0^P = \Phi\exp(Bt)\Psi_0, \qquad -\infty < t < \infty . \tag{3.8b}$$

Using these observations in (3.7), it is easily verified that, for each $t \geq 0$, (3.7) is equivalent to the equations

$$x_t = \Phi_L^0 u(t) + x_t^Q , \tag{3.9a}$$

$$\dot{u}(t) = B_L^0 u(t) + \Psi_L^0(0)h(x_t,\alpha) , \tag{3.9b}$$

$$x_t^Q = T_L^0(t)x_0^Q + \int_0^t T_L^0(t-s)X_0^Q h(x_t,\alpha)ds . \tag{3.9c}$$

3.2.4 The Centre-Manifold Reduction

The principal result of this section is contained in the following theorem which is a variant of the centre-manifold theorem presented by Chafee [1971] and Hale [1974] for functional differential equations of the finitely retarded type. An outline proof of the theorem, valid for infinite-delay functional differential equations, can be found in Stech [1985].

Centre-Manifold Theorem. If $\dot{x}(t) = f(x_t,\alpha)$ (denoted FDE(f,α)) is a given functional differential equation as defined in §3.2.1 with $f(0,\alpha_0) = 0$ and p roots of the characteristic equation for $L(\alpha_0) = f'(0,\alpha_0)$ lying on the imaginary axis, then there is an open neighbourhood $\mathcal{A}'$ in $\mathbb{R}^m$ of α_0, $\mathcal{A}' \subset \mathcal{A}$, open neighbourhoods V and W in X of $\varphi = 0$, positive constants K, ε and a C^k-diffeomorphism

$$m_f^\alpha : \pi(\alpha_0)X \cap V \to W$$

for every $\alpha \in \mathcal{A}'$, such that m_f^α is continuously differentiable in α and the set

$$M_f^\alpha = \{\varphi \in X : \varphi = m_f^\alpha \psi,\ \psi \in \pi(\alpha_0)X \cap V\}$$

is a local integral manifold of FDE(f,α) (that is, is composed of local solution curves of these equations) with M_f^0 tangent to $\pi(\alpha_0)X$ at $\varphi = 0$. On M_f^α, the local solution history of FDE(f,α) is equivalent to the solution of the ordinary differential equation

$$\dot{u}(t) = B_L^0 u(t) + \Psi_L^0(0)h(m_f^\alpha(\Phi_L^0 u(t)),\alpha) \qquad (3.10)$$

having initial value u_0, $\Phi_L^0 u_0 = \pi(\alpha_0)\varphi$, at time $t = 0$.

Furthermore, any solution $x(\varphi,\alpha)$ of FDE(f,α) satisfies

$$\|x_t(\varphi,\alpha) - m_f^\alpha \pi(\alpha_0)x_t(\varphi,\alpha)\|_X \le K \exp(-\varepsilon t)\ \|\varphi - \pi(\alpha_0)\varphi\|_X$$

for all $t \ge 0$ for which $x_t(\varphi,\alpha) \in W$, $\pi(\alpha_0)x_t(\varphi,\alpha) \in V$. □

The centre-manifold is characterized by two fundamental properties - *local invariance* and *local attractivity*. Local invariance of the centre-manifold implies that, for each $\alpha \in \mathcal{A}'$ and $t \geq 0$ for which $x_t(\varphi,\alpha) \in W$ and $\pi(\alpha_0)x_t(\varphi,\alpha) \in V$, if $\varphi \in M_f^\alpha$ then $x_t(\varphi,\alpha) \in M_f^\alpha$, while local attractivity implies that for all $t \geq 0$ for which $x_t(\varphi,\alpha) \in W$ and $\pi(\alpha_0)x_t(\varphi,\alpha) \in V$, $x_t(\varphi,\alpha) \to M_f^\alpha$ as $t \to \infty$. The family of invariant manifolds $\{M_f^\alpha, \alpha \in \mathcal{A}'\}$ completely captures the bifurcational behaviour locally in a neighbourhood of $(0,\alpha_0)$ if, for each $\alpha \in \mathcal{A}'$, $x_t(\varphi,\alpha) \in W$ and $\pi(\alpha_0)x_t(\varphi,\alpha) \in V$ for all $t \geq 0$ (see Figure 3.2). To obtain a complete local characterization of the bifurcational behaviour, including information on the creation of new attracting and repelling solutions, it is only necessary to study an equivalent finite-dimensional set of parameterized ordinary differential equations of the form (3.10). This equation set describes the dynamics of the projection of x_t onto P_0 when x_t resides on the centre-manifold (see Figure 3.3). By virtue of the attractivity of the centre-manifold and the diffeomorphic relation between elements of P_0 and elements of M_f^α, (3.10) determines the long term qualitative behaviour of x_t in X. The particular *fading memory* properties implied in the definition of the phase space X ensure that, for large t, the asymptotic behaviour of x_t in X follows, in a natural way, the asymptotic behaviour of x(t) in $\mathbb{R}^n$ (Murakami & Naito [1989])[1]. Consequently, there exists an equivalence between the behaviour of x(t) in $\mathbb{R}^n$ and the solution of (3.10). Local stability and bifurcation characteristics of the hereditary system (3.1) can therefore be inferred directly from the form of (3.10).

[1] For aeroelastic systems defined on more general phase spaces, the asymptotic properties of the state can differ from those of the state-history (Woodcock [1979]).

3.3 PROTOTYPES FOR NON-LINEAR DIVERGENCE AND FLUTTER

The archetypal aeroelastic phenomena of divergence and flutter are synonymous with *degenerate* behaviour of the aeroelastic operator at criticality. To characterize the type of behaviour that can be obtained in a neighbourhood of bifurcation, it is sufficient to consider a reduced equation set of the form (3.10), describing the qualitative characteristics of the dynamics of the aeroelastic initial-value problem on the centre-manifold. The *Centre-Manifold Theorem*, however, does not provide a constructive method for computing the necessary reduced equation set. Moreover, explicit representation of the aerodynamic force response functional is generally not possible. Nevertheless, the dynamics on the centre-manifold is not completely arbitrary. The system behaviour is conditioned, primarily, by the degenerate form of the reduced equation set at criticality. Qualitative features of the aeroelastic response which persist under perturbation are contained in the versal unfolding of the degeneracy. However, for *hereditary* aeroelastic systems governed by functional differential equations of the form (3.1), the nature of the functional in the reduced equation set imposes certain restrictions on the types of bifurcations that can occur, although, in general, details of these restrictions, and their influence on the versal unfolding of the degeneracy, are incompletely understood (*cf.* Hale [1985], 1986]). In the present application, and in the absence of evidence to the contrary, the versal unfolding of the reduced aeroelastic equation set is assumed to coincide with the versal unfolding of the generic vector field, of corresponding codimension, possessing the same degeneracy.

3.3.1 Preliminaries

The basic object of interest is a system of *ordinary* differential equations of the form

$$\dot{u} = F(u,\alpha) = F_\alpha(u) \tag{3.11}$$

where $u \in \mathbb{R}^p$, $\alpha \in \mathbb{R}^m$ and $F : \mathbb{R}^p \times \mathbb{R}^m \to \mathbb{R}^p$ or $F_\alpha : \mathbb{R}^p \to \mathbb{R}^p$. Here F is a smooth vector field which depends smoothly on the parameters.

The system (3.11) is assumed to possess an *equilibrium* point $(0,\alpha_0)$ which is *non-hyperbolic.* In this case, the Jacobian derivative of F with respect to the u variables has zero or pure imaginary eigenvalues and the equilibrium point is said to be *degenerate.* Of particular interest is the extent to which one can use the results of power series expansions of F (or F_α) to deduce the qualitative[2] properties of solutions of (3.11) near a degenerate equilibrium.

Multiple degeneracies of equilibria impose special conditions (defining conditions) on the Taylor series expansion of F. The number of independent conditions is (equal to) the *codimension* of the vector field. In addition, certain inequalities (transversality conditions) must be satisfied by the Taylor series - a working hypothesis in the qualitative theory of bifurcations is that *generic* perturbations of $F_0 \equiv F(.,\alpha_0)$ are *transversal* to the set of all vector fields on $\mathbb{R}^p$ with an equilibrium at the origin which are

[2] The meaning of the term 'qualitative' is made precise by a definition of an equivalence relation which specifies when two vector fields are to be regarded as qualitatively the same.

equivalent to F_0 (transversal intersections retain their topology under perturbation). These conditions and inequalities determine the type of bifurcation exhibited by an equilibrium. Further inequalities (non-degeneracy conditions) are imposed on the non-linear terms in the Taylor expansion at the equilibrium in order to have the desired properties of *qualitative stability* or *persistence* with respect to perturbations.

In discussing stability with respect to perturbations, it is necessary to specify whether the perturbations should be restricted to those which satisfy certain *symmetries* or other special *constraints*. Applications often involve systems which possess symmetries. Typically, symmetries of the physical problem are inherited by the reduced bifurcation problem which emerges from the centre-manifold reduction. The vector field $F(u,\alpha)$ has symmetry Γ if $\gamma \cdot F(u,\alpha) = F(\gamma \cdot u,\alpha)$ for each $\gamma \in \Gamma$ of the symmetry group Γ. Here, Γ may be represented by matrices acting on the variables u so that $\gamma \cdot u$ denotes multiplication of the vector u by the appropriate matrix γ. Thus if u(t) solves (3.11), so does $\gamma \cdot u(t)$. If only symmetric perturbations are considered, one obtains a different set of bifurcations of given codimension for each symmetry group. Additionally, the nature of the bifurcations is dependent on whether or not the trivial equilibrium at α_0 is maintained under perturbation. Customarily, the equilibrium at $u = 0$ remains an equilibrium for all values of parameters by imposition of the constraint that $F_\alpha(0) \equiv 0$ for all α. However, the general situation in which $u = 0$ is an equilibrium only at α_0 can also be treated and leads to a different bifurcation set.

3.3.2 Normal Forms and Generic Bifurcations of Vector Fields

The process of establishing the universal unfolding appropriate to a given degenerate form is greatly simplified by the use of smooth, near-identity non-linear co-ordinate changes to reduce the arbitrariness in the Taylor expansion of the vector field. The *normal form transformation* (Holmes [1981]) is a procedure for transforming co-ordinates near a degenerate equilibrium so that the Taylor series in the transformed system is particularly simple. The normal form of a vector field emphasizes those non-linear terms which control the interaction of the degenerate modes which undergo bifurcation. A feature of the normal form transformation is that it preserves the qualitative dynamics of the original vector field.

The idea of the normal form transformation is to simplify the degenerate system of ordinary differential equations

$$\dot{u} = F_0(u) \quad , \quad F_0(0) = 0 \tag{3.12}$$

by using successive polynomial changes of co-ordinates to set to zero as many terms as possible in the Taylor expansion of F_0 at degree k,

$$F_0(u) = Bu + \tilde{f}_k(u) + \mathcal{O}(|u|^{k+1}) \quad , \tag{3.13}$$

where B is the linear part of F_0, $\tilde{f}_k$ consists of terms of degree between 2 and k and $\mathcal{O}(|u|^{k+1})$ indicates terms of degree k+1 or higher. Here, B is assumed to be in real equivalent Jordan form.

A change of co-ordinates of the form

$$u = v + P_k(v) \tag{3.14}$$

is considered in which P_k denotes a homogeneous polynomial of degree k.

One can show (Guckenheimer & Holmes [1983]) that any *homogeneous* term of degree k in F_0 of the form

$$BP_k(v) - (DP_k)_v Bv \tag{3.15}$$

may be eliminated from (3.12) by a change of co-ordinates of the type (3.14). Moreover, the change of co-ordinates does not disturb terms of degree < k.

Since the terms of degree > k impose no constraint, the process of putting a system of ordinary differential equations in normal form is a recursive one. The necessary co-ordinate change is effected by the transformation, $\Phi : \mathbb{R}^p \to \mathbb{R}^p$, and is constructed iteratively:

$$\Phi(v) = v + P_2(v) + P_3(v) + \ldots + P_k(v) \tag{3.16}$$

where $P_2(v)$ is chosen to eliminate as many quadratic terms in F_0 as possible (possibly at the expense of modifying the remaining terms and adding terms of orders three and higher), $P_3(v)$ as many of the cubic terms as possible, and so forth. The terms that cannot be removed are determined by the nature of the linear operator B.

These observations may be abstracted as follows. If $\mathcal{P}_k$ is the space of homogeneous polynomials of degree k on $\mathbb{R}^p$, then L_B^k, defined by

$$L_B^k(P_k(v)) = BP_k(v) - (DP_k)_v Bv \quad , \tag{3.17}$$

is a linear map $\mathcal{P}_k \to \mathcal{P}_k$. Thus the terms in the Taylor expansion of F_0 that can be eliminated by the aforementioned process are precisely those in the subspace $L_B^k(\mathcal{P}_k) \subset \mathcal{P}_k$. This generalization is embodied in the following theorem (Guckenheimer & Holmes [1983]).

(Poincare-Birkhoff) Normal Form Theorem: If $B = (DF_0)_0$ and for each k the complementary subspace $\mathcal{G}_k \subset \mathcal{P}_k$, is defined such that $\mathcal{P}_k = \mathcal{G}_k \oplus \text{Range } L_B^k$, then there exists a polynomial change of co-ordinates of degree k such that in the new co-ordinates the system $\dot{u} = F_0(u)$ has the form

$$\dot{v} = Bv + \tilde{g}_k(v) + \mathcal{O}(|v|^{k+1}) \tag{3.18}$$

where $\tilde{g}_k(v) = \sum_{j=2}^{k} g_j(v)$ and $g_j \in \mathcal{G}_j$. Moreover, the dynamics of the truncated normal form $\dot{v} = Bv + \tilde{g}_k(v)$ are (locally) *topologically equivalent*[3] to the dynamics of the truncated system $\dot{u} = Bu + \tilde{f}_k(u)$; that is, minimally, information about the existence and stability properties of fixed points, closed orbits and limit sets is preserved.

[3] Two systems are topologically equivalent if there is a homeomorphism (that is, a continuous change of co-ordinates) mapping trajectories of one system onto those of the other. A system is qualitatively stable if all allowable C^1 perturbations of the system are topologically equivalent to one another.

For systems possessing simple symmetries, Γ, (in addition to the 'internal' symmetries of the normal forms themselves), the computation of the normal forms is performed within the class of vector fields equivariant with respect to Γ by restricting L_B^k to act on the subspaces of the $\mathcal{P}_k$ which are Γ-equivariant.

A basic strategy for the construction of the universal unfolding associated with the vector field (3.11) is to first transform a finite degree truncation of the Taylor expansion of the degenerate vector field F_0 to normal form and then to compute the transversal family containing the truncated normal form. The normal form is unfolded by adding small linear and non-linear terms describing the effects of varying α away from α_0. If the original vector field is equivariant with respect to some symmetry group, then both the normal form transformation and transversal unfolding are computed within the appropriate class of equivariant vector fields. Analysis of the dynamics of the resulting transversal family yields the desired bifurcation information. If the structural properties of the solutions obtained are insensitive to perturbations (including the addition of higher-order terms in the Taylor series) then the analysis is considered complete. The *universal unfolding* of F_0 is the transversal family G_μ^k of dimension equal to the codimension of F_0 which is stable to perturbations. This family will contain all the (local) qualitative dynamical features that exist in perturbations of F_0; that is, the perturbed vector field F_α is locally topologically equivalent to $G_{\mu(\alpha)}^k$ in the neighbourhood of α_0.

3.4 IDENTIFICATION OF AEROELASTIC BEHAVIOUR : A RÉSUMÉ

The aeroelastic initial-value problem is presumed to be defined by a notional parameterized functional differential equation of the form

$$\dot{x}(t) = f(x_t, \alpha) \qquad t > 0 \qquad (3.19a)$$

subject to $$x_0 = \varphi \in D \subset X \quad , \qquad (3.19b)$$

where $x(t) \in \mathbb{R}^n$ denotes the structural state, $x_t \in X$ denotes the structural state-history with X the phase space and $\alpha \in \mathbb{R}^m$ denotes the physical parameter set.

Under quite general hypotheses on f, the phase space X may be represented as the direct sum decomposition $X = P_0 \oplus Q_0$ where P_0 is the subspace spanned by the initial eigenhistories corresponding to the critical eigenvalues of the linearized aeroelastic operator at bifurcation ($\alpha = \alpha_0$) and Q_0 is the complement of P_0 in X. In the neighbourhood of bifurcation, the *Centre-Manifold Theorem* defines the precise nature of the equivalence between the asymptotic behaviour of the structural state-history x_t in the phase space X and the behaviour of the projection of x_t onto the eigenspace P_0. The assumed finite-dimensionality of the eigenspace P_0 implies that the qualitative characteristics of the projected state-history are described by a finite-dimensional set of ordinary differential equations of the form $\dot{u} = F_\alpha(u)$ where F_α may be interpreted as the composite function appearing in equation (3.10). The special fading memory properties assigned to the phase space X ensure that the

asymptotic behaviour of $x(t)$ in $\mathbb{R}^n$ follows, in a natural way, the behaviour of x_t in X. Consequently, the qualitative bifurcational characteristics (as observed in $\mathbb{R}^n$) of non-linear hereditary aeroelastic systems possessing the requisite fading memory properties may be inferred from an equivalent finite-dimensional set of ordinary differential equations.

Formal reduction of the aeroelastic initial-value problem to an equivalent equation set, $\dot{u} = F_\alpha(u)$, is generally not feasible. Nevertheless, one can postulate a qualitatively equivalent hypothetical degenerate form of a finite-degree truncation of the reduced equation set, $\dot{v} = G_0^k(v) \sim \dot{u} = F_0^k(u)$. The form of the postulated model derives from an examination of the symmetry properties of the aeroelastic system and from assertions on the spectral characteristics of the linearized equations of motion in the physical parameter range of interest. Equivalence between the degenerate form of the physical reduced equation set and the postulated degenerate form is established via a notional normal form transformation. Subject to the fundamental behavioural assumption that the physical reduced equation set is qualitatively stable, one can attempt to deduce the persistent qualitative characteristics of the aeroelastic system from the qualitatively distinct perturbations of the universal unfolding of the postulated degenerate form, $\dot{v} = G_\mu^k(v)$, via the notional equivalence $\dot{v} = G_{\mu(\alpha)}^k(v) \sim \dot{u} = F_\alpha(u)$. The precise topological class of the normal form corresponding to the unfolding of the postulated degenerate form is identified from observations of the aeroelastic response. Figure 3.4 summarizes the relationships between the various equation sets.

3.5 SUMMARY

Hereditary dynamical systems possessing appropriate fading memory properties exhibit a strong two-time-scale structure in the vicinity of bifurcation. Locally, the phase space is characterized by a stable manifold and a centre-manifold to which solution curves are locally attracted. In the neighbourhood of bifurcation, the qualitative characteristics of the system response are determined by a finite-dimensional set of ordinary differential equations, describing the dynamic on the centre-manifold. The dimension of the reduced model is determined by the order of the linear degeneracy at bifurcation. Formal reduction to an equivalent low-dimensional system is generally not possible without explicit representation of the governing evolution equation. In the absence of such information, the qualitative characteristics of the initial-value problem are identified with the generic bifurcations of vector fields and their associated normal forms. This association forms the basis of a qualitative model identification strategy for a general class of hereditary aeroelastic systems.

CHAPTER FOUR

A PROTOTYPE FOR DIVERGENCE/FLUTTER INTERACTION

4.1 INTRODUCTION

Bifurcations which accompany loss of stability of equilibrium solutions of systems of non-linear evolution equations $\dot{u} = F_\alpha(u)$ as a single control parameter passes quasi-statically through critical values are, generically, of two elementary types. These are the *steady-state* bifurcations, associated with a zero eigenvalue of the linearized operator $DF_\alpha(u)$ crossing the imaginary axis, and the *Hopf* bifurcation of time-periodic solutions, originating from a pair of (complex conjugate) imaginary eigenvalues of $DF_\alpha(u)$. By introducing an additional auxiliary parameter, the two elementary bifurcations can be made coincident, thereby forming a coupled Hopf and steady-state bifurcation. In the neighbourhood of the coincident bifurcation point, zero and imaginary eigenvalues of $DF_\alpha(u)$ occur for two different sets of parameter values. At these parameter values, elementary steady-state and Hopf bifurcations can be expected. However, at other parameter values, more complex bifurcational phenomena can occur as a result of non-linear interactions between stationary and periodic modes (Langford [1983]).

The nature of both the elementary and interacting bifurcations is strongly influenced by the presence of symmetry. If the system possesses a reflectional symmetry, then the generic steady-state

bifurcation is the so-called *pitchfork* bifurcation. A complete classification of the steady-state and periodic bifurcations associated with the *pitchfork/Hopf* degeneracy is presented by Langford & Iooss [1980]. This chapter summarizes the development of the classification and the principal solution types identified.

4.2 ELEMENTARY BIFURCATIONS OF EQUILIBRIA

The features of two classical bifurcations are described. The first of these bifurcations - the pitchfork bifurcation - involves one-dimensional dynamics and changes only in the steady-state. In contrast, the Hopf bifurcation gives rise to a periodic orbit with essentially two-dimensional dynamics.

4.2.1 Steady-State Bifurcations

If the vector field, F_α, is constrained to satisfy the symmetry condition $F_\alpha(Su) = SF_\alpha(u)$, where S is a linear operator such that $S^2 = I$, $S \neq I$, then the generic one-parameter steady-state bifurcation (the so-called pitchfork bifurcation) is characterized by two smooth solution branches, one of which is trivial. The non-trivial branch possesses a reflectional symmetry about the trivial equilibrium branch. The generic bifurcation diagram for the pitchfork bifurcation is shown, schematically, in Figure 4.1a. Here, the abscissa is the bifurcation parameter and the ordinate is some real functional of the solution u.

4.2.2 Periodic Bifurcations

The simplest type of bifurcation in which a unique periodic orbit is born from an isolated steady-state is the Hopf bifurcation (Marsden & McCracken [1976]). A family of periodic orbits (limit cycles) emerges from an equilibrium as the eigenvalues associated with the Jacobian of $F_\alpha(u)$ at the equilibrium cross the imaginary axis transversely at the critical parameter value. At the bifurcation point, the surface of periodic orbits is tangent to the the critical parameter surface $\alpha = \alpha_0$. The bifurcation diagram is illustrated in Figure 4.1b with the ordinate the periodic amplitude.

4.3 STEADY-STATE AND PERIODIC MODE INTERACTIONS

In the vicinity of a *coincident* critical point at which a simple zero eigenvalue and a pair of pure imaginary eigenvalues of the Jacobian $DF_\alpha(u)$ occur simultaneously under the influence of two parameters, the bifurcating equilibrium solutions and limit cycles can interact non-linearly to generate secondary (and tertiary) bifurcation phenomena. The nature of the generic steady-state and periodic interactions corresponding to a coincident Hopf and pitchfork bifurcation is inferred from the *normal form* of the degeneracy and its associated *universal unfolding*. In this section, a brief account of the construction of the pitchfork/Hopf normal form is presented, in conjunction with an analysis of the persistent steady-state and periodic solution behaviour. The various solution types are identified and classified accordingly.

4.3.1 Interacting Bifurcations with Symmetry

To characterize the persistent steady-state and periodic behaviour of a system of non-linear evolution equations as two independent parameters are varied in the vicinity of a coincident pitchfork/Hopf bifurcation point, it is sufficient (Shearer [1981]) to consider the three-dimensional system of ordinary differential equations

$$\dot{u} = F_\alpha(u) \tag{4.1}$$

where $u \in \mathbb{R}^3$ and $\alpha \in \mathbb{R}^2$. Here, F_α is a smooth vector field which depends smoothly on the parameters and satisfies

$$\text{(a)} \qquad F_\alpha(Su) = SF_\alpha(u) \quad , \quad S = -I$$

$$\text{(b)} \qquad F_\alpha(0) \equiv 0$$

$$\text{(c)} \qquad DF_0(0) = \begin{bmatrix} 0 & 0 & 0 \\ 0 & 0 & -\omega \\ 0 & \omega & 0 \end{bmatrix} \tag{4.2}$$

In effect, it is assumed that $u = 0$ is an equilibrium for all α and that the Jacobian $DF_0(0)$ has simple eigenvalues $0, \pm i\omega$, $\omega > 0$. The eigenvalues and corresponding eigenvectors of $DF_0(0)$ are assumed to possess smooth extensions for α near 0 such that if $\gamma(\alpha)$ and $\sigma(\alpha) = \zeta(\alpha) \pm i\nu(\alpha)$ are appropriate eigenvalues of $DF_\alpha(0)$ with $\gamma(0) = 0$ and $\sigma(0) = \pm i\omega$, then $\left|\partial(\gamma,\zeta)/\partial(\alpha_1,\alpha_2)\right| \neq 0$ at $\alpha = 0$ which represents a generalization of Hopf's *transversality* condition guaranteeing that the neutral stability curves $\gamma(\alpha) = 0$ and $\zeta(\alpha) = 0$ are not tangential at $\alpha = 0$ (Langford [1979]).

By a series of symmetry preserving non-linear co-ordinate transformations on the power series representation of F_0 in terms of u, it can be shown (Langford & Iooss [1980], Holmes [1980]) that the local dynamics of the degenerate system $\dot{u} = F_0(u)$ is qualitatively equivalent (in the sense that, minimally, branches of steady-state and periodic bifurcations are preserved) to the dynamics of the truncated system

$$\frac{d\hat{x}}{dt} = a(\hat{x}^2, \hat{y}^2 + \hat{z}^2)\hat{x} \tag{4.3a}$$

$$\frac{d\hat{y}}{dt} = b(\hat{x}^2, \hat{y}^2 + \hat{z}^2)\hat{y} - c(\hat{x}^2, \hat{y}^2 + \hat{z}^2)\hat{z}$$

$$\frac{d\hat{z}}{dt} = b(\hat{x}^2, \hat{y}^2 + \hat{z}^2)\hat{z} + c(\hat{x}^2, \hat{y}^2 + \hat{z}^2)\hat{y}$$

where $\hat{x}$ is the co-ordinate in the one-dimensional eigenspace of $DF_0(0)$ corresponding to 0 and $(\hat{y},\hat{z})$ are co-ordinates in the two-dimensional eigenspace corresponding to $\pm i\omega$. By (4.2c), the finite degree polynomials a, b, c satisfy

$$a(0,0) = b(0,0) = 0 \text{ and } c(0,0) = \omega \ . \tag{4.3b}$$

The normal form (4.3) may be written in cylindrical co-ordinates $(\hat{x},\hat{r},\hat{\theta})$ where $\hat{y} + i\hat{z} = \hat{r}e^{i\hat{\theta}}$. Formal expansion of (4.3) then yields

$$\begin{aligned}
\frac{d\hat{x}}{dt} &= (a_1\hat{x}^2 + a_2\hat{r}^2)\hat{x} + \mathcal{O}(|\hat{x},\hat{r}|^5) \\
\frac{d\hat{r}}{dt} &= (b_1\hat{x}^2 + b_2\hat{r}^2)\hat{r} + \mathcal{O}(|\hat{x},\hat{r}|^5) \\
\frac{d\hat{\theta}}{dt} &= \omega + c_1\hat{x}^2 + c_2\hat{r}^2 + \mathcal{O}(|\hat{x},\hat{r}|^4) \ .
\end{aligned} \tag{4.4}$$

The assumption that F_0 is odd introduces an implicit rotational, or phase-shift, symmetry in the $(\hat{r},\hat{\theta})$ co-ordinates of the truncated normal form. This symmetry mimics the natural phase-shift symmetry inherent in the assumed periodicity of the solutions. The form (4.4) therefore, automatically, accounts for enforced reflectional symmetry and assumed phase-shift symmetry.

4.3.2 Persistent Steady-State and Periodic Bifurcations

Examination of (4.4) reveals that the azimuthal component can be decoupled to yield the planar system

$$\begin{aligned} \frac{d\hat{x}}{dt} &= (a_1\hat{x}^2 + a_2\hat{r}^2)\hat{x} + O(|\hat{x},\hat{r}|^5) \\ \frac{d\hat{r}}{dt} &= (b_1\hat{x}^2 + b_2\hat{r}^2)\hat{r} + O(|\hat{x},\hat{r}|^5) \end{aligned} \tag{4.5}$$

describing, respectively, the steady-state and periodic amplitudes.

Re-scaling (4.5) by the linear transformation $x = \hat{x}|a_1|^{1/2}$, $r = \hat{r}|b_2|^{1/2}$ and requiring that a_1 and $b_2 \neq 0$ gives to third-order

$$\begin{aligned} \frac{dx}{dt} &= (\pm x^2 + mr^2)x \\ \frac{dr}{dt} &= (nx^2 \pm r^2)r \end{aligned} \tag{4.6}$$

where $m = a_2/a_1$ and $n = b_1/b_2$.

To unfold the degenerate two-dimensional field (4.6) under the constraints of symmetry and preservation of a fixed point at the origin, it is sufficient to add a (transversal) linear perturbation of the form $\begin{bmatrix} \pm\lambda x \\ \pm\mu r \end{bmatrix}$. The perturbed system is of the general form

$$\frac{dx}{dt} = x(\varepsilon_1 x^2 + mxr^2 + \varepsilon_2\lambda) \qquad (4.7)$$

$$\frac{dr}{dt} = r(\varepsilon_3 r^2 + nx^2 r + \varepsilon_4\mu)$$

where $\varepsilon_1 = \pm 1$.

The system (4.7) is a universal unfolding of (4.6) provided m and n satisfy the non-degeneracy conditions[1]

$$m \neq \varepsilon_3\varepsilon_2\varepsilon_4 \quad , \quad n \neq \varepsilon_1\varepsilon_2\varepsilon_4 \quad , \quad mn \neq \varepsilon_1\varepsilon_3 \quad ; \qquad (4.8)$$

that is, up to qualitative (topological) equivalence, (4.7) subject to the non-degeneracy conditions (4.8) contains all perturbations (equivalence classes) of (4.7). Minimally, topological equivalence preserves information about the existence and stability of fixed points, closed orbits and limit sets. Consequently, branches of steady-state and periodic solutions are preserved along with linearized stability information along branches. One can show (Langford & Iooss [1980]) that a precise correspondence exists

[1] The non-degeneracy conditions (4.8) ensure that, to all orders, the coefficients in the expressions for non-trivial stationary mixed-mode solutions of (4.7) do not vanish. The qualitative characteristics of (4.7) therefore persist under perturbation.

between small-amplitude steady-state and periodic solutions of the system (4.1) (where the periodic solutions have period near $2\pi/\omega$) and stationary solutions of the planar system of equations (4.7) in which $r = 0$ and $r \neq 0$ equilibria of the planar system translate to steady-state and periodic solutions of the original system.

4.3.3 Perturbed Bifurcation Diagrams

Stationary solutions of (4.7) correspond to zeros of the system

$$G(x,r,m,n,\lambda,\mu) = \begin{bmatrix} \varepsilon_1 x^3 + mxr^2 + \varepsilon_2 \lambda x \\ \varepsilon_3 r^3 + nx^2 r + \varepsilon_4 \mu r \end{bmatrix} \quad . \qquad (4.9)$$

The problem of determining the persistent steady-state and periodic behaviour of (4.1) is therefore reduced to enumerating the qualitatively distinct perturbations of $G(x,r,m,n,\lambda,\mu)$.

The perturbed bifurcation diagrams associated with the universal unfolding (4.9), which describe the persistent steady-state and periodic behaviour for the two-parameter pitchfork/Hopf problem, are defined, for non-degenerate m and n, by the set

$$\{(x,r,\lambda):\ G(x,r,m,n,\lambda,\lambda-\sigma) = 0,\ \sigma \neq 0\} \quad . \qquad (4.10)$$

Here, the parameter λ is regarded as a bifurcation parameter and the parameter σ as an imperfection parameter which, for $\sigma \neq 0$, divides the degenerate bifurcation point into two.

In most applications, the trivial solution of (4.9) is initially stable but loses stability as the bifurcation parameter increases. To reflect this observation, and to fix the orientation of the bifurcation diagrams, the convention $\varepsilon_2 = \varepsilon_4 = 1$ is adopted. A complete classification of the bifurcation diagrams for this case is described in Langford & Iooss [1980]. The present account is restricted to a summary of the solution types identified by Langford & Iooss.

The trivial solution of (4.9) is

$$x = 0 \quad , \quad r = 0 \qquad . \tag{4.11}$$

The stability of the trivial solution is determined by the signs of the real parts of the eigenvalues of the Jacobian matrix

$$DG(x,r) = \begin{bmatrix} 3\varepsilon_1 x^2 + mr^2 + \varepsilon_2\lambda & 2mxr \\ 2nxr & 3\varepsilon_3 r^2 + nx^2 + \varepsilon_4(\lambda-\sigma) \end{bmatrix} \tag{4.12}$$

evaluated at $x = 0$, $r = 0$. With $\varepsilon_2 = \varepsilon_4 = 1$, the *x-mode* and *r-mode* stability assignments of the trivial solution are indicated by $\mathrm{sgn}(\lambda)$ and $\mathrm{sgn}(\lambda-\sigma)$, respectively. Changes in stability associated with variations in the parameters λ and σ are accompanied by local codimension-one bifurcations of solutions at points of linear degeneracy. Two primary solution branches are associated with zero eigenvalues of the Jacobian DG(0,0). These branches bifurcate from the trivial solution when $\det(DG(0,0)) = 0$ and are identified with x-mode and r-mode instabilities of the trivial solution.

The x-mode or *pitchfork* branch defined by the equilibrium condition

$$\varepsilon_1 x^2 + \lambda = 0 \quad , \quad r = 0 \tag{4.13}$$

bifurcates from the trivial solution at $\lambda = 0$ and is super(sub)-critical if $\varepsilon_1 < 0$ (> 0).

The r-mode branch defined by the equilibrium condition

$$x = 0 \quad , \quad \varepsilon_3 r^2 + (\lambda - \sigma) = 0 \tag{4.14}$$

bifurcates from the trivial solution at $\lambda = \sigma$ and is super(sub)-critical if $\varepsilon_3 < 0$ (> 0). The r-mode branch corresponds to the Hopf branch for the original three-dimensional system.

The stability assignment of the primary x-mode branch is determined by the eigenvalues of DG(x,r) evaluated along the non-trivial solution branch defined by (4.13). In this case,

$$DG(x,0) = \begin{bmatrix} 2\varepsilon_1 x^2 & 0 \\ 0 & nx^2 + (\lambda - \sigma) \end{bmatrix} \tag{4.15}$$

where $\varepsilon_1 x^2 + \lambda = 0$. Since $\lambda = -\varepsilon_1 x^2$ along the primary x-mode branch, a change in stability assignment is possible if $(n-\varepsilon_1)$ and σ are of the same sign[2]. Secondary bifurcation from the primary x-mode branch then occurs at the degenerate point defined by $\det(DG(x,0)) = 0$

[2]The coefficients ε_1 and ε_3 are assumed to be of fixed sign. Hence, bifurcations of the primary x- and r-mode branches can occur only as a result of sign changes of the eigenvalues $nx^2+(\lambda-\sigma)$ and $mr^2+\lambda$.

which is associated with the zero eigenvalue condition

$$nx^2 + (\lambda-\sigma) = 0 \quad , \quad \varepsilon_1 x^2 + \lambda = 0 \quad . \qquad (4.16)$$

In the (λ,σ) parameter plane, secondary bifurcation from the x-mode branch occurs along the line

$$\lambda = \lambda_x(\sigma) = -\varepsilon_1\sigma/(n-\varepsilon_1) \quad , \quad \sigma(n-\varepsilon_1) > 0 \quad . \qquad (4.17)$$

The secondary solution branch is defined by the non-trivial equilibrium condition

$$\varepsilon_1 x^2 + mr^2 + \lambda = 0 \quad , \quad \varepsilon_3 r^2 + nx^2 + (\lambda-\sigma) = 0 \quad . \qquad (4.18)$$

Since DG(x,0) is diagonal, secondary bifurcation from the primary x-mode branch is initially in the r-mode direction.

Solving for x^2 in the second of (4.18) and substituting in the first of (4.18) yields

$$(mn-\varepsilon_1\varepsilon_3)r_s^2 + (n-\varepsilon_1)\lambda + \varepsilon_1\sigma = 0 \quad . \qquad (4.19)$$

Comparison of (4.19) with (4.17) reveals that

$$r_s^2 = -(\lambda-\lambda_x)(n-\varepsilon_1)/(mn-\varepsilon_1\varepsilon_3) \qquad (4.20)$$

and, hence, the secondary bifurcation from the primary x-mode branch is super(sub)-critical if $(n-\varepsilon_1)/(mn-\varepsilon_1\varepsilon_3) < 0$ (> 0).

In a similar manner, the stability assignment of the primary r-mode branch is determined by the eigenvalues of

$$DG(0,r) = \begin{bmatrix} mr^2 + \lambda & 0 \\ 0 & 2\varepsilon_3 r^2 \end{bmatrix} \qquad (4.21)$$

where $\varepsilon_3 r^2 + (\lambda-\sigma) = 0$. Secondary bifurcation from the primary r-mode branch is possible if $(m-\varepsilon_3)$ and σ are of opposite sign in which case the linear degeneracy condition $\det(DG(0,r)) = 0$ is

$$mr^2 + \lambda = 0 \quad , \quad \varepsilon_3 r^2 + (\lambda-\sigma) = 0 \qquad (4.22)$$

and bifurcation occurs along the line

$$\lambda = \lambda_r(\sigma) = m\sigma/(m-\varepsilon_3) \quad , \quad \sigma(m-\varepsilon_3) < 0 \quad . \qquad (4.23)$$

In this case, secondary bifurcation from the primary r-mode branch occurs initially in the x-mode direction. Solving for the first of (4.18) and substituting in the second of (4.18) yields

$$(mn-\varepsilon_1\varepsilon_3)x_s^2 + (m-\varepsilon_3)\lambda - m\sigma = 0 \quad . \qquad (4.24)$$

Comparison of (4.24) with (4.23) shows that

$$x_s^2 = -(\lambda-\lambda_r)(m-\varepsilon_3)/(mn-\varepsilon_1\varepsilon_3) \qquad (4.25)$$

and, hence, the secondary bifurcation from the primary r-mode branch is super(sub)-critical if $(m-\varepsilon_3)/(mn-\varepsilon_1\varepsilon_3) < 0$ (> 0).

The resulting secondary solution branches are given by

$$x_s^2 = -(\lambda-\lambda_r)(m-\varepsilon_3)/(mn-\varepsilon_1\varepsilon_3)$$

$$r_s^2 = -(\lambda-\lambda_x)(n-\varepsilon_1)/(mn-\varepsilon_1\varepsilon_3) \quad . \tag{4.26}$$

Following Langford & Iooss [1980], one can show that these secondary branches exist in the sector of the (λ,σ) plane bounded by the lines defined by (4.17) and (4.23), subtending an angle less than π but non-zero. If $(n-\varepsilon_1)(m-\varepsilon_3) < 0$, this sector lies entirely inside the half-plane defined by $\sigma(n-\varepsilon_1) > 0$, so both secondary bifurcations occur for the same sign of σ, and there exist no secondary bifurcations for σ of the opposite sign. In the bifurcation diagrams, the secondary branches form a closed loop, with λ in the interval having the endpoints λ_x and λ_r. If $(n-\varepsilon_1)(m-\varepsilon_3) > 0$, then this sector contains one half of the λ-axis, the two bifurcations occur for opposite signs of σ, and the two secondary branches exist for λ in intervals extending in the same direction from λ_x and λ_r.

Tertiary bifurcations from the secondary branches, involving only stationary solutions of (4.7), are not possible since det(DG(x,r)) is non-zero everywhere on the secondary branches. However, the possibility of *time-dependent* behaviour for x and r arises. By a classical theorem of Hopf (Marsden & McCracken [1976]), the system (4.7) has a bifurcation of a family of periodic solutions from a stationary solution if the Jacobian matrix evaluated at the stationary solution has a pair of simple complex eigenvalues crossing the imaginary axis, with real part having non-zero

derivative with respect to λ. One can show that these conditions are never satisfied on the trivial or primary branches of solutions of (4.9), but can be satisfied on the secondary branches. In this case, the Jacobian has pure imaginary eigenvalues if

$$\det(DG(x_s,r_s)) > 0 \quad \text{and} \quad \mathrm{tr}(DG(x_s,r_s)) = 0 \quad . \qquad (4.27)$$

It is easily verified that

$$DG(x_s,r_s) = \begin{bmatrix} 2\varepsilon_1 x_s^2 & 2mx_s r_s \\ 2nx_s r_s & 2\varepsilon_3 r_s^2 \end{bmatrix} \qquad (4.28)$$

and with $x_s^2 > 0$, $r_s^2 > 0$, the conditions (4.27) are satisfied only if

$$(mn-\varepsilon_1\varepsilon_3) < 0 \quad \text{and} \quad \varepsilon_1\varepsilon_3 < 0 \quad . \qquad (4.29)$$

Assuming (4.29), (4.26) and (4.27) define a unique line in the $(\lambda.\sigma)$ plane which lies inside the previously described sector in which x_s and r_s exist. Provided the Hopf transversality condition is satisfied, a bifurcation of periodic solutions of (4.7) from the secondary branch occurs along this line. Periodic solutions of (4.7) correspond to doubly periodic solutions of the original three-dimensional problem. In fact, the crossing condition for the eigenvalues of the planar problem implies a corresponding crossing of the Floquet exponents for the corresponding periodic solution of the three-dimensional problem (Langford & Iooss [1980]). This implies a bifurcation from the periodic orbit to an invariant torus, provided additional non-degeneracy conditions are satisfied.

From the above description of the various solution types, four broad classes of bifurcation diagrams can be identified according to whether the two primary bifurcations are supercritical or subcritical. Each of these classes may be further subclassified according to the signs of $(n-\varepsilon_1)$, $(m-\varepsilon_3)$, $(mn-\varepsilon_1\varepsilon_3)$ and σ. The diagrams are symmetric under reflections in x and in r. Branches which correspond under reflections in r represent the same periodic solutions but reflections in x represent distinct solutions in general.

The four classes are :

Class I : $\varepsilon_1 < 0$, $\varepsilon_3 < 0$. Both primary bifurcations are supercritical. There are no tertiary bifurcations.

Class II : $\varepsilon_1 < 0$, $\varepsilon_3 > 0$. The x-mode bifurcation is supercritical and the r-mode bifurcation is subcritical. Tertiary bifurcation is possible.

Class III : $\varepsilon_1 > 0$, $\varepsilon_3 < 0$. The x-mode bifurcation is subcritical and the r-mode bifurcation is supercritical. The bifurcation diagrams are permutations of those for Class II, with the roles of the x-mode and r-mode bifurcations reversed.

Class IV : $\varepsilon_1 > 0$, $\varepsilon_3 > 0$. Both primary bifurcations are subcritical. The bifurcation diagrams map onto those of Class I after reflections and sign reversals. Again, there are no tertiary bifurcations.

4.4 SUMMARY

Under the action of an auxiliary parameter, the generic one-parameter steady-state and periodic bifurcations of a system of non-linear evolution equations can be made coincident, thereby forming a coupled steady-state and periodic bifurcation. The pitchfork/Hopf bifurcation describes the interaction of steady-state and periodic modes in the presence of reflectional symmetry in the steady-state mode. Enumeration of the persistent steady-state and periodic bifurcations is facilitated by successive non-linear co-ordinate transformations of the vector field containing the appropriate degenerate linearization to eliminate non-essential terms in its Taylor series expansion. Generic two-parameter unfoldings of the resulting normal form yield the qualitatively distinct solution sets corresponding to the degeneracy. For the case most commonly encountered in applications, four main solution classes are identified, two of which exhibit tertiary bifurcation to tori.

CHAPTER FIVE

MODE INTERACTION PHENOMENA IN TRANSONIC FLOW

5.1 INTRODUCTION

Preliminary computational studies of the effects of coupling between the full unsteady Euler aerodynamics in the transonic regime and a simple linear structure (Kousen [1989] and Bendiksen [1989]) have revealed hitherto unanticipated results involving the non-linear interaction between divergence and flutter. The observed aeroelastic phenomena differ substantially from the linear notions of divergence and flutter. Interpretation of the observed behaviour is made difficult, primarily as a consequence of the aerodynamic origins of the non-linearities and by the fact that most of the interesting behaviour is observed under variation of aerodynamic parameters, the action of which is not easily discernible. The complexity of the coupled aerodynamic and structural equations of motion and the limitations of conventional *quantitative* model simplification techniques applied to the transonic aeroelastic problem motivate an attempt to interpret the observed aeroelastic behaviour cited by Kousen and Bendiksen in a *geometrical*, or *topological*, sense. The present chapter describes an application of the qualitative dynamical systems concepts established in Chapters Two and Three. Based on a notional functional description of the unsteady aerodynamic force response and partial bifurcational information derived from published time-histories of the structural response, a

reduced model is identified which captures the local bifurcational behaviour of the transonic aeroelastic system investigated by Bendiksen and Kousen. The reduced model is then used to study the qualitative effects of parameter variations on the system response in an attempt to understand the underlying topological mechanisms responsible for some of the more unusual aeroelastic behaviour observed in numerical simulations.

5.2 OBSERVATIONS OF NON-LINEAR FLUTTER AND DIVERGENCE

The archetypal aeroelastic problem is the typical section aerofoil in two-dimensional flow. The utility of the typical section model in capturing the fundamental features of bending-torsion flutter is well established (see, for example, Bisplinghoff *et al* [1955]). The simple structural model contains two degrees-of-freedom : the plunge displacement of the elastic axis[1] measured from the undeformed position, positive downwards, and the angle of incidence between the aerofoil chord and the incoming uniform freestream (the pitch), measured positive nose-up. Plunging and pitching stiffnesses are modelled by a linear spring element and a torsional spring element, respectively. Relevant structural parameters are the elastic axis location, the centre of mass position, the mass of the aerofoil, the radius of gyration about the elastic axis, the ratio of the uncoupled natural frequency in plunge to that in pitch and the

[1] The point on the aerofoil where a pure load at this point will result in plunging with no pitching, and a pure moment will result in pitching with no plunging, is referred to as the 'elastic axis'.

reduced velocity - a coupling parameter between the structural model and the uniform freestream in which it is immersed. The typical section model is illustrated in Figure 5.1.

Figures 5.2 and 5.3 derive from numerical simulations (Bendiksen [1989]), Kousen [1989]) based on simultaneous time-marching solutions of the unsteady Euler equations and the equations of motion for a structurally linear symmetric (NACA 64A006) typical section aerofoil. The time histories shown relate to the response in pitch and plunge degrees of freedom following initial perturbation of the aerofoil from the zero equilibrium position[2]. The asymptotic and transient aeroelastic behaviour depicted is representative of the non-linear phenomena observed in these simulations for a range of Mach numbers, M, and reduced velocities, $\bar{U}$, in the transonic regime. Three broad categories of solution characterize the asymptotic aeroelastic behaviour; namely, steady-state, periodic and coupled steady-state and periodic. Under variation of the control parameters M and $\bar{U}$, the aeroelastic response exhibits transitions from one solution type to another. Numerical experiments demonstrating the persistence of the observed behaviour under progressive refinement of the aerodynamic computational mesh (Kousen [1989]) suggest that the observed qualitative behaviour is credible. Similar behaviour is reported by van der Peet [1991] in an independent study of the same aeroelastic configuration based on a modified version of the unsteady transonic small-disturbance equations (ULTRAN-V).

[2]The free motion of the aerofoil is preceded by several cycles of a prescribed sinusoidal motion with amplitude 0.1 degrees.

5.2.1 Non-Linear Flutter

Flutter in the subsonic regime exhibits the classical exponential growth in response above the linear flutter speed and the characteristic exponential decay below the linear flutter speed. For a range of Mach numbers in the transonic regime, however, amplitude limited periodic behaviour, in the form of stable (symmetric) limit cycles, is evident. Limit cycle flutter is observed only in the transonic regime when shocks are present in the flow. The development of an inherently non-linear phase lag between the shock motion and the aerofoil pitch is believed to play an important rôle in the transition from exponential growth to limit cycle behaviour.

Typical time-histories in pitch and plunge corresponding to transonic Mach numbers are shown in Figure 5.2. The amplitude of the limit cycles and the rate of growth to a stationary cycle increases with increasing reduced velocity. This general trend is reported to occur for a range of transonic Mach numbers. The variation of limit cycle amplitude in pitch versus reduced velocity is illustrated in Figure 5.2b[3]. Typically, the limit cycle amplitude develops monotonically from zero after the linear flutter point is exceeded. In general, the linear flutter velocity increases with increasing Mach number while the limit cycle amplitudes tend to decrease with increasing Mach number. The plunge limit cycle amplitude is reported to follow similar trends (Kousen & Bendiksen [1988]).

[3]Physically, an increasing reduced velocity at constant Mach number represents either a decrease in the aerofoil chord or a decrease in the uncoupled natural frequency in pitch.

5.2.2 Non-Linear Divergence and Divergence/Flutter Interaction

At Mach number 0.85, the linear flutter point is ill-defined and the qualitative behaviour of the aeroelastic response is sensitive to changes in reduced velocity. Figure 5.3 illustrates the progressive change in behaviour as the reduced velocity is varied, quasi-statically, from a value of 1.80 to a value of 2.00. At $\bar{U} = 1.80$, the response exhibits a dynamic approach to a (stable) non-zero equilibrium (Figure 5.3a). Similar behaviour is reported at $\bar{U} = 1.75$ with a correspondingly smaller offset in both pitch and plunge. Since the aerofoil is symmetric, it is reasonable to assume that, for these values of reduced velocity, the zero equilibrium is surrounded by two reflectionally symmetric non-zero equilibria.

At $\bar{U} = 1.90$, the response is characterized by an initial divergence in both pitch and plunge, followed by an apparent secondary flutter instability (Figure 5.3b). While the pitch response appears to settle to a symmetric limit cycle about the zero equilibrium position, it is unclear from the time history of the plunge response whether or not the ultimate stationary behaviour in plunge is also symmetric about the zero equilibrium. Kousen and Bendiksen suggest that the observed behaviour in plunge at $\bar{U} = 2.00$ (Figure 5.3c) is representative of the asymptotic behaviour in plunge at $\bar{U} = 1.90$. At $\bar{U} = 2.00$, the initial divergence is regulated, and eventually suppressed, by the presence of a stable symmetric limit cycle. However, despite the general similarities in stationary behaviour, qualitative differences remain in the origins of the flutter instabilities in each case.

5.2.3 The Influence of Structural Asymmetry

Destroying the symmetry of the system by the imposition of a structural pre-twist reveals additional new and subtle aeroelastic phenomena. Figure 5.4 illustrates the progressive change in the qualitative nature of the aeroelastic response as the pre-twist angle, α_0, is varied over the range zero to five degrees for fixed values of Mach number and reduced velocity ($M = 0.85$, $\bar{U} = 1.85$). The response shown in Figure 5.4a, corresponding to $\alpha_0 = 2.0$ degrees, is basically as expected. The pitch response approaches a limit cycle centred around a non-zero, positive angle of attack near 2.0 degrees. The plunge motion also oscillates about a finite offset.

Slightly below a pre-twist angle of four degrees, however, the response displays significant higher harmonics. At $\alpha_0 = 4.0$ degrees, the response is characterized by the absence of any obvious periodicity (Figure 5.4b). Further increase in the pre-twist angle results in the behaviour shown in Figure 5.4c ($\alpha_0 = 4.75$ degrees). Here, some form of doubly periodic cycle is clearly present. At $\alpha_0 = 5.0$ degrees, the oscillatory motion decays into a stable negative offset as depicted in Figure 5.4d. Quite remarkably, at each of these *positive* angles of pre-twist, the asymptotic response in pitch contains a *negative* steady-state component. The steady-state component of the plunge degree-of-freedom also displays a tendency to change sign as the pre-twist angle is increased beyond 2.00 degrees. The nature of the aeroelastic response suggests the effects of structural pre-twist are inherently non-linear.

5.3 A GENERIC BIFURCATION MODEL FOR DIVERGENCE/FLUTTER INTERACTION

The sensitivity to variation in Mach number and reduced velocity which characterizes the (symmetric) non-linear divergence and flutter phenomena described in §5.2 suggests an analogy with the generic behaviour of systems of non-linear ordinary differential equations as two independent parameters are varied in the neighbourhood of a coupled *steady-state* and *periodic* bifurcation point. This bifurcation is defined by the condition that the linearized system at criticality possesses, simultaneously, a zero eigenvalue and pure imaginary pair of eigenvalues. That is, after an appropriate similarity transformation and re-arrangement to real equivalent form, the system contains the degenerate linearization

$$\begin{bmatrix} 0 & 0 & 0 \\ 0 & 0 & -\omega \\ 0 & \omega & 0 \end{bmatrix} \quad . \tag{5.1}$$

A class of candidate (two-parameter) bifurcation models which characterizes the persistent steady-state and periodic behaviour of such systems under the constraint of reflectional symmetry of the steady-state mode is defined by the universal unfolding of the *pitchfork/Hopf* degeneracy (*cf.* Chapter Four). The simplest form of this degeneracy, for which the neutral stability curves of the perturbed system are transversal at criticality and do not re-intersect in the vicinity of the coupled bifurcation point, is of codimension-two. Subject to the additional constraint of phase-shift symmetry, the steady-state and periodic characteristics of the nominally three-dimensional normal form corresponding to this

degeneracy may be represented by the planar system of equations

$$\dot{x} = x(\varepsilon_1 x^2 + mxr^2 + \varepsilon_2 \lambda) \qquad (5.2)$$

$$\dot{r} = r(\varepsilon_3 r^2 + nx^2 r + \varepsilon_4 \mu)$$

describing, respectively, the steady-state and periodic amplitudes.

Here, λ and μ are the perturbation, or unfolding, parameters, $\varepsilon_1 = \pm 1$ and the parameters m and n satisfy the non-degeneracy conditions

$$m \neq \varepsilon_3\varepsilon_2\varepsilon_4 \quad , \quad n \neq \varepsilon_1\varepsilon_2\varepsilon_4 \quad , \quad mn \neq \varepsilon_1\varepsilon_3 \quad . \qquad (5.3)$$

The implied spatial and temporal symmetries incorporated in this model are representative of the physical symmetries present in the aeroelastic system of §5.2. Both the reflectional symmetry and (apparent) phase-shift symmetry of the stationary aeroelastic response are assumed to be maintained under perturbation of Mach number and reduced velocity. The existence of a coincident divergence and flutter point in the physical system, implied by the analogy with the coupled steady-state and Hopf bifurcation, defines a *bifurcation centre* $(\bar{U}_0, M_0)$ in physical parameter space. The underlying structure of the transitions observed in the aeroelastic response, as Mach number and reduced velocity are varied, quasi-statically, in the vicinity of the bifurcation centre, is assumed to be characterized by one of the qualitatively distinct stationary solution sets from within the class defined by the family of models (5.2).

5.3.1 Model Identification

The selection, from the family of candidate models (5.2), of an appropriate bifurcation model for the aeroelastic system of §5.2 is guided by the partial bifurcational information summarized in Figures 5.2 and 5.3. Certain qualitative features of the stationary aeroelastic response are immediately discernible from these figures. Reference to Figures 5.2 and 5.3 indicates that, at least locally, the trivial equilibrium is stable subcritically and that stable pure divergence solutions co-exist with stable supercritical flutter solutions in the vicinity of the bifurcation point $(\bar{U}_0, M_0)$ - an arrangement which persists only for *supercritical* pure divergence solutions (Langford & Iooss [1980]). Consequently, it is only necessary to consider as candidate models those cases of (5.2) for which the trivial solution of the unperturbed system is stable subcritically, and for which the pure mode solutions bifurcate supercritically. An analysis of (5.2) shows that these conditions prevail when $\varepsilon_1 = \varepsilon_3 = -1$ and $\varepsilon_2 = \varepsilon_4 = 1$. This case has been considered in detail by Golubitsky & Schaeffer [1985].

The non-degeneracy conditions (5.3) are, in this case,

$$mn \neq 1 \quad , \quad m \neq -1 \quad , \quad n \neq -1 \quad . \tag{5.4}$$

These conditions divide the (m,n) parameter plane into seven qualitatively distinct regions as indicated in Figure 5.5. Perturbations of (5.2) are qualitatively similar at all points within a given region except in regions 3, ,3′ and 4.

Regions 3 and 3′ each divide into two qualitatively distinct sub-regions within which perturbations of (5.2) are qualitatively similar. Region 4 similarly divides into four qualitatively distinct sub-regions. These sub-divisions reflect the invariance of the order of bifurcation under equivalence transformation.

The stationary solution branches defined by (5.2) are

$$\begin{aligned}
&\text{(a)}\quad x = r = 0 \ , && \text{(trivial)} \quad (5.5)\\
&\text{(b)}\quad \lambda = x^2 \ , \quad r = 0 \ , && \text{(x-mode)}\\
&\text{(c)}\quad x = 0 \ , \quad \mu = r^2 \ , && \text{(r-mode)}\\
&\text{(d)}\quad (1 + n)x^2 - (m + 1)r^2 = \lambda - \mu \ , \quad \lambda = x^2 - mr^2, && \text{(mixed-mode)}
\end{aligned}$$

corresponding to trivial equilibrium, steady-state, periodic and coupled steady-state and periodic solutions of the original system.

The persistent perturbed bifurcation diagrams derived from these solutions are illustrated, schematically, for regions 1, 2, 3a,b, 4a,b,c, and 5 of the (m,n) parameter plane in Figure 5.6. To indicate the structure of the bifurcations more clearly, it is convenient to introduce the new perturbation parameter $\sigma \triangleq \lambda - \mu$. The diagrams for regions 2′, 3a′,b′ and 4b′ can be obtained from those for regions 2, 3a,b and 4b by interchanging x and r and reversing the sign of σ. The stability assignments along each branch are indicated by solid and dashed lines, denoting stable and unstable equilibria, respectively. These stability assignments derive from an examination of the signs of the real parts of the eigenvalues of the Jacobian matrix associated with (5.2) along each

branch. The eigenvalue sign designations are summarized in (5.6)

(a)	$\text{sgn}(\lambda)$,	$\text{sgn}(\lambda - \sigma)$	(trivial) (5.6)
(b)	- ,	$\text{sgn}((1 + n)\lambda - \sigma)$	(x-mode)
(c)	$\text{sgn}((1 + m)\lambda - m\sigma)$,	-	(r-mode)
(d)	$\text{sgn}(mn - 1)$,	-	(mixed-mode)

Examination of the bifurcation diagrams reveals a close similarity between the generic bifurcations associated with region 3 of the (m,n) parameter plane (see Figure 5.6) and the symmetric non-linear divergence and flutter phenomena illustrated in Figure 5.3. The progression from a divergent steady-state, through an apparent stable mixed-mode solution, to a symmetric flutter condition is consistent with the generic behaviour in region 3 for $\sigma > 0$. In this region, the x-mode (divergence mode) solution branch looses stability at a secondary bifurcation and a smooth transition to the r-mode (symmetric flutter) branch takes place along a stable mixed-mode branch. Contrasted with this, for $\sigma < 0$, the generic behaviour is characterized by loss of stability of the trivial equilibrium via a primary bifurcation to a stable r-mode branch. This latter behaviour is typical of the simple limit-cycle flutter shown in Figure 5.2.

Region 3 in the (m,n) parameter plane divides into two qualitatively distinct sub-regions 3a and 3b. The perturbed bifurcation diagrams for the regions 3a and 3b differ in detail for $\sigma > 0$ by the position of the secondary bifurcation relative to the second primary bifurcation. In region 3a, the second primary bifurcation precedes

the secondary bifurcation whereas in region 3b, the order of bifurcation is reversed. While the resolution of the reduced velocity changes in Figure 5.3 is too coarse to establish the order of bifurcation directly, the transient behaviour observed at $M = 0.85$, $\bar{U} = 1.90$ is consistent with the occurrence of a secondary instability of the initial divergence mode in close proximity to the linear flutter point. It is reasonable to surmise, therefore, that the bifurcation diagram 3b is representative of the underlying transition structure of the aeroelastic system of §5.2, locally, in a neighbourhood of the bifurcation centre $(\bar{U}_0, M_0)$.

A more detailed description of the perturbed bifurcation diagram for region 3b is presented in Figure 5.7. Here, the stability assignments of each solution branch are indicated explicitly by the appropriate eigenvalue sign designations defined by (5.6). The parameters λ and σ in the bifurcation diagram are identified with general curvilinear co-ordinates in the physical $(\bar{U}, M)$ parameter plane. The origin of these co-ordinates is the bifurcation centre $(\bar{U}_0, M_0)$. The linear divergence and flutter boundaries define the curves $\lambda = 0$ and $\lambda = \sigma$, respectively. These lines correspond to the primary bifurcation points on the bifurcation diagram. The secondary bifurcation points on the x- and r-mode branches, which occur for $\sigma > 0$ at the points $\lambda_x = \sigma / (1 + n)$ and $\lambda_r = m\sigma / (1 + m)$, respectively, define two additional boundaries in the $(\bar{U}, M)$ plane. The hypothetical bifurcation sets in physical parameter space are shown in Figure 5.8. Qualitatively, a one-to-one correspondence is assumed to exist between the constant Mach number solutions shown in Figure 5.3 and the bifurcation diagram 3b.

5.3.2 The Nature of Symmetric Mode Interactions

The bifurcation diagram (Figure 5.7) is a useful aid to interpretation of the unusual transient behaviour exhibited by the divergence/flutter interaction solutions in Figure 5.3. Much of this behaviour can be attributed to the presence of unstable solution branches which co-exist with the stable stationary solution branch. For example, in the range $\lambda_x < \lambda < \sigma$, $\sigma > 0$, a stable mixed-mode branch co-exists with an x-mode branch, locally unstable in the r-mode. The trivial equilibrium is locally unstable in the x-mode but locally stable in the r-mode. Perturbation of the system close to the trivial equilibrium results in an initial divergence attracted to the (locally x-mode stable) x-mode branch. Initial r-mode perturbations which persist to this point are amplified as a consequence of the local r-mode instability of the x-mode branch. The final stationary solution is a combined steady-state/ limit cycle. This behaviour is consistent with the aeroelastic response history at $M = 0.85$, $\bar{U} = 1.90$. Similar effects are also present for $\lambda > \lambda_r$. However, the dominant features here are the local instability of the trivial equilibrium in both the x- and r-modes and the presence of a stable r-mode branch. The initial divergence which accompanies the stationary symmetric flutter solution at $M = 0.85$, $\bar{U} = 2.00$ is regulated, and eventually suppressed, by this solution.

While both of these cases display stationary limit-cycle behaviour, the origins of the non-linear flutter are quite different in each case. The former derives from secondary instability of a non-linear

divergence whereas the latter results from a primary instability of the trivial equilibrium. This distinction is most apparent in the initial growth rates of the oscillatory motion. This observation has significant implications with regard to the definition and interpretation of flutter boundaries. In the present application, secondary flutter precedes primary flutter in a region of 'weak' or 'limit deflection' divergence (the primary (classical) flutter boundary is, in fact, unobservable in regions of physical parameter space corresponding to $\sigma > 0$).

5.3.3 Imperfection Sensitivity and Symmetry-Breaking

Interpretation of the observed asymmetric behaviour in the neighbourhood of $(\bar{U}_0, M_0)$ is a somewhat more difficult task. The underlying structure of the transitions is not immediately apparent, particularly as the computational evidence relates only to the variation of a *single* parameter (the structural pre-twist). The identified model for the symmetric mode interactions described in §5.3.1 does, however, provide a framework for a first-order analysis of the effects of imperfections from which the bifurcations for the non-symmetric case can be discussed; that is, the degenerate model form for the symmetric case may be interpreted as an *organizing centre* for the asymmetric problem. The essentially three-dimensional nature of the model normal form satisfies the minimum pre-requisite for compatibility with the observed asymmetric behaviour - the apparent doubly periodic asymptotic behaviour observed for moderate angles of pre-twist demands, at least, a

three-dimensional (centre) phase space. Physical considerations indicate that the dominant symmetry-breaking effects result from steady-state structural generalized forces associated with the pre-twisted aeroelastic configuration. The special symmetry properties of the problem; namely, that the anti-symmetry of the generalized aerodynamic forces is maintained under asymmetric perturbation due to structural pre-twist, and the fact that the non-linearities are exclusively aerodynamic in origin, imply that the notional centre-manifold is also anti-symmetric in the projected state-history and the structural pre-twist (*cf.* Holmes [1981]). Perturbation of the normal form (5.2) by a *constant* term is the simplest asymmetric continuation of the pitchfork/Hopf degeneracy compatible with the physics of the problem. While an affine unfolding of the pitchfork/Hopf degeneracy is not universal, it is indicative of the asymmetric dynamics in the immediate neighbourhood of the pitchfork/Hopf bifurcation point. The modified normal form corresponding to region 3b in the (m,n) plane in the symmetric case is of the form

$$\dot{x} = \varepsilon + \lambda x + x(-x^2 + mr^2) \qquad (5.7)$$

$$\dot{r} = \mu r + r(-r^2 + nx^2)$$

where ε is the (α_0-dependent) symmetry-breaking perturbation parameter. The unfolding parameters λ, μ, and the parameters m and n, are, in general, functions of the physical parameters $(\bar{U}-\bar{U}_0)$, $(M-M_0)$ and α_0. Here, it is implicitly assumed that, at least locally, the degenerate form of (5.7) remains of the same topological type in the physical parameter range of interest.

The simplicity of the modified normal form is deceptive. Analysis of the bifurcation sets of (5.7) in $(\lambda,\mu,\varepsilon)$ parameter space (see Appendix One) reveals that the asymmetrically perturbed planar normal form organizes local codimension-two bifurcations which correspond to complex periodic and quasi-periodic solution behaviour in the original three-dimensional centre phase space after reinstatement of the phase component. Figure 5.9a depicts the general structure of the local bifurcation sets in the (λ,μ) plane for fixed $\varepsilon > 0$[4]. Superimposed on this diagram are the local bifurcation sets corresponding to the symmetric case $\varepsilon = 0$. In $(\lambda,\mu,\varepsilon)$ space, the *local* bifurcation structure for $\varepsilon \neq 0$ scales in proportion to $\varepsilon^{-2/3}$; re-scaling of the parameters by the transformation $\tilde{\lambda} = \lambda\varepsilon^{-2/3}$, $\tilde{\mu} = \mu\varepsilon^{-2/3}$ means that the *topological* structure of the local bifurcation sets is independent of ε in the $(\tilde{\lambda},\tilde{\mu})$ plane. In general, each of the perturbation parameters may be regarded as a function of the physical pre-twist and hence variation of this parameter alone is sufficient to traverse different regions of the $(\tilde{\lambda},\tilde{\mu})$ plane.

The projections onto the (λ,μ) plane of the intersections of the local codimension-one bifurcation surfaces in $(\lambda,\mu,\varepsilon)$ space with the plane ε = constant are denoted by B_1, $B_2^{\pm}$, B_3 and B_4 (Figure 5.9b). The bifurcation sets B_1, $B_2^{\pm}$, B_3 are associated with steady-state bifurcations of the planar system (5.7) while the set B_4 is associated with periodic bifurcations. Here, B_1 defines the parameter set corresponding to the *saddle-node* bifurcation which results from asymmetric perturbation of the supercritical pitchfork

[4]Figure 5.9 is based on the parameter values $\varepsilon = 1$, $m = -2$, $n = 1$.

bifurcation in the x-mode at $\varepsilon = 0$. The pitchfork bifurcation is perturbed into a continuous stable branch and a saddle-node bifurcation for which two $r = 0$, $x \neq 0$ solutions appear. For $\varepsilon > 0$, the continuous branch has $x > 0$ and the saddle-node bifurcation appears for $x < 0$ with both solutions emanating from this x value remaining negative for all parameter values. Bifurcations occurring on $B_2^{\pm}$ involve the creation/annihilation of $r \neq 0$ equilibria from/to those on the $r = 0$ axis in the (x,r) phase plane. The lines $B_2^{\pm}$ are asymptotic to the secondary bifurcation line $\lambda = \lambda_x$ for the symmetric case in which $r \neq 0$ equilibria are born from the primary x-mode branches on the pitchfork. In the absence of x-mode symmetry, the bifurcations from the $x > 0$, $r = 0$ solutions and the $x < 0$, $r = 0$ solutions (associated with B_2^- and B_2^+, respectively) no longer occur simultaneously. Steady-state bifurcations of $r \neq 0$ equilibria of the planar system (5.7) are associated with the parameter set B_3. In the original three-dimensional centre phase space, these bifurcations correspond to saddle-nodes of periodic orbits. The parameter set defined by B_4 is associated with periodic bifurcations of the Hopf type in the (x,r) phase plane. These bifurcations occur only for $r \neq 0$ and correspond to bifurcations to two-tori in the original three-dimensional centre phase space.

The various intersections and tangencies which exist between the bifurcation sets in the (λ,μ) plane (for the same equilibria) correspond to codimension-two bifurcation points. In Figure 5.9b, these points are denoted by p_1, p_2, and p_3. The point p_1 represents the point of tangency between B_2^+ and B_1. This point is also a point of intersection between B_4 and B_1 and B_2^+. The tangency at p_1

corresponds to a *saddle-node/Hopf* bifurcation point for the original three-dimensional system in the centre phase space and is the $\varepsilon \neq 0$ counterpart of the *pitchfork/Hopf* bifurcation for the symmetric case $\varepsilon = 0$. The point p_2 represents the point of tangency between B_3 and B_4. In the (x,r) phase plane, the local linearization of the normal form (5.7) in the neighbourhood of the equilibrium associated with p_2 possesses a zero eigenvalue with algebraic multiplicity two. The degeneracy at p_2 is associated with a codimension-two *Takens/ Bogdanov* bifurcation in the (x,r) phase plane. Similarly, the point of tangency of B_2^+ with B_3 defines p_3. This point corresponds to a *degenerate Hopf* bifurcation point for the original system in the centre phase space. The unfoldings of these bifurcations are discussed in detail in Guckenheimer & Holmes [1983].

Examination of the phase portraits in the neighbourhood of the origin in the (λ,μ) plane reveals the nature of the dynamics for the asymmetrically perturbed system. A partial set of phase portraits based on those described in the monograph by Guckenheimer & Holmes [1983], and verified, independently, by direct numerical simulation, is shown, schematically, in Figure 5.10 (note that, to maintain the clarity of the phase portraits, the scale of the negative x-axis is exaggerated). The addition of $\varepsilon \neq 0$ to the normal form (5.2) breaks the $x \rightarrow -x$ invariance of the equations. The results shown are for $\varepsilon > 0$, small. It is easily verified from (5.7) that the results for $\varepsilon < 0$ can be obtained by simply changing $x \rightarrow -x$ in the various phase portraits. Since the $r \rightarrow -r$ invariance is assumed to persist in the asymmetric case, the $r < 0$ and $r > 0$ stationary points at the same x value and r magnitude correspond to

the same periodic orbit; consequently, only the $r \geq 0$ cases are shown. Here, a fixed point on the $r = 0$ axis represents a static equilibrium solution. Any fixed point with $r \neq 0$ represents a periodic solution in the full three-dimensional system. A (stable) closed orbit represents motion on a two-torus in the three-dimensional centre phase-space and corresponds to an amplitude modulated periodic, or quasi-periodic, motion with mean amplitude of the motion also modulating as a result of the periodic change in the x variable. The implied phase-shift symmetry, or $r \rightarrow -r$ invariance, forces the motion on the tori to be periodic or quasi-periodic depending on whether the *rotation number* is, respectively, rational or irrational (Guckenheimer [1984]). In the absence of phase-shift symmetry, periodic motion on a torus is a highly unstable phenomenon.

The dynamical behaviour in the neighbourhood of the codimension-two points p_1 ,p_2 and p_3 is of particular interest. The degeneracy at p_1 admits Hopf bifurcation to (unstable) time-periodic solutions in the (x,r) phase plane - a feature absent from the corresponding degeneracy in the symmetric case. Numerical simulations indicate that the repulsion of the unstable orbits is relatively weak and one can envisage quite complicated transient behaviour in the neighbourhood of these orbits. The Hopf bifurcation line B_4 emanating from the point p_1 also extends to the codimension-two point p_2. Here, unstable limit-cycle behaviour of the planar system is also present. Global bifurcations, which must accompany the various Hopf bifurcations to maintain path consistency in the (λ,μ) plane, involve *heteroclinic* or *homoclinic* loops connecting

saddle-nodes in the (x,r) plane (Guckenheimer & Holmes [1983]). In the vicinity of such bifurcations, further irregular motions can be expected. The point p_3 corresponds to a degenerate (codimension-two) Hopf bifurcation in the original three-dimensional system. Here, a saddle-node bifurcation of periodic orbits emerges upon crossing from region b to region h in the (λ,μ) plane.

Since stability types are generally preserved between corresponding motions in the equivalent planar and three-dimensional systems, only stable hyperbolic solution sets of the planar system correspond to solutions which are physically observable. Consequently, relatively few of the rich dynamical structures present in the perturbed normal form (5.7) represent motions that occur in (numerical) experiment. Moreover, the stable fixed point in the positive quadrant of the (x,r) plane dominates all trajectories emanating from initial conditions close to the origin, thereby excluding even transient exploration of the more interesting structures. This pattern of behaviour is consistent with the observed aeroelastic response for relatively small values of structural pre-twist and might have been anticipated on physical grounds alone.

While it is reasonable to speculate that the bifurcational characteristics of the model defined by (5.7) for $\varepsilon \neq 0$ are representative of the qualitative behaviour of the aeroelastic system of §5.2, locally, in some neighbourhood of the symmetric case, the absence of stable dynamical solution structures of the type depicted in Figures 5.4(b)-(d) suggests that the range of validity of the model (5.7) is too narrow to encompass the behaviour

observed for large angles of pre-twist and that, in the physical parameter range of interest, a change of topological type takes place in which higher-order asymmetric perturbation terms originally omitted from the model normal form assume a more prominent role .

The general asymmetric perturbation of the pitchfork/Hopf normal form which maintains $r \to -r$ invariance, and which is x-mode anti-symmetric with respect to a change of sign of the asymmetric perturbation parameters, is (to third-order)

$$\begin{aligned} \dot{x} &= \varepsilon + \beta x^2 + \gamma r^2 + \lambda x + x(-x^2 + mr^2) \\ \dot{r} &= \qquad\qquad \delta r x + \mu r + r(-r^2 + nx^2) \quad . \end{aligned} \tag{5.8}$$

The mechanism whereby quadratic perturbation terms appear in the normal form of the reduced aeroelastic model can be traced to the special symmetry properties of the problem. By analogy with the centre-manifold reduction for parameterized *ordinary* differential equations (Holmes [1981]), in which the physical parameter α_0 is interpreted as an augmented state component with trivial dynamics $\dot{\alpha}_0 = 0$, the unfolding parameters ε, β, γ, δ can be shown to be $\mathcal{O}(|\alpha_0|)$ while the parameters λ, μ and m, n are $\mathcal{O}(|\alpha_0|^2)$ in α_0.

A complete classification of the topologically distinct bifurcation structures associated with the asymmetric perturbation model (5.8) is a formidable task. The general unfolding can be expected to organize degeneracies of particularly high (topological) codimension (typically, greater than two, but less than five) whose local unfoldings are only partially complete (*cf.* Dangelmayr &

Armbruster [1983] and Armbruster *et al* [1985]). However, by restricting attention to existing local (codimension-two) structures exposed by the analysis of the simple perturbed normal form (5.7) (with $m < -1$, $n > 0$), one can establish the nature of local qualitative changes induced by the higher-order unfolding terms. In particular, restoration of quadratic unfolding terms in the asymmetrically perturbed model, typically, will modify third-order terms in the normal form of the Taylor expansion in the neighbourhood of the saddle-node/Hopf point p_1 in Figure 5.10. Locally, third-order terms of the normal form determine the stability of any bifurcating tori (limit cycles in the (x,r) plane). Consequently, while the primary influence of a first-order asymmetric perturbation is to shift and split the double degeneracy, higher-order perturbations provide a mechanism whereby changes to the qualitative nature of the degeneracy are possible.

The *local* bifurcation structure of the general unfolding (5.8) is determined by

$$G_{\varepsilon,\beta,\gamma,\delta} = \begin{bmatrix} \varepsilon + \beta x^2 + \gamma r^2 + \lambda x + x(-x^2 + mr^2) \\ \delta r x + \mu r + r(-r^2 + nx^2) \end{bmatrix} . \qquad (5.9)$$

To detect regions of $(\varepsilon,\beta,\gamma,\delta)$ space in which saddle-node/Hopf intersections are *feasible*, it is sufficient to consider those regions in which $\partial \det(DG_{\varepsilon,\beta,\gamma,\delta})/\partial r^2 > 0$ at points of double degeneracy in $DG_{\varepsilon,\beta,\gamma,\delta}$ (that is, points at which, simultaneously, $\mathrm{tr}(DG_{\varepsilon,\beta,\gamma,\delta})$ and $\det(DG_{\varepsilon,\beta,\gamma,\delta})$ are identically zero for the same

equilibrium). If $r = 0$, $x = x^*$ denotes an equilibrium at which such a degeneracy occurs, then the existence of a continuous Hopf bifurcation 'surface' emanating from this point requires

$$\partial \det(DG_{\varepsilon,\beta,\gamma,\delta})/\partial r^2\big|_{r=0,x=x^*} > 0 \qquad (5.10)$$

since $\det(DG_{\varepsilon,\beta,\gamma,\delta}) > 0$, $r^2 > 0$ on the Hopf surface.

From the definition of $G_{\varepsilon,\beta,\gamma,\delta}$, it is easily verified (see Appendix One) that, with $\mathrm{tr}(DG_{\varepsilon,\beta,\gamma,\delta})\big|_{r=0,x=x^*} = 0$ (the requirement $\det(DG_{\varepsilon,\beta,\gamma,\delta})\big|_{r=0,x=x^*} = 0$ is automatically satisfied with $r = 0$), the inequality (5.10) implies that

$$(mx^* + \gamma)(2nx^* + \delta) < 0 \quad , \qquad (5.11)$$

so that

$$(2nx^* + \delta) > 0 \Rightarrow (mx^* + \gamma) < 0 \qquad (5.12a)$$

$$(2nx^* + \delta) < 0 \Rightarrow (mx^* + \gamma) > 0 \quad . \qquad (5.12b)$$

The inequalities (5.12) define partitions in the (δ,γ) plane in which saddle-node/Hopf intersections are feasible. For each $\varepsilon > 0$, $\beta < 3\varepsilon^{1/3}$, there exists a single $x^* < 0$ (*cf.* equation (A1.42)), dependent only on ε and β, and hence with $m < -1$, $n > 0$, the (δ,γ) plane divides into four regions of the form illustrated in Figure 5.11. The feasible saddle-node/Hopf regions are denoted by region I and region II.

Empirical evidence suggests that the saddle-node/Hopf degeneracies in region I of the (δ,γ) plane are topologically distinct from those in region II. In the neighbourhood of the origin in region I of the (δ,γ) plane, the structure of the local bifurcation sets of $G_{\varepsilon,\beta,\gamma,\delta}$ can be inferred from the first-order perturbation model defined by G_{ε} in (5.7). The saddle-node/Hopf degeneracy organized by this model is of the type depicted in Figure 5.9 as a projection in the (λ,μ) plane. In contrast, the nature of the saddle-node/Hopf degeneracy in region II of the (δ,γ) plane is determined by the quadratic unfolding terms in $G_{\varepsilon,\beta,\gamma,\delta}$. A coarse sample of the local bifurcation sets associated with parameters in $(\varepsilon,\beta,\gamma,\delta)$ space mapping to region II in the (δ,γ) plane indicates that the qualitative structure of those sets which organize a saddle-node/Hopf point is of the form[5] illustrated in Figure 5.12. The bifurcation set shown may be regarded as a *topological conjugate* of those sets in region II admitting a saddle-node/Hopf degeneracy.

Since variation of the physical symmetry-breaking parameter alone is sufficient to explore, simultaneously, different regions of the (δ,γ) and (λ,μ) planes, the transition from the type A degeneracy of region I to the type B degeneracy of region II provides a simple topological mechanism for the apparently disparate aeroelastic behaviour reported by Bendiksen and Kousen for moderate to high

[5] In general, the system (5.8) may be re-scaled such that

$$\tilde{x} = x\varepsilon^{-1/3},\ \tilde{r} = r\varepsilon^{-1/3},\ \tilde{\lambda} = \lambda\varepsilon^{-2/3},\ \tilde{\mu} = \mu\varepsilon^{-2/3},\ \tilde{t} = t\varepsilon^{2/3},$$

$$\tilde{\beta} = \beta\varepsilon^{-1/3},\ \tilde{\gamma} = \gamma\varepsilon^{-1/3},\ \tilde{\delta} = \delta\varepsilon^{-1/3},$$

and hence there is no loss of generality in assuming $\varepsilon = 1$ in (5.8).
The parameters m and n in the normal form are unaffected by the scaling.

angles of pre-twist. Figure 5.13 illustrates the nature of the phase portraits for the perturbation model (5.8) in the vicinity of a region II saddle-node/Hopf point. Examination of the 'global' phase plane characteristics, as the parameters (λ,μ) are varied in the neighbourhood of the saddle-node/Hopf point, reveals a close similarity with the qualitative pattern of aeroelastic behaviour depicted in Figures 5.4(a)-(d). The large transient excursion of trajectories in the positive x half-plane, terminating, initially, in stable limit cycle behaviour and progressing, with variation of λ and μ, through $r \neq 0$ equilibria to $r = 0$ equilibria in the negative x half-plane is entirely consistent with the observed aeroelastic response over the range of pre-twist angles from 4.00 degrees to 5.00 degrees in which a change of sign of the steady-state component of the response is evident.

Interpretation of the observed aeroelastic response in terms of the asymmetric perturbations of the pitchfork/Hopf degeneracy provides a comprehensive picture of the local and global organization of the dynamics as a function of the structural pre-twist. The global scenario indicated by the bifurcation model explains much of the counter-intuitive aeroelastic behaviour. The transient excursion of the aeroelastic response captured by the reduced bifurcation model can be attributed to the presence of an x-mode stable, r-mode unstable saddle equilibrium on the positive x axis from which a bifurcation to a $r \neq 0$ equilibrium occurs. The location of this equilibrium in the (x,r) plane shifts in the direction of the negative x half-plane under the action of the higher-order asymmetric perturbation parameters. During this process, the

equilibrium changes from a stable node to a stable focus with slow decay. Progressively, the stability of the equilibrium is relaxed until a Hopf bifurcation to a periodic orbit occurs. This behaviour is consistent with the observation, noted by Bendiksen and Kousen, of higher harmonics in the response at a pre-twist angle just below that at which quasi-periodic behaviour appears. The local behaviour in the negative x half-plane can be interpreted in terms of the generic unfoldings of the type B saddle-node/Hopf degeneracy illustrated in Figure 5.14. Here, the *stable* limit cycle behaviour corresponds to motion on a two-torus in the original three-dimensional centre phase space while the $r = 0$ and $r \neq 0$ equilibria correspond to steady-state and periodic solution behaviour, respectively. The motion on the torus has one 'fast' frequency associated with the angular variable θ in three-dimensional phase space and a 'slow' frequency associated with the secondary Hopf bifurcation of the planar system. The motion is characterized by a rapid oscillation with a slow modulation and is periodic or quasi-periodic depending on whether the ratio of the 'slow' and 'fast' frequencies - the rotation number - is rational or irrational. The implied interpretation of the irregular aeroelastic response at $\alpha_0 = 4.00$ degrees is that of quasi-periodic motion on a two-torus corresponding to an irrational rotation number. The more regular aeroelastic response at $\alpha_0 = 4.75$ degrees suggests periodic motion associated with a rational rotation number. However, the limited duration of the time-history of the response at $\alpha_0 = 4.75$ degrees makes it difficult to distinguish stationary and transient behaviour. This fact necessitates some caution in the interpretation of the aeroelastic response at this angle of pre-twist.

5.4 CONJECTURES ON NEW TRANSONIC AEROELASTIC PHENOMENA

The bifurcation sets associated with the reduced bifurcation model defined by $G_{\varepsilon,\beta,\gamma,\delta}$ correspond to legitimate unfoldings of the pitchfork/Hopf degeneracy in the absence of reflectional symmetry. In conjunction with appropriate bifurcation diagrams or phase portraits, these bifurcation sets illustrate the range of behaviour possible in some neighbourhood of the bifurcation centre. Notionally, each of the parameters in the perturbed normal form is functionally dependent on the three physical parameters - structural pre-twist, Mach number and reduced velocity. The precise nature of this dependence is determined by the physical characteristics of the transonic aeroelastic problem. Under variation of the physical parameters, however, only certain 'paths' through (normal form) parameter space are possible. Consequently, not all of the *potential* behaviour contained in the general unfoldings is necessarily *realizable*. Nevertheless, continuity arguments suggest that behaviour associated with parameter values in the neighbourhood of regions of (normal form) parameter space identified with observed aeroelastic behaviour corresponding to prescribed values of the physical parameters *may* be realized for some perturbation of the physical parameter set. In particular, the 'global' bifurcation structure associated with saddle-node/Hopf intersections in Region II of the (δ,γ) plane contains additional degeneracies, remote from the saddle-node/Hopf point, which organize new phenomena detectable only by a comprehensive survey of parameter space. Generically, one might expect to encounter similar phenomena in the original aeroelastic system.

Figure 5.15 illustrates the nature of the phase portraits at other locations in the (λ,μ) plane in the neighbourhood of the Region II saddle-node/Hopf point previously identified with the observed aeroelastic response corresponding to pre-twist angles in the range 4.00 degrees to 5.00 degrees for fixed values of Mach number and reduced velocity ($M = 0.85$, $\bar{U} = 1.85$). The stable limit cycle behaviour depicted for region b is fundamentally different from that which occurs in the negative x half-plane close to the saddle-node/Hopf point. Here, the limit cycle is centred in the positive x half-plane and the range of amplitudes of the steady-state and periodic components of the cycle is significantly greater. The time responses of the (x,r) variables shown in Figure 5.16 indicate that this range of amplitudes is experienced in a relatively short time interval[6]. In the three-dimensional centre phase space, this behaviour is manifest as ('slow' frequency) periodic 'bursts' of large amplitude steady-state and ('fast' frequency) periodic behaviour followed by relatively quiescent periods of response. To the right of the $r = 0$ saddle-node line in the (λ,μ) plane, stable limit cycle behaviour is no longer possible and the phase portraits exhibit more complicated behaviour. Here, the controlling influence is the local double zero degeneracy which results from the tangency of the Hopf bifurcation line and the $r \neq 0$ saddle-node line (saddle-node of periodic orbits in the centre phase space) in the positive quadrant of the (λ,μ) plane. Path consistency dictates that a global bifurcation line, also emanating from the point of tangency, exists below the Hopf line to ensure compatibility with the behaviour far removed from the Hopf line.

[6] For $\varepsilon > 1$, the simulation timescale is generally compressed.

Physically, the stable limit cycle behaviour in the (x,r) plane represents an 'intermittent' type of divergence/flutter interaction. Since the behaviour persists under perturbation, it is feasible that this kind of mode interaction is realized by the original coupled aerodynamic and structural equations of motion. Although the behaviour cited derives from a *supercritical secondary* bifurcation of the primary flutter solution (and is therefore of limited practical significance), similar behaviour is present at other combinations of the asymmetric perturbation parameters in which the route to stable limit cycle behaviour occurs *subcritically* to the classical flutter boundary as a result of a *cusp* bifurcation associated with the equilibrium in the positive x half-plane[7] (an example of the bifurcation structure corresponding to this type of behaviour is illustrated in Figure 5.17). While the existence of such behaviour in the original aeroelastic equations of motion is more speculative, qualitatively, behaviour of this kind is not inconsistent with the known characteristics of unsteady transonic flow. Empirical evidence indicates that the dominant asymmetric perturbation parameters responsible for shaping the stable limit cycle behaviour are the parameters γ and δ. These parameters control, respectively, the r^2 and xr contributions to the unfolding of the pitchfork/Hopf degeneracy. This suggests a strong dependence of the response on the periodic component of the motion. The inherent non-linearity of the transonic aeroelastic problem and instances of anomalous behaviour can be traced to the presence of moving shocks on the lifting surface. In the aeroelastic problem, the shocks evolve in response to the aerofoil motion, but with an

[7] This bifurcation occurs only for $\beta > 3\varepsilon^{1/3}$.

important phase lag. The shock excursion amplitude and strength are functions of the amplitude, frequency, and type of aerofoil motion. In unsteady transonic flow, the motion of shock waves makes an important contribution to the overall unsteady aerodynamic forces. Under certain flow conditions, shocks form intermittently on the aerofoil surface (Tijdeman B-type shock development (Tijdeman & Seebass [1980])) resulting in large variations of the aerodynamic pitching moment amplitude and phase relative to the aerofoil motion. The existence of this type of shock development is reported by Kousen for Mach numbers and reduced velocities in the physical parameter range of interest. The inference here is that shock effects alone are sufficient to induce the conjectured aeroelastic behaviour. Details of the physical mechanisms responsible for such behaviour, however, remain unidentified.

5.6 SUMMARY

An analogy exists between the transitions in qualitative behaviour which characterize divergence/flutter interaction phenomena in transonic flow and the persistent bifurcations of a class of non-linear ordinary differential equations which arise, generically, in the vicinity of a coupled steady-state and Hopf bifurcation point (the pitchfork/Hopf degeneracy). Several interesting physical consequences for aeroelastic divergence and flutter can be drawn from this analogy (strictly, a formal qualitative equivalence) which are computationally verifiable and add new insight into the phenomenology of non-linear transonic aeroelasticity. The analogy is

suggestive of the existence of a coincident divergence and flutter point in the Mach number/reduced velocity parameter plane. In regions of divergence/flutter interaction, the nature and origin of non-linear flutter changes markedly. Examples in which secondary flutter emanating from unstable 'weak' divergence solutions precedes primary flutter suggest that the classical notion of flutter boundary is of limited applicability. The imposition of a structural pre-twist leads to changes in the topological nature of the divergence/flutter interaction point and to the appearance of new aeroelastic behaviour. The 'global' organization of divergence/ flutter interaction phenomena observed in the computational studies of Bendiksen and Kousen can be interpreted in terms of the asymmetric perturbations of the pitchfork/Hopf degeneracy. The anomalous flutter characteristics observed for medium to high values of pre-twist are identified with stable perturbations corresponding to quasi-periodic motion on a two-torus. Genericity and continuity arguments indicate the existence of additional aeroelastic phenomena not contained in previous numerical computations. The conjectured aeroelastic behaviour is reminiscent of an 'intermittent' type of divergence/flutter interaction.

CHAPTER SIX

CONCLUSIONS AND RECOMMENDATIONS FOR FURTHER RESEARCH

6.1 GENERAL CONCLUSIONS

The complexity of the governing aeroelastic equations of motion in transonic flow precludes the direct use of these equations in analytical bifurcation studies. Direct numerical integration of the aeroelastic equations of motion is feasible only for a limited number of initial conditions and parameter values. Determining the nature of the solution behaviour, as reflected in the bifurcations which occur as the parameters are varied, and understanding the structure of these bifurcations in parameter space, is more readily accommodated by an *inductive* approach in which partial bifurcational data is used to reason an appropriate *internal* model which characterizes the *qualitative* features of the observed behaviour. The utility of *generic modelling* as an *interpretive* device in the study of non-linear hereditary aeroelastic phenomena is demonstrated by the application of the technique to a model transonic aeroelastic problem. The approach adds new insight into the phenomenology of transonic aeroelastic behaviour and complements observations derived from computational studies of the coupled aerodynamic and structural equations of motion. The strategy for exploring aeroelastic bifurcational behaviour is based upon mathematical considerations of a general, non-constructive nature which encompass the key geometrical concepts of model reduction, qualitative equivalence,

genericity and persistence. Implementation of the strategy in problems which embody realistic unsteady aerodynamic behaviour is shown to be feasible without the requirement for explicit knowledge of the unsteady aerodynamic environment. The principal assumption is the existence of a notional aerodynamic force response functional, possessing requisite smoothness and fading memory properties consistent with the absence of aerodynamic bifurcations, which adequately models the unsteady aerodynamic behaviour. Representation of the aeroelastic initial-value problem as an infinite-delay functional differential equation in the structural state, in conjunction with the centre-manifold theorem, facilitates description of the qualitative characteristics of the aeroelastic response by a (generally low-dimensional) system of ordinary differential equations. Non-linear divergence and flutter characteristics are identified with the generic bifurcations of parameterized vector fields and their normal forms. The description of the observed aeroelastic behaviour (at least locally) is based on the qualitatively stable perturbations of an appropriate class of degenerate vector fields.

Transitions in qualitative behaviour which characterize the symmetric divergence/flutter interaction phenomena observed in the computational aeroelastic response studies of Bendiksen and Kousen under variation of Mach number and reduced velocity are identified, *uniquely*, with the persistent bifurcations of a two-parameter class of non-linear ordinary differential equations which arises, generically, in the neighbourhood of a coincident steady-state and periodic bifurcation point (the pitchfork/Hopf degeneracy). The

local nature of the bifurcation model, and its ability to capture large amplitude aeroelastic behaviour 'in embryo', is consistent with the observation that, in transonic flow, non-linear effects become important at relatively small amplitudes. The correspondence between the observed and generic behaviour poses important questions with regard to the definition and interpretation of flutter boundaries. For certain parameter regimes, in which secondary flutter emanating from unstable 'weak divergence' solutions precedes primary flutter, the classical notion of flutter boundary is of limited applicability - the classical (linear) flutter boundary is, in fact, unobservable in this case and secondary flutter is the principal aeroelastic instability.

The persistence of secondary flutter of this kind is a consequence of the reflectional symmetry of the aeroelastic system. The imposition of structural asymmetry leads to changes in the topological nature of the divergence/flutter interaction point and to the appearance of new aeroelastic phenomena. The anomalous behaviour observed by Bendiksen and Kousen for moderate to high values of structural pre-twist can be interpreted in terms of the 'global' response characteristics associated with asymmetric perturbation of the pitchfork/Hopf degeneracy identified for the zero pre-twist configuration. In the absence of reflectional symmetry, this degeneracy organizes complex steady-state and periodic mode interactions corresponding to *stable* quasi-periodic motion on a two-torus, the existence of which could not have been anticipated *a priori*. Qualitatively, there exists a high degree of correlation between the pattern of behaviour reported by Bendiksen

and Kousen and that generated by the asymmetrically perturbed bifurcation model. The confidence engendered by this similarity leads one to speculate, on the basis of genericity and continuity assumptions, the existence of additional aeroelastic phenomena not contained in previous numerical computations but realized by nearby unfoldings of the equivalent asymmetric perturbation model. The conjectured aeroelastic behaviour, which results from motion on a two-torus in the equivalent centre phase space, is manifest as an 'intermittent' type of divergence/flutter interaction. While the detailed physical mechanisms responsible for such behaviour remain unidentified, it is not unreasonable to suggest that behaviour of this kind is attributable, principally, to unsteady shock motion and is therefore, primarily, a *transonic* aeroelastic phenomenon.

6.2 TOPICS FOR FURTHER RESEARCH

Verification of the hypothesized aeroelastic behaviour is possible only by a detailed parametric survey of numerical solutions of the coupled aerodynamic and structural equations of motion. The topological structure established for the local bifurcation sets provides for an intelligent search of parameter space in which likely locations for the existence of new behaviour can be determined, qualitatively, in relation to known solution behaviour. Whether or not the existing and postulated behaviour is an artifact of the Euler aerodynamic model requires further investigation. An implicit assumption adopted in the present study is that of the qualitative stability of the notional aeroelastic model; that is,

qualitative details of the dynamics are assumed to persist under certain allowable perturbations. The persistence of the behaviour predicted by the Euler aerodynamic formulation of the aeroelastic equations of motion to perturbations introduced by the Navier-Stokes representation of the unsteady flowfield is a necessary pre-requisite for the *physical* realization of the observed computational behaviour. For the high Reynolds number flows of interest, the fundamental physical differences which exist between the two flowfield models are generally assumed to be important only where extensive flow separation or shock/ boundary-layer interaction occurs. That most of the observed Euler aeroelastic solutions involve amplitudes below that at which viscous effects are known to be significant, suggests that the qualitative stability of the previously identified reduced bifurcation model extends to perturbations associated with differences in the Euler and Navier-Stokes aerodynamic models. The main caveat is that the assumed phase-shift symmetry of the perturbations is maintained. In the absence of phase-shift symmetry, not all of the behaviour exhibited by the original bifurcation model can be expected to persist. For example, motion on a two-torus is not qualitatively stable and may lead to transverse homoclinic orbits which are associated with the appearance of chaotic behaviour. Subject to the aforementioned proviso, however, the qualitative characteristics of the bifurcation model can be expected to persist in experiment, although at slightly modified values of the physical parameters. Experimental validation of this conjecture would establish, in part, the physical processes responsible for the anomalous aeroelastic behaviour predicted by the model.

Further insight to the non-linear characteristics of the transonic aeroelastic problem is to be gained from a detailed analysis of the spectral properties of the linearized aeroelastic equations of motion under variation of the parameters. Root locus patterns can be identified with specific linear and non-linear degeneracies which, in turn, determine the form of the appropriate generic bifurcation model and the topological characteristics of the aeroelastic system. At an intermediate level, a more formal analysis of non-linear hereditary aeroelastic models, in which explicit representation of the reduced equation set at bifurcation is sought, can be expected to yield information on the relationship between aerodynamic non-linearity and delay structure in shaping the local bifurcational characteristics of the aeroelastic response and, hence, indirectly, indicate the nature of the physical processes involved. This is in contrast to the topological interpretation of non-linear aeroelastic behaviour described in the present work in which associations of this kind are not possible or, at best, heuristic. The validity of the geometrical approach is ultimately related to the formulation of the aeroelastic initial-value problem and, in particular, to the precise nature of the functional approximation to the aerodynamic force response and to the subsequent definition of the phase space. The assumptions adopted in the present model, although retrospectively shown to be legitimate, are somewhat restrictive in a more general context and are inconsistent with the *detailed* characteristics of the aerodynamic force response in transonic flow. Relaxation of these assumptions demands a re-evaluation of the conventional hereditary model of unsteady aerodynamic behaviour to account for such effects as thermodynamic irreversibility,

path-dependency and asymptotic invariance in plunge while embracing a broader class of motion histories. Similarly, the issue of aerodynamic bifurcation must be addressed if qualitative techniques are to applied to aeroelastic problems involving non-linear aerodynamic phenomena such as dynamic stall or shock/boundary-layer interaction. For more complex multi-degree-of-freedom structural configurations, these complications are compounded by the fact that the definition of an appropriate set of observables for aeroelastic systems of this kind is not immediately apparent[1]. These generalizations impinge on the geometrical description of the aeroelastic initial-value problem in the neighbourhood of bifurcation. In particular, the underlying assumption that the bifurcational characteristics of the reduced equation set correspond to the generic bifurcations of vector fields without further constraint cannot be expected to apply universally. This is an important issue which should be addressed in future qualitative studies of the aeroelastic initial-value problem.

[1]There are, however, parallels with the work of Baldock [1978] on the reduction of linear multi-degree-of-freedom aeroelastic systems to equivalent binary systems.

APPENDIX ONE

ASYMMETRIC PERTURBATION OF THE PITCHFORK/HOPF BIFURCATION

A1.1 INTRODUCTION

A comprehensive unfolding of the pitchfork/Hopf bifurcation in the absence of reflectional symmetry in the x-mode requires the addition of unfolding terms involving even ordered powers of the x and r variables. The high codimension of this bifurcation (Dangelmayr & Armbruster [1983]) suggests that a formal analysis of the associated universal unfolding is likely to prove prohibitive, both in terms of construction and interpretation. A simplified account of the effects of asymmetric perturbation of the pitchfork/Hopf bifurcation is provided by the constant term perturbation model described in §5.3. This model provides a framework for a first-order analysis of the effects of symmetry-breaking imperfections from which the relevant bifurcations for the universal unfolding can be discussed. This appendix outlines the calculation procedures for the enumeration of the local bifurcation sets and corresponding phase portraits associated with the simplified and higher-order unfoldings of the pitchfork/Hopf bifurcation model identified in Chapter Five. The analysis described here is adapted from that of Sethna & Shaw [1987] (as applied to the imperfection sensitivity analysis of a similar, but topologically distinct, bifurcation model) and the presentation closely parallels that of the cited reference.

A1.2 FIRST-ORDER ASYMMETRIC PERTURBATION AND LOCAL BIFURCATIONS

The simplified asymmetric perturbation model corresponding to Region 3b in the (m,n) parameter plane is defined by the system

$$\begin{aligned} \dot{x} &= \varepsilon + \lambda x + x(-x^2 + mr^2) \\ \dot{r} &= \mu r + r(-r^2 + nx^2) \end{aligned} \qquad \text{(A1.1)}$$

where $m < -1$, $n > 0$ and $mn < 1$.

The right-side of (A1.1) is represented concisely in the form

$$G_\varepsilon(x,r) = \begin{bmatrix} \varepsilon + \lambda x + x(-x^2 + mr^2) \\ \mu r + r(-r^2 + nx^2) \end{bmatrix} . \qquad \text{(A1.2)}$$

Determination of the local (codimension-one) bifurcation conditions derives from two main criteria; the existence of an equilibrium point and the degeneracy in the linearization of $G_\varepsilon(x,r)$ at that point. These conditions define surfaces in $(\lambda,\mu,\varepsilon)$ space which reduce to curves in the $\varepsilon = 0$ plane. Codimension-two bifurcation conditions correspond to curves in $(\lambda,\mu,\varepsilon)$ space formed by the intersection or tangency of codimension-one bifurcation surfaces. The codimension-two curves must pass through the origin in $(\lambda,\mu,\varepsilon)$ space since, locally, there exists only one codimension-two point in the $\varepsilon = 0$ plane - the pitchfork/Hopf point. Calculation of the local bifurcation sets in $(\lambda,\mu,\varepsilon)$ space commences with the enumeration of all codimension-one surfaces. Intersections and tangencies of the codimension-one surfaces are then analyzed to detect the existence of codimension-two curves.

A1.2.1 Bifurcations Associated with a Zero Eigenvalue

A zero eigenvalue corresponds to a *saddle-node* or a *pitchfork* bifurcation. Pitchfork bifurcations occur from r = 0 and, as in the $\varepsilon = 0$ case, these correspond to Hopf bifurcations for the full third order system. All other zero eigenvalues correspond to saddle-node bifurcations.

The condition for a zero eigenvalue is $\det(DG_\varepsilon(x,r)) = 0$.

Now,

$$DG_\varepsilon(x,r) = \begin{bmatrix} \lambda - 3x^2 + mr^2 & 2mxr \\ 2nxr & \mu - 3r^2 + nx^2 \end{bmatrix} \qquad (A1.3)$$

and hence

$$\det(DG_\varepsilon(x,r)) = (\lambda - 3x^2 + mr^2)(\mu - 3r^2 + nx^2) - 4mnx^2r^2 \; . \qquad (A1.4)$$

r = 0 Equilibria: For the r = 0 case, $\dot{r} = 0$ is automatically satisfied and the condition $\dot{x} = 0$ becomes

$$\varepsilon + \lambda x - x^3 = 0 \qquad (A1.5)$$

and $\det(DG_\varepsilon(x,r)) = 0$ becomes

$$(\lambda - 3x^2)(\mu + nx^2) = 0 \qquad (A1.6)$$

which has roots

$$x_{1,2} = \pm \sqrt{\frac{\lambda}{3}} \quad , \quad x_{3,4} = \pm \sqrt{\frac{-\mu}{n}} \quad . \qquad (A1.7)$$

Substitution of $x_{1,2}$ into (A1.5) yields

$$\varepsilon \pm 2\left(\frac{\lambda}{3} \right)^{3/2} = 0 \quad . \qquad (A1.8)$$

For $\varepsilon > 0$ and $\lambda > 0$, (A1.8) is satisfied only in the case of the negative $x_{1,2}$ root.

Hence, the bifurcation condition becomes

$$B_1: \qquad \lambda = + 3\left(\frac{\varepsilon}{2} \right)^{2/3} \quad . \qquad (A1.9)$$

Condition (A1.9) represents a standard perturbation of a pitchfork bifurcation. The supercritical pitchfork bifurcation at $\varepsilon = 0$ is perturbed into a continuous stable root and a saddle-node bifurcation for which two $r = 0$, $x \neq 0$ solutions appear. For $\varepsilon > 0$, the continuous root has $x > 0$ and the pair of roots appears at $x = -\sqrt{\lambda/3}$ with both roots emanating from this x value remaining negative for all parameter values.

For $r = 0$, $x = x_{1,2}$, and where (A1.9) is satisfied, DG_ε has only one non-zero element, in the lower right entry of DG_ε. The centre-manifold for this bifurcation must be parallel to the x-axis and since $r = 0$ here, it must in fact be the x-axis. Consequently, the saddle-node bifurcation involves only $r = 0$ equilibria.

Substitution of $x_{3,4}$ into (A1.5) gives

$$\varepsilon \pm \sqrt{\frac{-\mu}{n}} \left(\lambda + \frac{\mu}{n} \right) = 0 \quad . \qquad \text{(A1.10)}$$

For $\varepsilon > 0$, $n > 0$ and $\mu < 0$, (A1.10) is satisfied for both positive and negative $x_{3,4}$ roots depending on the sign of the term $(\lambda + \mu/n)$.

Hence, the bifurcation condition, for fixed ε, is

$$B_2: \qquad \lambda = -\frac{\mu}{n} \mp \varepsilon \sqrt{\frac{n}{-\mu}} \quad . \qquad \text{(A1.11)}$$

DG_ε for this bifurcation contains a non-zero element only in the upper left entry and hence the centre-manifold associated with this bifurcation must be tangent to a parallel of the r-axis at the value $x = x_3$ or $x = x_4$ at $r = 0$. Consequently, these bifurcations involve the creation/annihilation of $r \neq 0$ equilibria from/to those on the $r = 0$ axis.

It can be inferred that (A1.11) represents a condition for *pitchfork* bifurcations in which $r \neq 0$ equilibria are born (r-symmetry is still present). The reason for two branches of (A1.11) extending asymptotically towards $\lambda = \frac{-\mu}{n}$ $(\mu < 0)$ for large μ is simply that the bifurcations from the $x > 0$, $r = 0$ and the $x < 0$, $r = 0$ roots no longer occur simultaneously. This is expected in the absence of x-symmetry. Consideration of (A1.5) and (A1.11) indicates that (A1.11+) corresponds to the $x < 0$ equilibrium and (A1.11-) corresponds to the $x > 0$ equilibrium.

$r \neq 0$ Equilibria: For $r \neq 0$, the equation $\dot{r} = 0$ is satisfied by

$$r^2 = \mu + nx^2 \quad . \qquad \text{(A1.12)}$$

Substitution of (A1.12) into the equation $\dot{x} = 0$ yields an expression for equilibrium which involves only the x variable and the parameters,

$$\varepsilon + (\lambda + m\mu)x + (mn - 1)x^3 = 0 \quad . \qquad \text{(A1.13)}$$

Substitution of condition (A1.12) into the zero determinant condition $\det(DG_\varepsilon) = 0$ yields

$$(\lambda + m\mu + (mn - 3)x^2)(-2\mu - 2nx^2) - 4mn\mu x^2 - 4mn^2x^4 = 0 \quad . \qquad \text{(A1.14)}$$

This equation factors to give

$$(\lambda + m\mu + (3mn-3)x^2)(-2\mu - 2nx^2) = 0 \qquad \text{(A1.15)}$$

which has roots

$$x_{3,4} = \pm \sqrt{\frac{-\mu}{n}} \quad , \quad x_{5,6} = \pm \sqrt{\frac{\lambda+m\mu}{3(1-mn)}} \quad . \qquad \text{(A1.16)}$$

Substitution of $x_{3,4}$ into condition (A1.13) returns expression (A1.11). This confirms the observation that bifurcations associated with (A1.11) involve $r = 0$ and $r \neq 0$ equilibria.

Substitution of $x_{5,6}$ in (A1.13) results in a condition for bifurcation involving only $r \neq 0$ equilibria

$$\varepsilon \pm \frac{2}{3}\sqrt{\frac{\lambda+m\mu}{3(1-mn)}}\,(\lambda+m\mu) = 0 \qquad \text{(A1.17)}$$

For $\varepsilon > 0$, (A1.17) is satisfied only for negative real $x_{5,6}$. With $mn < 1$, this requires that $\lambda + m\mu > 0$. In addition, it is easily verified from (A1.12) and (A1.17) that the existence of a real non-zero r value requires that $n\lambda + (3 - 2mn)\mu > 0$.

Subject to these constraints, the bifurcation condition (A1.17) can be expressed as

$$B_3: \qquad \lambda = -m\mu + 3(1 - mn)^{1/3}\left(\frac{\varepsilon}{2}\right)^{2/3} \quad . \qquad \text{(A1.18)}$$

A1.2.2 Bifurcations Involving a Pure Imaginary Pair of Eigenvalues

For a pure imaginary pair of eigenvalues, the following condition must hold,

$$\mathrm{tr}(DG_{\varepsilon}(x,r)) = 0 \quad , \qquad \text{(A1.19)}$$

which is given by

$$\lambda + \mu + (n-3)x^2 + (m-3)r^2 = 0 \quad . \qquad \text{(A1.20)}$$

Additionally, $\det(DG_\varepsilon(x,r)) > 0$ which, from (A1.15), implies

$$\lambda + m\mu + (3mn-3)x^2 < 0 \quad , \tag{A1.21}$$

since $r^2 = n\mu + x^2 > 0$.

Hopf bifurcations occur only for $r \neq 0$. Substitution of (A1.12) into (A1.20) yields the condition for Hopf bifurcation in terms of x alone,

$$(\lambda + (m-2)\mu) + (mn - 2n - 3)x^2 = 0 \tag{A1.22}$$

which has solutions

$$x_{7,8} = \pm \sqrt{\frac{\mu(2-m)-\lambda}{n(m-2)-3}} \quad . \tag{A1.23}$$

Substitution of these solutions into the $\dot{x} = 0$ condition given in (A1.13) yields the Hopf bifurcation condition

$$\varepsilon = \pm 2 \sqrt{\frac{\mu(2-m)-\lambda}{n(m-2)-3}} \left(\frac{\mu(1+m) + \lambda(1+n)}{n(m-2)-3} \right) \tag{A1.24}$$

or

$$\lambda^3(1+n)^2 + \lambda^2\mu(1+n)(3m-n(2-m)) - \lambda\mu^2(1+m)(3(1-m)+2n(2-m))$$
$$- \mu^3(2-m)(1+m)^2 + \frac{\varepsilon^2}{4}(n(m-2)-3)^3 = 0 \quad .$$

B_4: (A1.25)

For the solution branches of equation (A1.25) to be meaningful, the associated r and x bifurcation values must be *real* with $r \neq 0$. Given $m < -1$, $n > 0$ and $mn < 1$, one can easily verify that real x, r can exist only for real λ, μ inside the sector in the right-half (λ,μ) plane defined by $3\mu + n\lambda > 0$ and $\lambda - \mu(2 - m) > 0$. The constraint (A1.21) further restricts the range of validity of solutions of (A1.25).

A1.2.3 Tangencies, Intersections and Codimension-Two Bifurcations

The various tangencies and intersections which are observed in Figure 5.9b can be shown to exist for general parameter values. This follows from the nature of the degeneracy at the relevant parameter values.

The surface (A1.11+), given by the 'plus' branch of (A1.11), is tangent to the saddle-node surface (A1.9). The tangency condition is obtained by eliminating λ from (A1.9) and (A1.11+). The calculation results in the cubic equation,

$$\zeta^3 + 6\zeta^2 + 9\zeta + 4 = 0 \qquad \text{(A1.26)}$$

where $\zeta \triangleq \frac{\mu}{n}\left(\frac{\varepsilon}{2}\right)^{-2/3}$.

The cubic has roots $\zeta = -4, -1, -1$ and these give the intersection curves in $(\lambda,\mu,\varepsilon)$ space.

The tangency curve

$$\mu = -n\left(\frac{\varepsilon}{2}\right)^{2/3} \quad , \quad \lambda = 3\left(\frac{\varepsilon}{2}\right)^{2/3} \qquad \text{(A1.27)}$$

provided by the double root also lies on the Hopf bifurcation surface; this can be shown by direct substitution. This result also confirms the observation that the tangency point p_1 in the (λ,μ) plane lies on the line $\mu = -n\lambda/3$.

The tangency between the 'plus' branch of (A1.11) and the surface defined by (A1.18) is similarly demonstrated. Eliminating λ results in the same cubic equation with $\zeta = \mu \frac{(1-mn)^{2/3}}{n}\left(\frac{\varepsilon}{2}\right)^{-2/3}$. The point at which this tangent curve intersects the (λ,μ) plane is labelled as p_3 in Figure 5.9b.

The existence of the tangency involving the Hopf condition (A1.25) and the saddle-node surface (A1.18) can be verified by eliminating μ from (A1.25) and showing that the discriminant of the cubic equation is zero. The corresponding point in Figure 5.9b is labelled p_2.

Local codimension-two bifurcations of equilibria occur along curves in the parameter space where two local codimension-one bifurcation conditions for the same equilibrium point are simultaneously satisfied. Only some of the intersections of the various bifurcation surfaces represent such curves since some of the intersections relate to bifurcation conditions involving different equilibrium points and therefore correspond to simultaneous but unconnected bifurcations.

Codimension-two bifurcations may be of two types - those which involve a double degeneracy in the linearization and those which, in addition to the (single) linear degeneracy required for bifurcation, involve a non-linear degeneracy. To determine the linearly degenerate codimension-two points, it is sufficient to note that for the planar equations under study all such local codimension-two bifurcations of equilibria involve double zero eigenvalues. Thus, at such points of equilibrium, $\det(DG_\varepsilon) = 0$ and $\mathrm{tr}(DG_\varepsilon) = 0$.

For $r = 0$, the zero determinant condition yields $x_{1,2}$ and $x_{3,4}$ while the zero trace condition gives, from (A1.20),

$$x_{9,10} = \pm \sqrt{\frac{\lambda+\mu}{3-n}} \quad . \tag{A1.28}$$

Equating either $x_{1,2}$ or $x_{3,4}$ to $x_{9,10}$ results in the condition

$$\frac{\mu}{n} = -\frac{\lambda}{3} \quad . \tag{A1.29}$$

Combining (A1.29) with the equilibrium condition (A1.5) and using any of the $x_{1,2}$, $x_{3,4}$, or $x_{9,10}$ leads to the condition

$$\lambda = 3\left(\frac{\varepsilon}{2}\right)^{2/3} \quad , \qquad \mu = -n\left(\frac{\varepsilon}{2}\right)^{2/3} \quad , \tag{A1.30}$$

which corresponds to the point p_1.

For $r \neq 0$, the zero determinant condition corresponds to $x_{3,4}$ and $x_{5,6}$ and the zero trace condition results in $x_{7,8}$. Combining $x_{3,4}$ with $x_{7,8}$, the equilibrium condition (A1.18) leads to p_1 again.

Combining $x_{5,6}$, $x_{7,8}$ and the $r \neq 0$ equilibrium condition (A1.18) yields

$$\lambda = (mn(1+m) + 3(1-mn))(1-mn)^{-2/3}\left(\frac{\varepsilon}{2}\right)^{2/3} \qquad \text{(A1.31a)}$$

$$\mu = -n(1+m)(1-mn)^{-2/3}\left(\frac{\varepsilon}{2}\right)^{2/3} \qquad \text{(A1.31b)}$$

which corresponds to p_2.

Consequently, p_1 and p_2 are the only points where a double zero eigenvalue occurs at the same equilibrium. One can show that at p_1 and p_2, the respective Jordan forms of DG_ε are

$$\begin{bmatrix} 0 & 0 \\ 0 & 0 \end{bmatrix} \quad \text{and} \quad \begin{bmatrix} 0 & 1 \\ 0 & 0 \end{bmatrix}, \qquad \text{(A1.32)}$$

corresponding, respectively, to the planar representation of the *saddle-node/Hopf* bifurcation and the *Takens/Bogdanov* bifurcation. The unfoldings for these bifurcations are available in the literature (Guckenheimer & Holmes [1983]) and no attempt is made to generate the specific normal forms for these cases.

The degeneracy at p_3 is also of codimension-two. Here, the degeneracy involves the vanishing of the cubic term in the bifurcation along the 'plus' branch of (A1.11). This bifurcation corresponds to a degenerate Hopf bifurcation in the original three-dimensional system. A rigorous treatment of this bifurcation can be found in the work of Takens [1973].

A1.3 HIGHER-ORDER ASYMMETRIC PERTURBATIONS

The general asymmetric perturbation of the pitchfork/Hopf normal form corresponding to region 3b of the (m,n) parameter plane, which maintains $r \to -r$ invariance, is (to third-order)

$$\begin{aligned} \dot{x} &= \varepsilon + \beta x^2 + \gamma r^2 + \lambda x + x(-x^2 + mr^2) \\ \dot{r} &= \delta r x + \mu r + r(-r^2 + nx^2) \end{aligned} \qquad \text{(A1.33)}$$

where $m < -1$, $n > 0$ and $mn < 0$.

The *local* bifurcation sets for the general perturbed normal form (A1.33) are determined in a similar manner to that adopted for the simplified perturbation model in §A2.2.

If the right-side of (A1.33) is denoted by

$$G_{\varepsilon,\beta,\gamma,\delta} = \begin{bmatrix} \varepsilon + \beta x^2 + \gamma r^2 + \lambda x + x(-x^2 + mr^2) \\ \delta r x + \mu r + r(-r^2 + nx^2) \end{bmatrix}, \qquad \text{(A1.34)}$$

then,

$$DG_{\varepsilon,\beta,\gamma,\delta} = \begin{bmatrix} \lambda + 2\beta x - 3x^2 + mr^2 & 2mxr + 2\gamma r \\ 2nxr + \delta r & \mu - 3r^2 + \delta x + nx^2 \end{bmatrix} \qquad \text{(A1.35)}$$

and

$$\det(DG_{\varepsilon,\beta,\gamma,\delta}) = (\lambda + 2\beta x - 3x^2 + mr^2)(\mu - 3r^2 + \delta x + nx^2) - (2\gamma r + 2mxr)(2nxr + \delta r) \quad . \tag{A1.36}$$

Equilibrium solutions of (A1.33) satisfy

$$\dot{x} = 0 : \begin{cases} \varepsilon + \beta x^2 + \lambda x - x^3 = 0 \quad , \quad r = 0 & \text{(A1.37a)} \\ (\varepsilon + \gamma\mu) + (\beta + n\gamma + m\delta)x^2 + (\lambda + m\mu + \gamma\delta)x + (mn - 1)x^3, \quad r \neq 0 \end{cases}$$

$$\dot{r} = 0 : \begin{cases} r = 0 \\ r^2 = \mu + \delta x + nx^2 \quad , \quad r \neq 0 \end{cases} \tag{A1.37b}$$

Bifurcations of equilibria associated with a *zero eigenvalue* of $DG_{\varepsilon,\beta,\gamma,\delta}$ are classified according to whether a bifurcation emanates from an $r = 0$ equilibrium or an $r \neq 0$ equilibrium.

r = 0 Equilibria : Here, $\dot{r} = 0$ is automatically satisfied and the condition $\dot{x} = 0$ is given by

$$\varepsilon + \beta x^2 + \lambda x - x^3 = 0 \tag{A1.38}$$

while, with $r = 0$, $\det(DG_{\varepsilon,\beta,\gamma,\delta}) = 0$ becomes

$$(\lambda + 2\beta x - 3x^2)(\mu + \delta x + nx^2) = 0 \quad . \tag{A1.39}$$

Consequently, $\det(DG_{\varepsilon,\beta,\gamma,\delta}) = 0$ when either

$$(\lambda + 2\beta x - 3x^2) = 0 \quad \text{or} \quad (\mu + \delta x + nx^2) = 0 \quad . \qquad \text{(A1.40)}$$

Re-arrangement of the $\dot{x} = 0$ condition (equation (A1.38)) in the form

$$\varepsilon + (\lambda + 2\beta x - 3x^2)x - \beta x^2 + 2x^3 = 0 \qquad \text{(A1.41)}$$

yields, by virtue of the first of equations (A1.40), the bifurcation condition

$$\varepsilon - \beta x^2 + 2x^3 = 0 \quad . \qquad \text{(A1.42)}$$

For $\varepsilon > 0$, $\beta < 3\varepsilon^{1/3}$, the discriminant of (A1.42) is positive and the equation possesses a single (negative) real x root and two complex conjugate roots. For $\varepsilon > 0$, $\beta > 3\varepsilon^{1/3}$, the discriminant is negative and equation (A1.42) possesses two positive real roots and one negative real root. At $\beta = 3\varepsilon^{1/3}$, the two positive roots coalesce at a *cusp* bifurcation point (see below).

For fixed ε, β, and for each real root $x = x_1^*$ of (A1.42), the corresponding bifurcation sets in the (λ,μ) plane are defined by :

$$B_1: \qquad \lambda = -2\beta x_1^* + 3x_1^{*2} \quad . \qquad \text{(A1.43)}$$

Similarly, the bifurcation sets in the (λ,μ) plane, corresponding to the second of equations (A1.40), are defined, implicitly, for fixed ε, β, δ, n and each real root of $\mu + \delta x + nx^2 = 0$, $x = x_2^*(\mu)$, by

$$B_2: \qquad \lambda = -\varepsilon/x_2^*(\mu) - \beta x_2^*(\mu) + x_2^*(\mu)^2 \quad . \qquad \text{(A1.44)}$$

$r \neq 0$ Equilibria : For $r \neq 0$, the equation $\dot{r} = 0$ is satisfied by

$$r^2 = \mu + \delta x + nx^2 \quad . \qquad \text{(A1.45)}$$

Substitution of (A1.45) into the condition $\det(DG_{\varepsilon,\beta,\gamma,\delta}) = 0$ yields

$$-2r^2((\lambda + m\mu + \delta\gamma) + 2(\beta + n\gamma + m\delta)x + 3(mn - 1)x^2) = 0 \quad . \qquad \text{(A1.46)}$$

Re-arrangement of the $\dot{x} = 0$ condition in the form

$$(\varepsilon + \gamma\mu) + x(2(\beta + n\gamma + m\delta)x + (\lambda + m\mu + \gamma\delta) + 3(mn - 1)x^2) - (\beta + n\gamma + m\delta)x^2 - 2(mn - 1)x^3 = 0 \qquad \text{(A1.47)}$$

yields, with $r \neq 0$ in equation (A1.46), the bifurcation condition

$$(\varepsilon + \gamma\mu) - (\beta + n\gamma + m\delta)x^2 - 2(mn - 1)x^3 = 0 \quad . \qquad \text{(A1.48)}$$

Considering only $\varepsilon > 0$ and values of β, γ, δ for which (A1.48) has real positive and negative roots $x = x_3^*(\mu)$, and for which there exist associated real non-zero r values, the appropriate bifurcation sets in the (λ,μ) plane are defined, implicitly, by the relation

$$B_3: \quad \lambda = -(m\mu + \gamma\delta) - 2(\beta + n\gamma + m\delta)x_3^*(\mu) - 3(mn - 1)x_3^*(\mu)^2 \quad . \tag{A1.49}$$

Bifurcations of equilibria associated with a *pure imaginary pair of eigenvalues* of $DG_{\varepsilon,\beta,\gamma,\delta}$ occur only for $x \neq 0$, $r \neq 0$. The existence of a pure imaginary pair of eigenvalues derives from the condition

$$\mathrm{tr}(DG_{\varepsilon,\beta,\gamma,\delta}) = 0 \tag{A1.50}$$

which, with $r^2 = \mu + \delta x + nx^2$ (*cf.* equation (A1.37b), is given by

$$\lambda + 2\beta x - 3x^2 + (m - 2)r^2 = 0 \quad . \tag{A1.51}$$

Additionally, the existence of a pure imaginary pair of eigenvalues of $DG_{\varepsilon,\beta,\gamma,\delta}$ requires that $\det(DG_{\varepsilon,\beta,\gamma,\delta}) > 0$ which, from (A1.36), implies

$$(\lambda + m\mu + \delta\gamma) + 2(\beta + n\gamma + m\delta)x + 3(mn - 1)x^2 < 0 \tag{A1.52}$$

since $r^2 > 0$.

Substitution of $r^2 = \mu + \delta x + nx^2$ in (A1.51) yields the trace condition in terms of x :

$$(\lambda + (m-2)\mu) + (2\beta + (m-2)\delta)x + ((m-2)n - 3)x^2 = 0 \quad . \tag{A1.53}$$

The $\dot{x} = 0$ condition may be expressed as

$$(\varepsilon + \gamma\mu) + ((\lambda + (m-2)\mu) + (2\beta + (m-2)\delta)x + ((m-2)n - 3)x^2)x$$
$$- (\beta - n\gamma - 2\delta)x^2 + (\gamma\delta + 2\mu)x + 2(n + 1)x^3 = 0 \tag{A1.54}$$

which, with $tr(DG_{\varepsilon,\beta,\gamma,\delta}) = 0$, yields the Hopf bifurcation condition

$$(\varepsilon + \gamma\mu) + (2\mu + \gamma\delta)x - (\beta - n\gamma - 2\delta)x^2 + 2(n + 1)x^3 = 0 \; . \tag{A1.55}$$

For $\varepsilon > 0$, β, γ, $\delta \neq 0$, the range of μ for which (A1.55) yields real roots $x = x_4^*(\mu)$ and real $r \neq 0$, $r^2 = \mu + \delta x_4^*(\mu) + n x_4^*(\mu)^2$, subject to the inequality (A1.52), defines, implicitly, the associated bifurcation sets in the (λ,μ) plane :

$$B_4: \qquad \lambda = - (m-2)\mu - (2\beta + (m-2)\delta)x_4^*(\mu) - ((m-2)n - 3)x_4^*(\mu)^2 \; . \tag{A1.56}$$

A1.4 GLOBAL BIFURCATIONS AND PATH CONSISTENCY

Bifurcations exist which are not reducible to elementary algebraic calculations which avoid numerical integration of trajectories. Bifurcations of this kind are generally of a *global* nature and are distinguished from the *local* bifurcations described in §A1.2 and §A1.3. The simplest global bifurcations are associated with transitions involving *heteroclinic* and *homoclinic* saddle-node connections. Local analyses cannot detect such bifurcations, except very near the degeneracies from which they emanate. The procedure involves the transformation the planar representation of the system at the point of degeneracy to an equivalent perturbed Hamiltonian system (Guckenheimer & Holmes [1983]). However, there are technical difficulties when applying the procedure in a general context. Less rigorously, the existence of global bifurcational phenomena can be detected by checking 'path consistencies'. The notion of path consistency is that the phase portrait arrived at for any combination of parameters must be the same regardless of the path taken (and hence which bifurcation surfaces are crossed) from any initial combination of parameters. By appealing to the known unfoldings of the relevant degeneracies, some idea of the location of global bifurcations in parameter space can be obtained, at least locally in some neighbourhood of the degenerate point. In the present analysis, the simplest arrangement of global bifurcation curves compatible with path consistency and the known unfoldings is assumed. For the systems defined by (A1.1) and (A1.33), the existence of global bifurcational phenomena in the (λ,μ) plane is established by checking path consistencies in the plane.

A1.5 SUMMARY

A simple first-order asymmetric perturbation of the pitchfork/Hopf degeneracy in the absence of reflectional symmetry in the steady-state mode reveals the essential features of the underlying bifurcation structure. The bifurcation sets admit a simple scaling rule which enables the bifurcation structure to be interpreted in a two-parameter control space. Intersections and tangencies are identified with specific codimension-two degeneracies. In particular, the perturbed system organizes codimension-two degeneracies corresponding to complex periodic and quasi-periodic behaviour in the original three-dimensional phase space. Topological changes in the basic structures are possible under the influence of higher-order asymmetric perturbation parameters. Detailed analysis of the more general unfoldings reveals the existence of further coincident bifurcation points which, again, organize stable subcritical and supercritical secondary bifurcations to tori.

REFERENCES

Anderson, J. [1991],

Qualitative Analysis of Non-Linear Transonic Aeroelastic Phenomena, in *Proceedings of the International Forum on Aeroelasticity and Structural Dynamics 1991*, pp.542-551, DGLR-Bericht 91-06, Bonn.

Armbruster, D. [1983],

An Organizing Center for Optical Bistability and Self-Pulsing, *Z. Phys.* B - *Condensed Matter*, **53**, 157-166.

Armbruster, D., Dangelmayr, G. and Güttinger, W. [1985],

Imperfection Sensitivity of Interacting Hopf and Steady-State Bifurcations and their Classification, *Physica* **16D**, 99-123.

Arnol'd, V.I. [1972],

Lectures on Bifurcations in Versal Families, *Russian Mathematical Surveys*, **27**(5), 54-123.

Ashley, H. [1980],

Role of Shocks in 'Sub-Transonic' Flutter Phenomena, *J. Aircraft*, **17**(3), 187-197.

Atkinson, F.V. and Haddock, J.R. [1988],

On Determining Phase Spaces for Functional Differential Equations, *Funkcialaj Ekvacioj*, **31**, 331-347.

Baldock, J.C.A. [1978],

The Identification of the Flutter Mechanism from a Large-Order Flutter Calculation, RAE TR 78017.

Ballhaus, W.F. and Goorjian, P.M. [1978],

Computation of Unsteady Transonic Flows by the Indicial Method, *AIAA J.*, **16**(2), 117-124.

Barkley, D. [1990],

Theory and Predictions for Finite-Amplitude Waves in Two-Dimensional Plane Poiseuille Flow, *Phys. Fluids* A, **2**(6), 955-970.

Batina, J.T. [1988],
Unsteady Transonic Small-Disturbance Theory Including Entropy and Vorticity Effects, AIAA Paper No.88-2278, Presented at the *AIAA/ASME/ASCE/AHS 29th Structures, Structural Dynamics and Materials Conference*, Williamsburg, Virginia, April 18-20.

Bendiksen, O.O [1989],
Nonlinear Flutter and Divergence in Transonic Flow, in *Proceedings of the European Forum on Aeroelasticity and Structural Dynamics 1989*, pp.669-686, DGLR-Bericht 89-01, Bonn.

Berry, M.V. [1976],
Waves and Thom's Theorem, *Advances in Physics*, **25**(1), 1-26.

Bisplinghoff, R.L., Ashley, H. and Halfman, R.L. [1955],
Aeroelasticity, Addison-Wesley, Cambridge, Mass.

Carr, J. [1981],
Applications of Center Manifold Theory, Springer-Verlag, Berlin.

Chafee, N. [1971],
A Bifurcation Problem for a Functional Differential Equation of Finitely Retarded Type, *J. Math. Anal. Appl.*, **35**, 312-348.

Chow, S.-N. and Hale, J.K. [1982],
Methods of Bifurcation Theory, Springer-Verlag, New York.

Chyu, W.J. and Schiff, L.B [1983],
Nonlinear Aerodynamic Modeling of Flap Oscillations in Transonic Flow : A Numerical Validation, *AIAA J.*, **21**(1), 106-113.

Coleman., B.D. and Mizel, V.J. [1966],
Norms and Semi-Groups in the Theory of Fading Memory,
Arch. Rational Mech. Anal., **23**, 87-123.

Coleman., B.D. and Mizel, V.J. [1968],
On the General Theory of Fading Memory,
Arch. Rational Mech. Anal., **29**, 18-31.

Corduneanu, C. and Lakshmikantham, V. [1980],
Equations with Unbounded Delay: A Survey, *Nonlinear Analysis, Theory, Methods & Applications*, **4**(5), 831-877.

Dangelmayr, G. and Armbruster, D. [1983],
Classification of Z(2)-Equivariant Imperfect Bifurcations with Corank 2, *Proc. London Math. Soc.*(3), **46**, 517-546.

Edwards, J.W., Bennett, R.M., Whitlow, W., and Seidel, D.A. [1983],
Time-Marching Transonic Flutter Solutions Including Angle-of-Attack Effects, *J. Aircraft*, **20**(11), 899-906.

Golubitsky, M. and Langford, W.F. [1981],
Classification and Unfoldings of Degenerate Hopf Bifurcations, *J. Differential Equations*, **41**, 375-415.

Golubitsky, M. and Schaeffer, D.G. [1985],
Singularities and Groups in Bifurcation Theory, Vol.1, Applied Mathematical Sciences 51, Springer-Verlag, New York.

Guckenheimer, J. [1981],
On a Codimension Two Bifurcation, in *Dynamical Systems and Turbulence*, D.A. Rand and L.S. Young (eds.), pp.99-142, Lecture Notes in Mathematics, Vol.898, Springer-Verlag, New York.

Guckenheimer, J. [1983],
Persistent Properties of Bifurcations, *Physica* **7D**, 105-110.

Guckenheimer, J. [1984],
Multiple Bifurcation Problems of Codimension Two, *SIAM J. Math. Anal.*, **15**(1), 1-49.

Guckenheimer, J. [1986],
Multiple Bifurcation Problems for Chemical Reactors, *Physica* **20D**, 1-20.

Guckenheimer, J. and Holmes, P.J. [1983],
Nonlinear Oscillations, Dynamical Systems, and Bifurcations of Vector Fields, Applied Mathematical Sciences 42, Springer-Verlag, New York.

Haddock, J.R. and Horner, W.E. [1988],
Precompactness and Convergence in Norm of Positive Orbits in a Certain Fading Memory Space, *Funkcialaj Ekvacioj*, **31**, 349-361.

Haddock, J.R. and Terjéki, J. [1990],
On the Location of Positive Limit Sets for Autonomous Functional Differential Equations with Infinite Delay, *J. Differential Equations*, **86**, 1-32.

Hale, J.K. [1974],
Behavior Near Constant Solutions of Functional Differential Equations, *J. Differential Equations*, **15**, 278-294.

Hale, J.K. [1977],
Theory of Functional Differential Equations, Applied Mathematical Sciences 3, Springer-Verlag, New York.

Hale,J.K. [1979],
Retarded Equations with Infinite Delays, in *Functional Differential Equations and Approximation of Fixed Points*, H.-O. Peitgen and H.-O.Walther (eds.), pp.157-193, Lecture Notes in Mathematics, Vol.730, Springer-Verlag, Berlin.

Hale, J.K. [1985],
Flows on Centre Manifolds for Scalar Functional Differential Equations, *Proc. Royal Soc. Edinburgh*, **101A**, 193-201.

Hale, J.K. [1986],
Local Flows for Functional Differential Equations, in *Multiparameter Bifurcation Theory*, M. Golubitsky and J.M. Guckenheimer (eds.), pp.185-192, Contemporary Mathematics Vol.56, American Mathematical Society, Providence, Rhode Island.

Hale, J.K. and Kato, J. [1978],
Phase Space for Retarded Equations with Infinite Delay, *Funkcialaj Ekvacioj*, **21**, 11-41.

Holmes, P.J. [1977],
Bifurcations to Divergence and Flutter in Flow-Induced Oscillations: A Finite Dimensional Analysis, *J. Sound & Vibration*, **53**(4), 471-503.

Holmes, P.J. [1980],
Unfolding a Degenerate Nonlinear Oscillator : A Codimension Two Bifurcation, in *Nonlinear Dynamics*, R.H.G. Helleman (ed.), pp.473-488, Annals of the New York Academy of Sciences, Vol.357, New York.

Holmes, P.J. [1981],
Center Manifolds, Normal Forms and Bifurcations of Vector Fileds with Application to Coupling Between Periodic and Steady Motions, *Physica* **2D**, 449-481.

Holmes, P.J. and Marsden, J.E. [1978a],
Bifurcation to Divergence and Flutter in Flow-Induced Oscillations: An Infinite Dimensional Analysis, *Automatica*, **14**, 367-384.

Holmes, P.J. and Marsden, J.E. [1978b],
Bifurcations of Dynamical Systems and Nonlinear Oscillations in Engineering Systems, in *Nonlinear Partial Differential Equations and Applications*, J.M. Chadam (ed.), pp.163-206, Lecture Notes in Mathematics, Vol.648, Springer-Verlag, New York.

Holmes, P.J. and Rand, D.A. [1975],
Identification of Vibrating Systems by Generic Modelling, with an Application to Flutter, Institute of Sound and Vibration Research Technical Report No.79, Southampton University, Southampton.

Hui, W.H. and Tobak, M. [1985],
Bifurcation Theory Applied to Aircraft Motions, in *Unsteady Aerodynamics - Fundamentals and Applications to Aircraft Dynamics*, Paper No.26, AGARD CP-386.

Kerlick, G.D. and Nixon, D. [1982],
Calculation of Unsteady Transonic Pressure Distributions by the Indicial Method, *J. Applied Mechanics*, **49**, 273-278.

Kousen, K.A. [1989],
Nonlinear Phenomena in Computational Transonic Aeroelasticity, PhD Thesis, Princeton University, Princeton, New Jersey.

Kousen, K.A. and Bendiksen, O.O. [1988],
Nonlinear Aspects of the Transonic Aeroelastic Stability Problem, AIAA Paper No.88-2306, Presented at the *AIAA/ASME/ASCE/AHS 29th Structures, Structural Dynamics and Materials Conference*, Williamsburg, Virginia, April 18-20.

Langford, W.F. [1979]
Periodic and Steady-State Mode Interactions Lead to Tori, *SIAM J. Appl. Math.*, **37**(1), 22-48.

Langford, W.F. [1983],
A Review of Interactions of Hopf and Steady-State Bifurcations, in *Nonlinear Dynamics and Turbulence*, G.I. Barenblatt, G. Iooss and D.D. Joseph (eds.), pp.215-237, Pitman, London.

Langford, W.F. [1988],

The Taylor-Couette System, in *Singularities and Groups in Bifurcation Theory*, Vol.II, M. Golubitsky, I. Stewart and D.G. Schaeffer, pp.485-512, Applied Mathematical Sciences 69, Springer-Verlag, New York.

Langford, W.F. and Iooss, G. [1980],

Interactions of Hopf and Pitchfork Bifurcations, in *Bifurcation Problems and their Numerical Solution*, H. Mittelmann and H. Weber (eds.), pp.103-134, International Series of Numerical Mathematics ISNM 42, Birkhäuser Verlag, Basel.

Lima, P.F. [1977],

Hopf Bifurcation in Equations with Infinite Delays, PhD Thesis, Brown University, Providence, Rhode Island.

Mabey, D.G. [1989],

Physical Phenomena Associated with Unsteady Transonic Flows, in *Unsteady Transonic Aerodynamics*, D. Nixon (ed.), pp.1-55, Progress in Astronautics and Aeronautics, Vol.120, AIAA, Washington, D.C.

Magnus, R. and Yoshihara, H. [1975],

Unsteady Transonic Flows over an Airfoil, *AIAA J.*, **13**(12), 1622-1628.

Marsden, J.E. and McCracken, M. [1976],

The Hopf Bifurcation and its Applications, Springer-Verlag, New York.

Murakami, S. and Naito, T. [1989],

Fading Memory Spaces and Stability Properties for Functional Differential Equations with Infinite Delay, *Funkcialaj Ekvacioj*, **32**, 91-105.

Naito, T. [1979],

On Linear Autonomous Retarded Equations with an Abstract Phase Space for Infinite Delay, *J. Differential Equations*, **33**, 74-91.

Palis, J. and Takens, F. [1977],

Topological Equivalence of Normally Hyperbolic Dynamical Systems, *Topology*, **16**, 335-345.

Scheidl, R., Troger, H. and Zeman, K. [1983],
Coupled Flutter and Divergence Bifurcation of a Double Pendulum, *Int. J. Non-Linear Mechanics*, **19**(2), 163-176.

Schiff, L.B. [1974],
A Study of the Nonlinear Aerodynamics of Bodies in Nonplanar Motion, NASA TR R-421.

Sethna, P.R. and Shaw, S.W. [1987],
On Codimension-Three Bifurcations in the Motion of Articulated Tubes Conveying a Fluid, *Physica* **24D**, 305-327.

Shearer, M. [1981],
Coincident Bifurcation of Equilibrium and Periodic Solutions of Evolution Equations, *J. Math. Anal. Appl.*, **84**, 113-132.

Stech, H.W. [1985],
Hopf Bifurcation Calculations for Functional Differential Equations, *J. Math. Anal. Appl.*, **109**, 472-491.

Takens, F. [1973],
Unfoldings of Certain Singularities of Vectorfields: Generalized Hopf Bifurcations, *J. Differential Equations*, **14**, 476-493.

Takens, F. [1974a],
Singularities of Vector Fields, *Publ. Math. IHES*, **43**, 47-100.

Takens, F. [1974b],
Forced Oscillations and Bifurcations, *Comm. Math. Inst. Rijkuniversiteit Utrecht*, 3, 1-59.

Thom, R. [1975],
Structural Stability and Morphogenesis, W.A. Benjamin, Reading, Massachusetts (Original edition, Paris, 1972).

Tijdeman, H. and Seebass, R. [1980],
Transonic Flow Past Oscillating Airfoils, *Ann. Rev. Fluid Mech.*, **12**, 181-222.

Tobak, M. and Chapman, G.T. [1985],
Nonlinear Problems in Flight Dynamics Involving Aerodynamic Bifurcations, in *Unsteady Aerodynamics - Fundamentals and Applications to Aircraft Dynamics*, Paper No.25, AGARD CP-386.

Tobak, M. and Pearson, W.E. [1964],
A Study of Nonlinear Longitudinal Dynamic Stability, NASA TR R-209.

Tobak, M. and Schiff, L.B. [1976],
On the Formulation of the Aerodynamic Characteristics in Aircraft Dynamics, NASA TR R-456.

Tobak, M. and Schiff, L.B. [1978],
The Role of Time-History Effects in the Formulation of the Aerodynamics of Aircraft Dynamics, in *Dynamic Stability Parameters*, Paper No.26, AGARD CP-235.

Tobak, M. and Schiff, L.B. [1981],
Aerodynamic Mathematical Modelling - Basic Concepts, in AGARD Lecture Series No.114, Paper No.1.

Ueda, T. and Dowell, E.H. [1984],
Flutter Analysis Using Nonlinear Aerodynamic Forces, *J. Aircraft*, **21**(2), 101-109.

Van der Peet, E.C. [1991],
Nonlinear Aspects of Aeroelastic Problems, Memorandum M-650, Delft University of Technology, Faculty of Aerospace Engineering, Delft, The Netherlands.

Woodcock, D.L. [1979],
The Form of the Solutions of the Linear Integro-Differential Equations of Subsonic Aeroelasticity, RAE TM Str 956.

Woodcock, D.L. [1981],
Aerodynamic Modelling for Studies of Aircraft Dynamics, RAE TR-81016.

Yu, P. and Huseyin, K. [1988],
A Perturbation Analysis of Interactive Static and Dynamic Bifurcations, *IEEE Trans. Automatic Control*, **33**(1), 28-41.

Zwaan, R.J. [1991],
Private Communication.

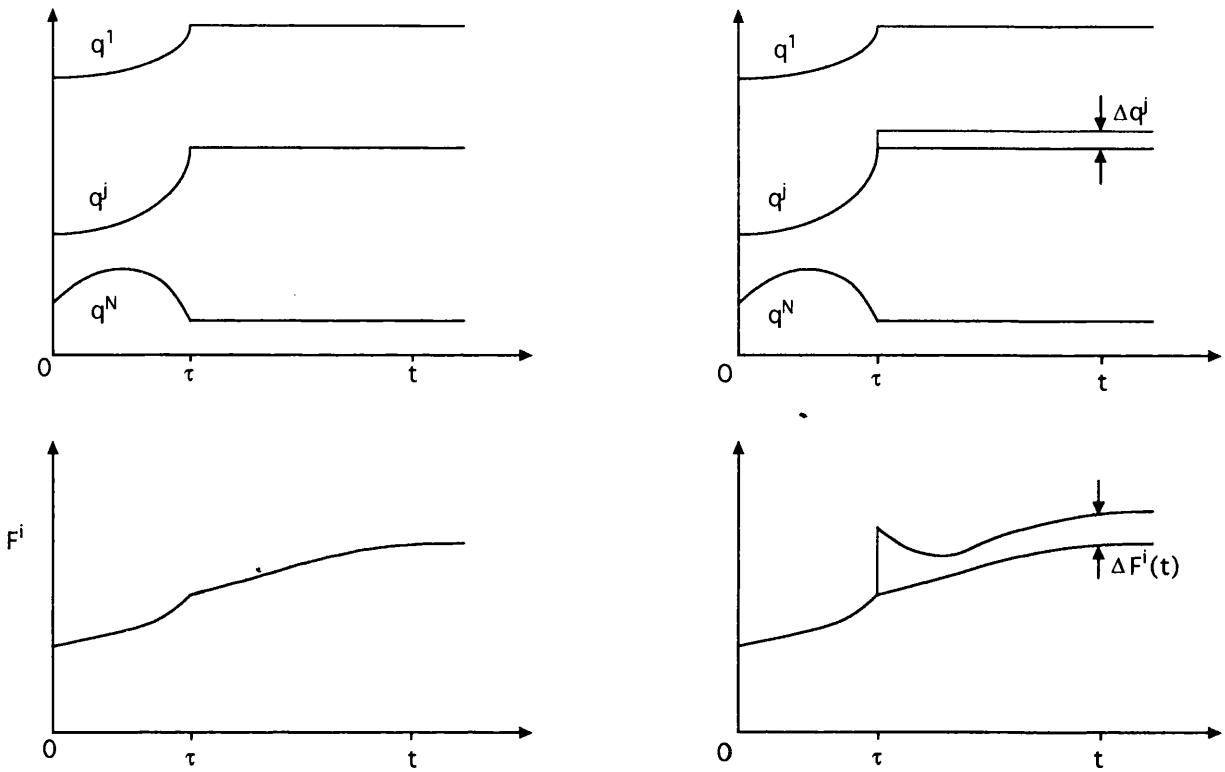

$$\mathcal{F}^{ij}_{q}(q_{\tau}, t, \tau) \triangleq \lim_{\Delta q^j \to 0} \frac{\Delta F^i}{\Delta q^j}$$

Figure 2.1 Definition of Non-Linear Indicial Response.
(Adapted from Schiff [1974])

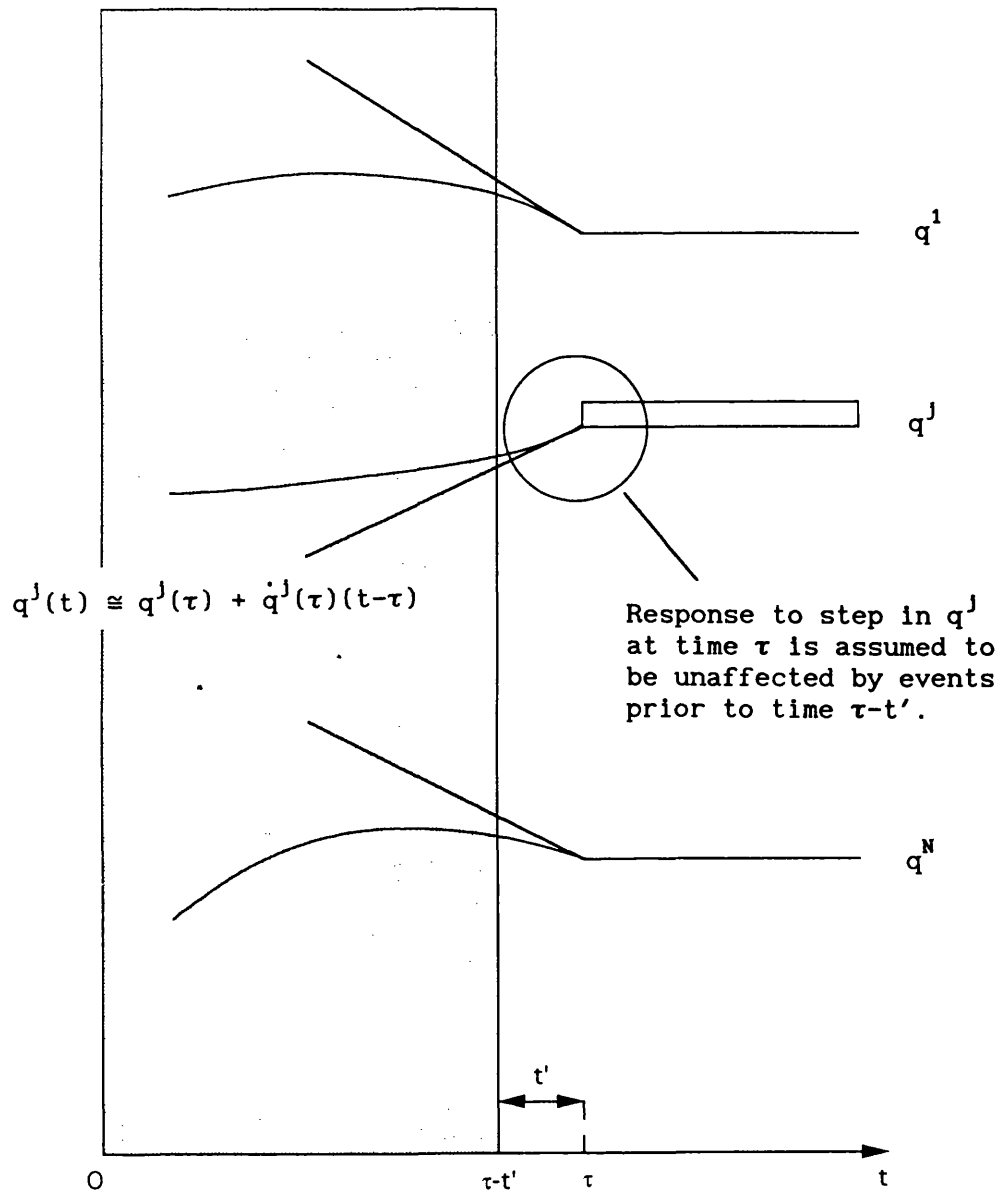

Figure 2.2 Dependence of Indicial Response on Recent Past.
(Adapted from Schiff [1974])

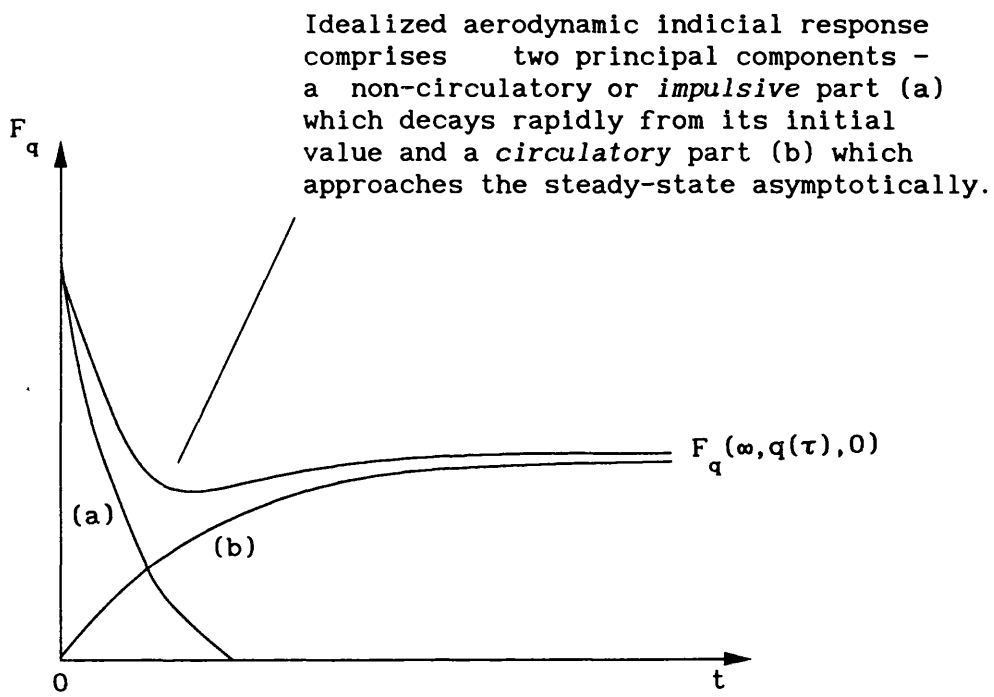

Figure 2.3 Generic Characteristics of the Indicial Response.

(Adapted from Tobak & Schiff [1981])

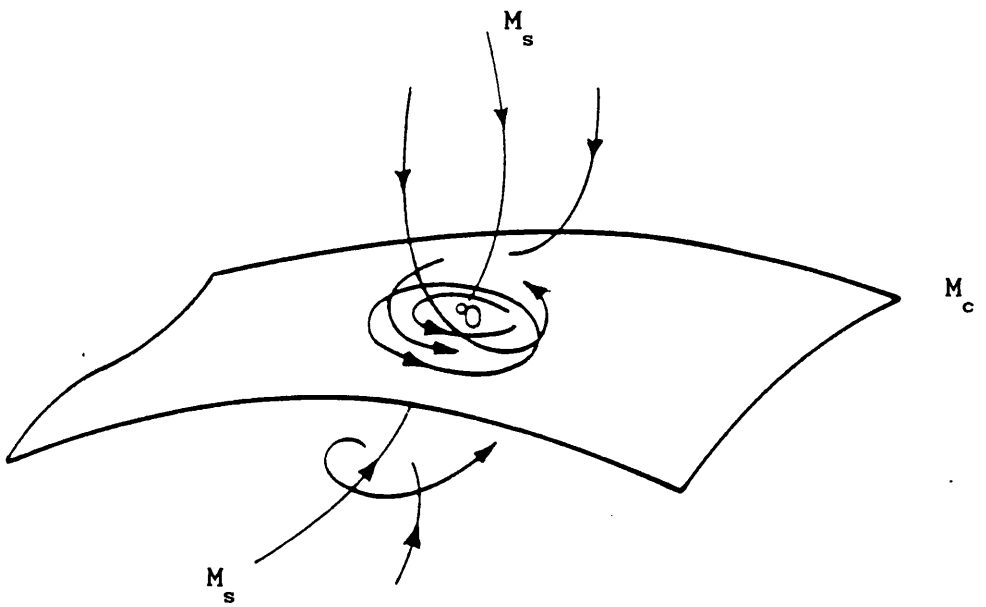

Figure 3.1 Two-Time-Scale Structure in the Neighbourhood of Bifurcation.
(Reproduced from Holmes & Marsden [1978])

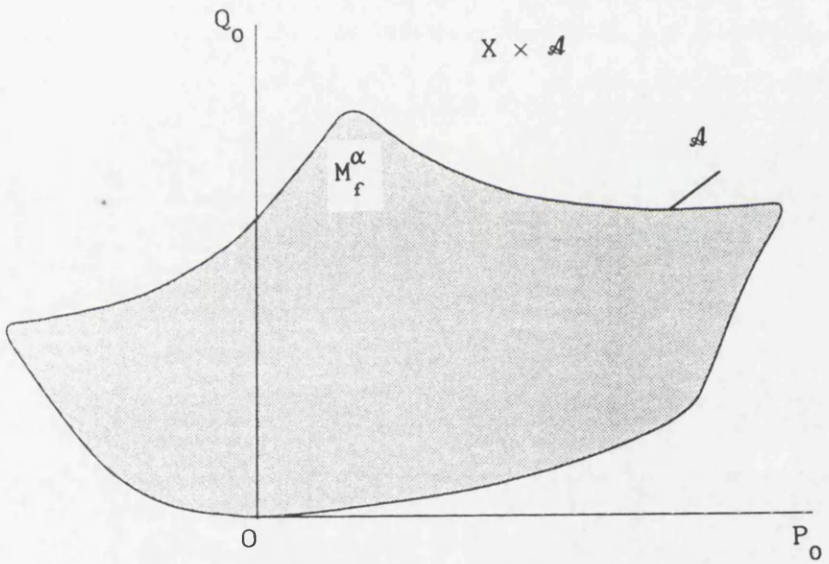

Figure 3.2 The Centre-Manifold in State-History ~ Parameter Space.

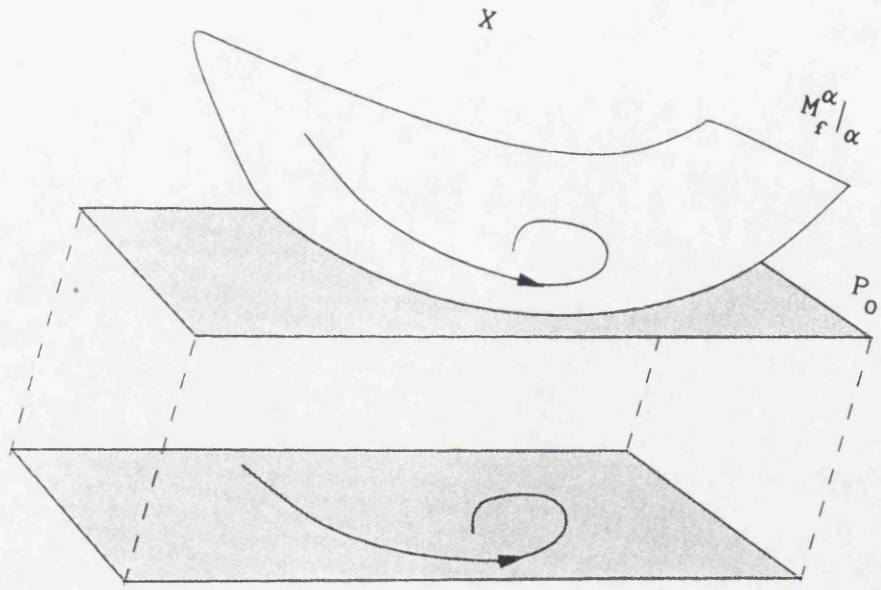

Figure 3.3 Eigenspace Projection of the State Trajectory on the Centre-Manifold.

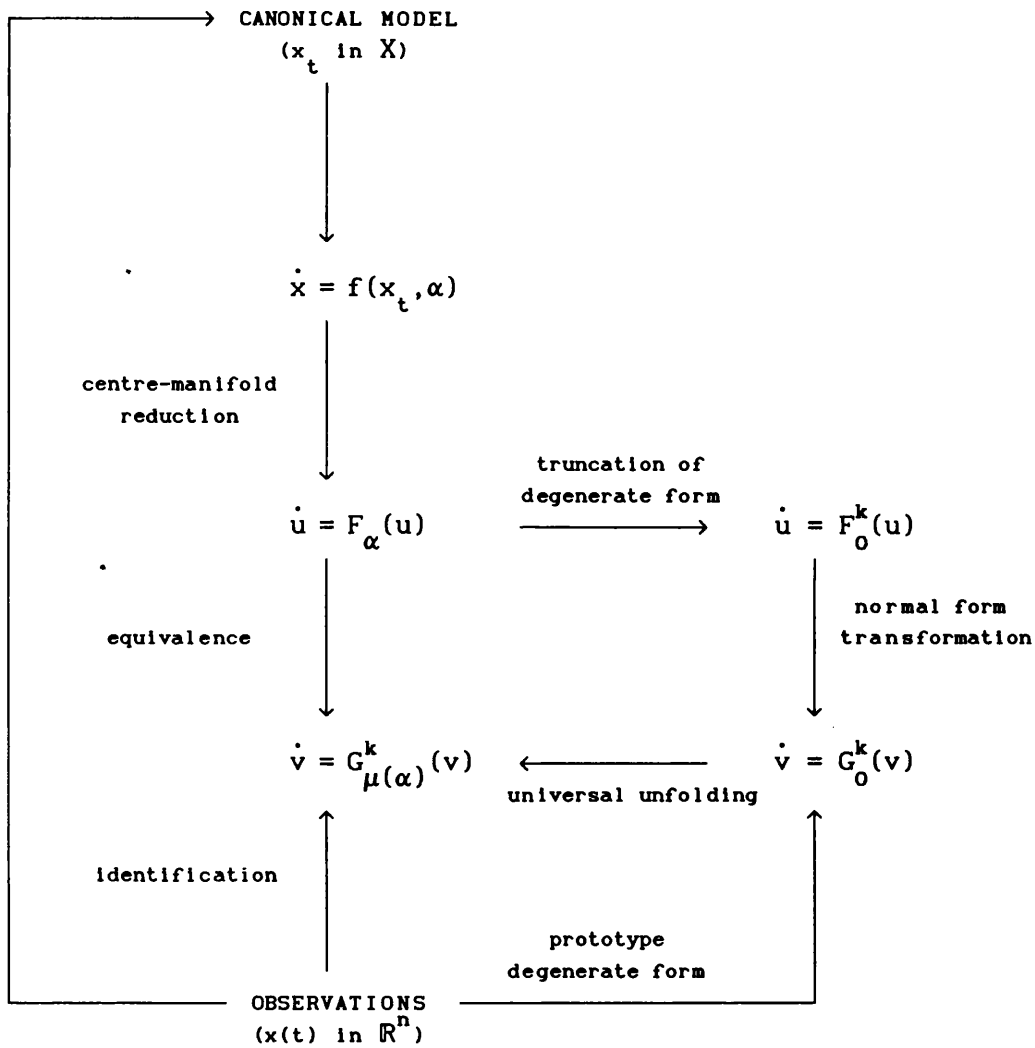

Figure 3.4 Qualitative Model Identification and Equivalence Map.

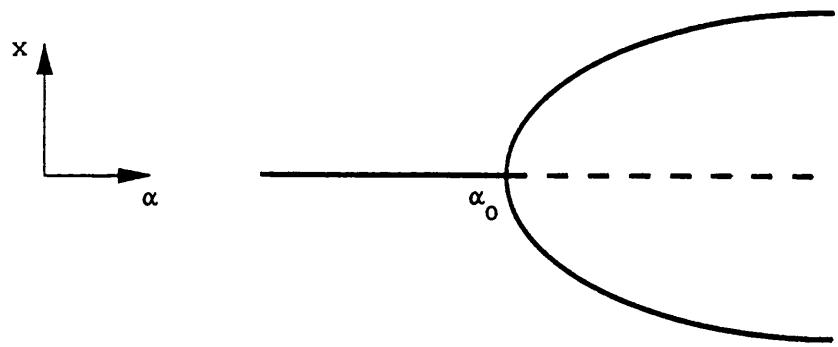

(a) Pitchfork Bifurcation

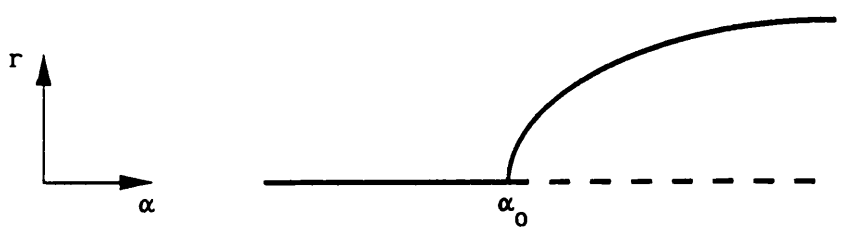

(b) Hopf Bifurcation

Figure 4.1 Generic One-Parameter Bifurcations of Equilibria.

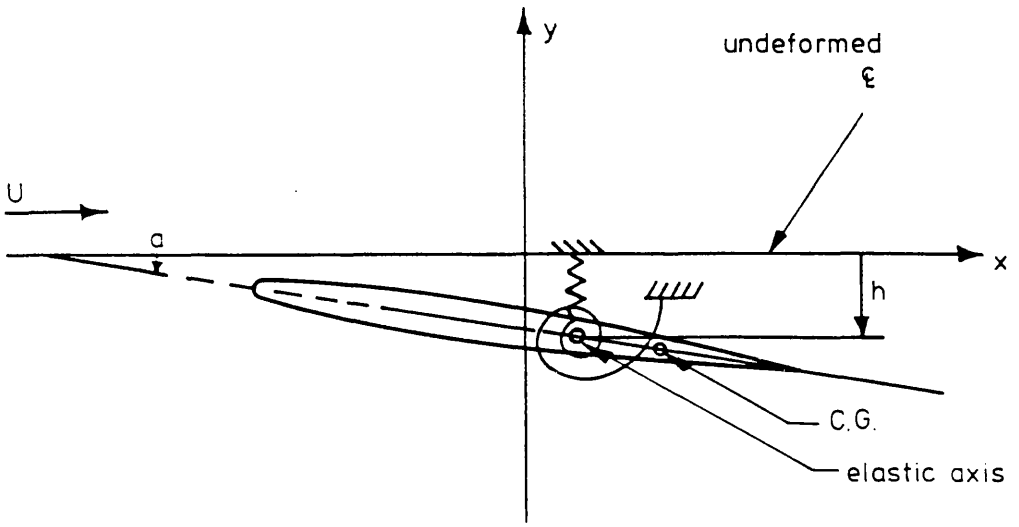

Figure 5.1 Typical Section Aerofoil.

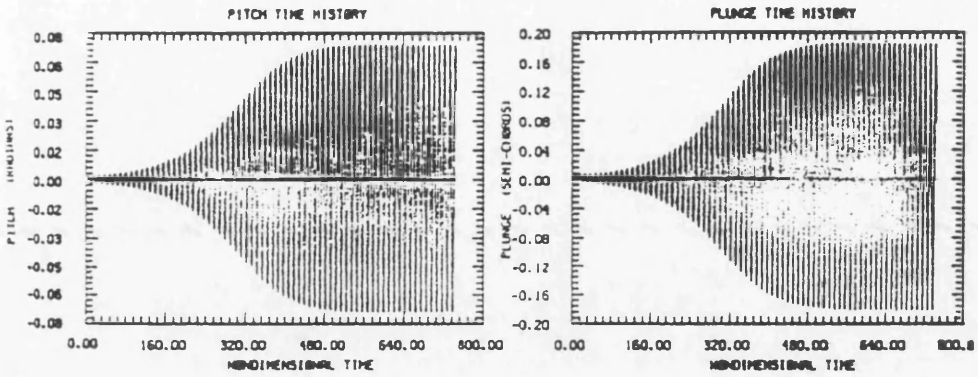

(a) Limit Cycle Flutter (M = 0.87, $\bar{U}$ = 2.00).

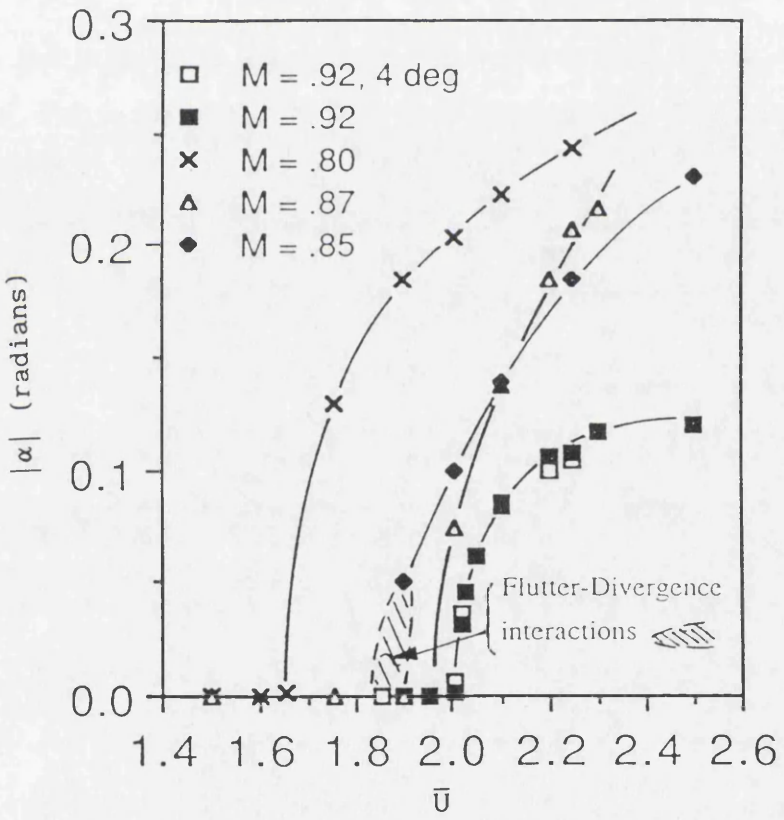

(b) Pitch Limit Cycle Amplitude vs Reduced Velocity

Figure 5.2 Non-Linear Flutter in Transonic Flow.
(Reproduced from Kousen [1989])

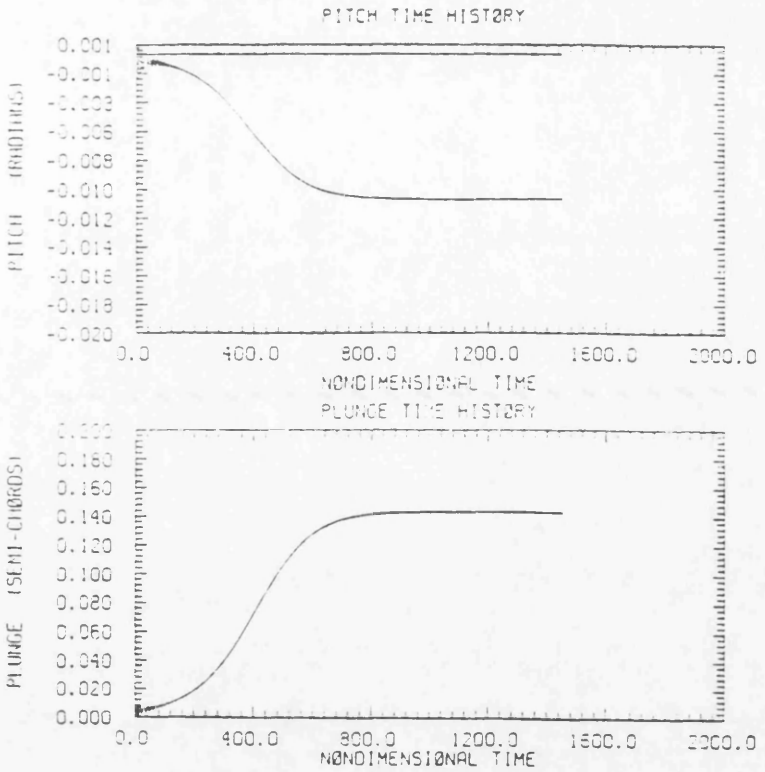

(a) ($M = 0.85$, $\bar{U} = 1.80$)

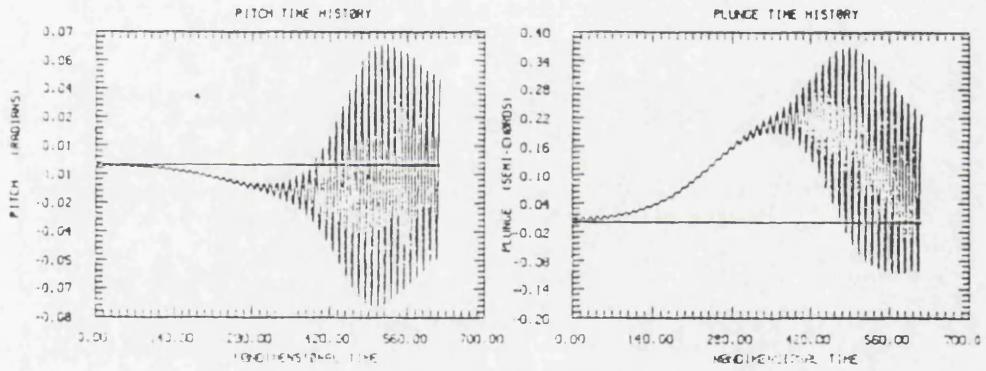

(b) ($M = 0.85$, $\bar{U} = 1.90$)

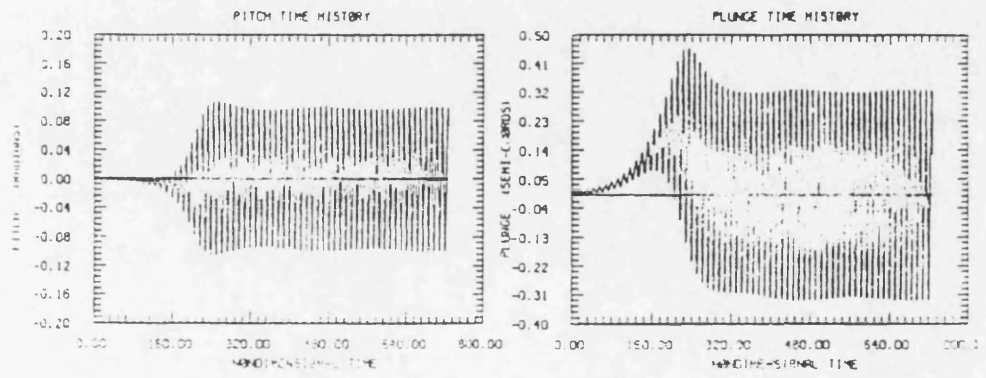

(c) ($M = 0.85$, $\bar{U} = 2.00$)

Figure 5.3 Non-Linear Divergence and Divergence/Flutter Interaction.
(Reproduced from Kousen [1989])

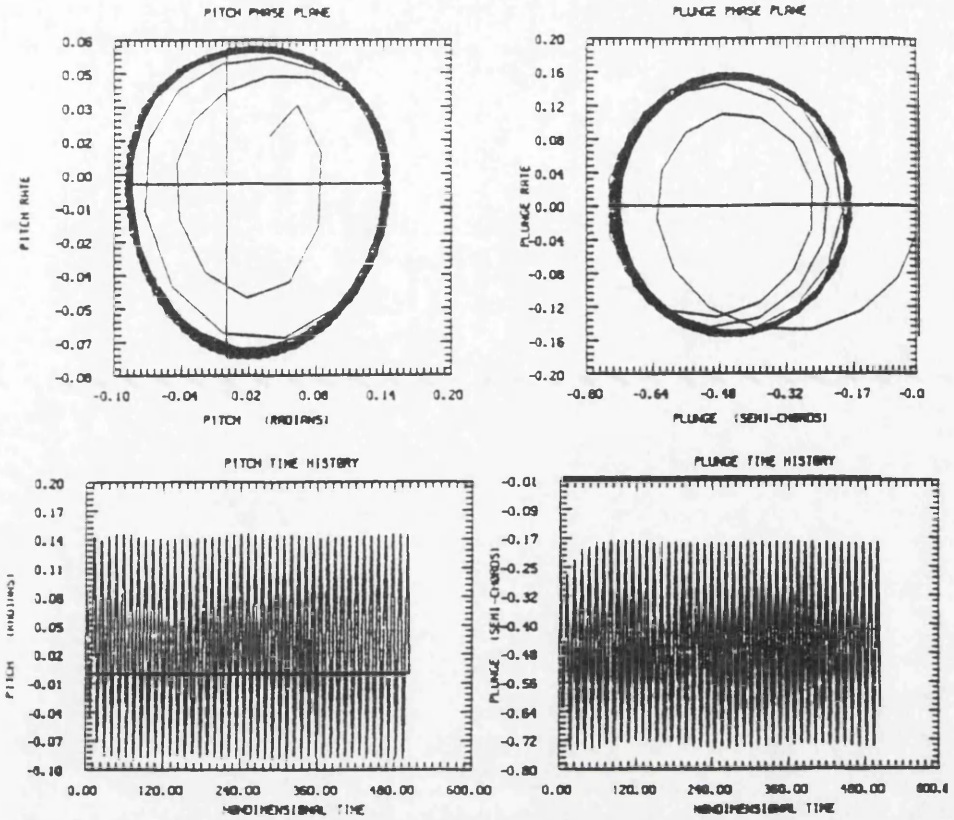

(a) α_0 = 2.00 degrees

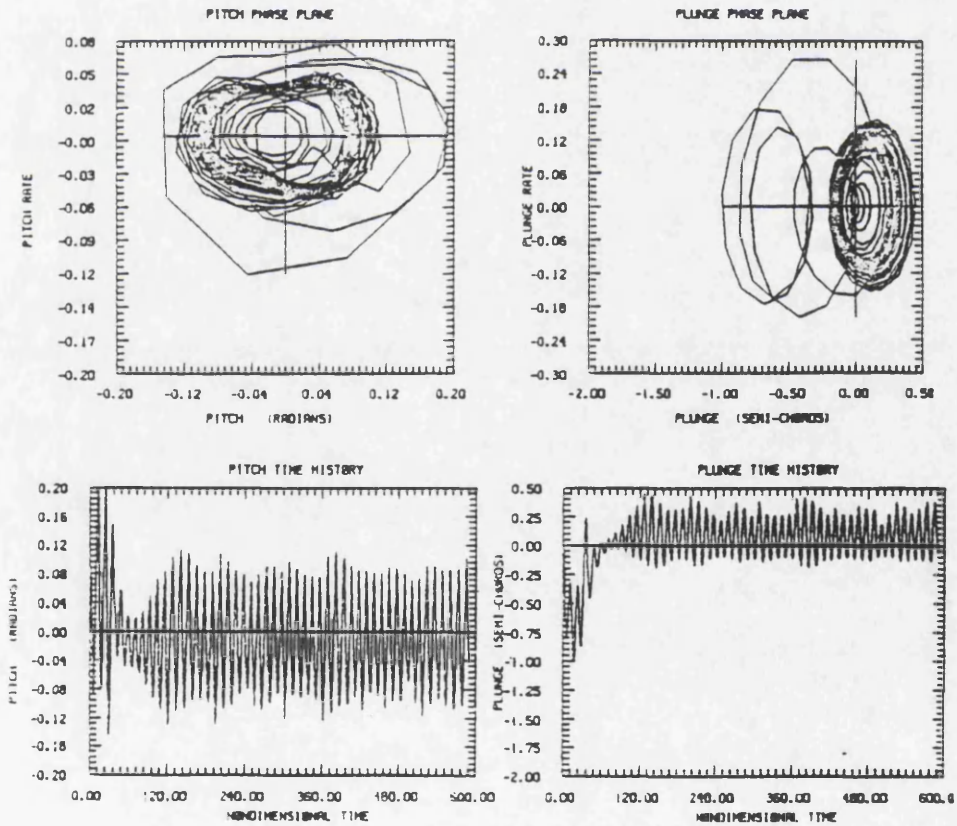

(b) α_0 = 4.00 degrees

Figure 5.4 Non-Linear Interactions with Structural Pre-twist.

($M = 0.85$, $\bar{U} = 1.85$)

(Reproduced from Kousen [1989])

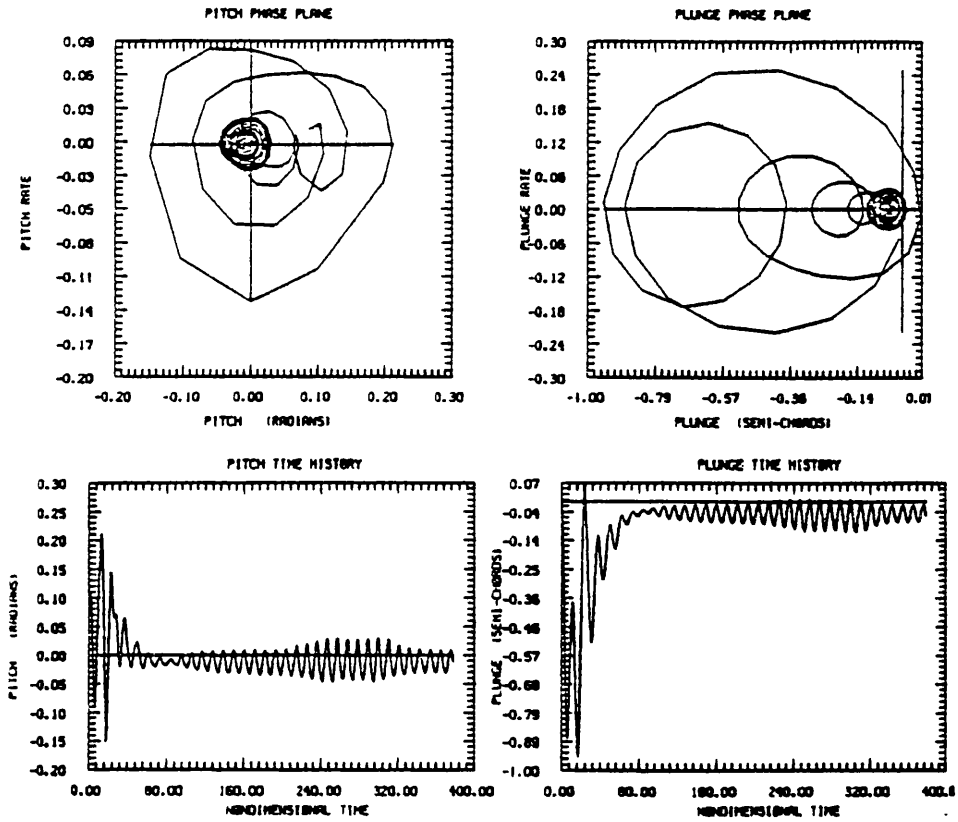

(c) α_0 = 4.75 degrees

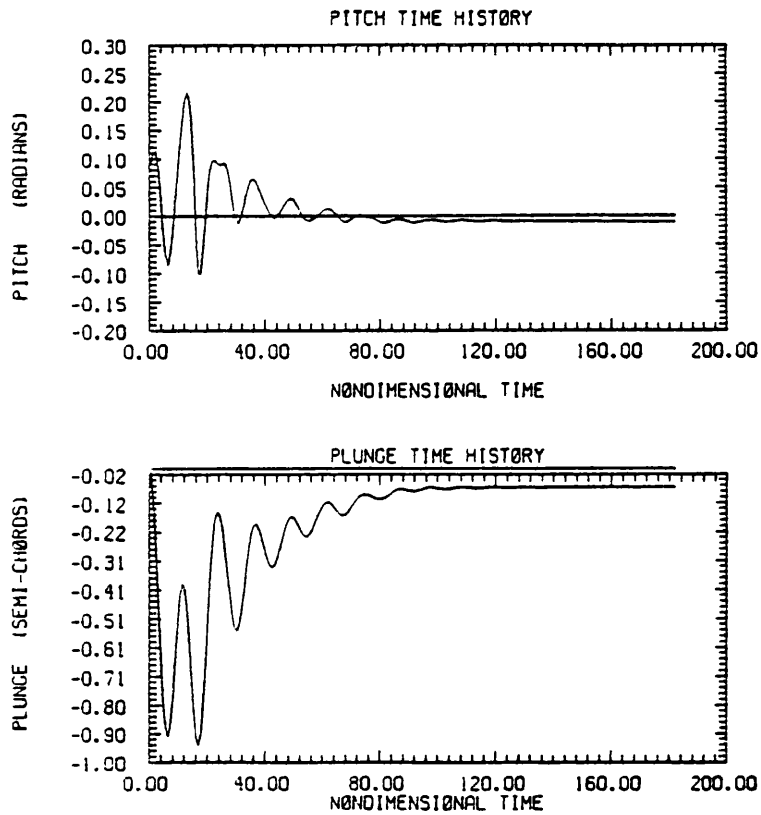

(d) α_0 = 5.00 degrees

Figure 5.4 (Cont'd)

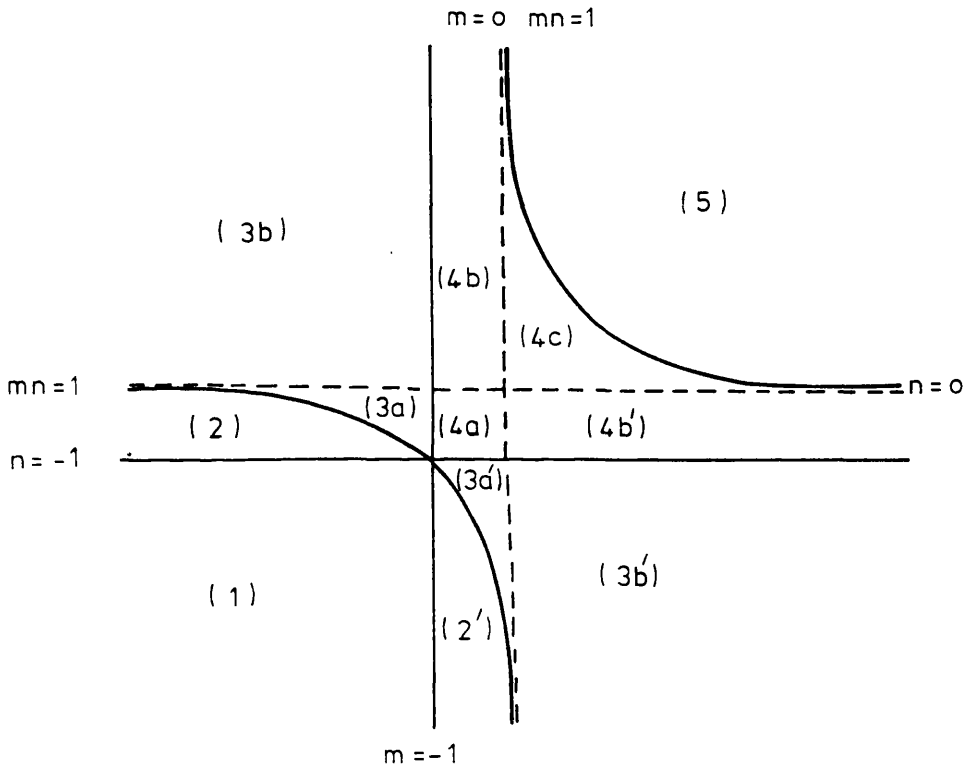

Figure 5.5 (m,n) Parameter Plane.
(Adapted from Golubitsky & Schaeffer [1985])

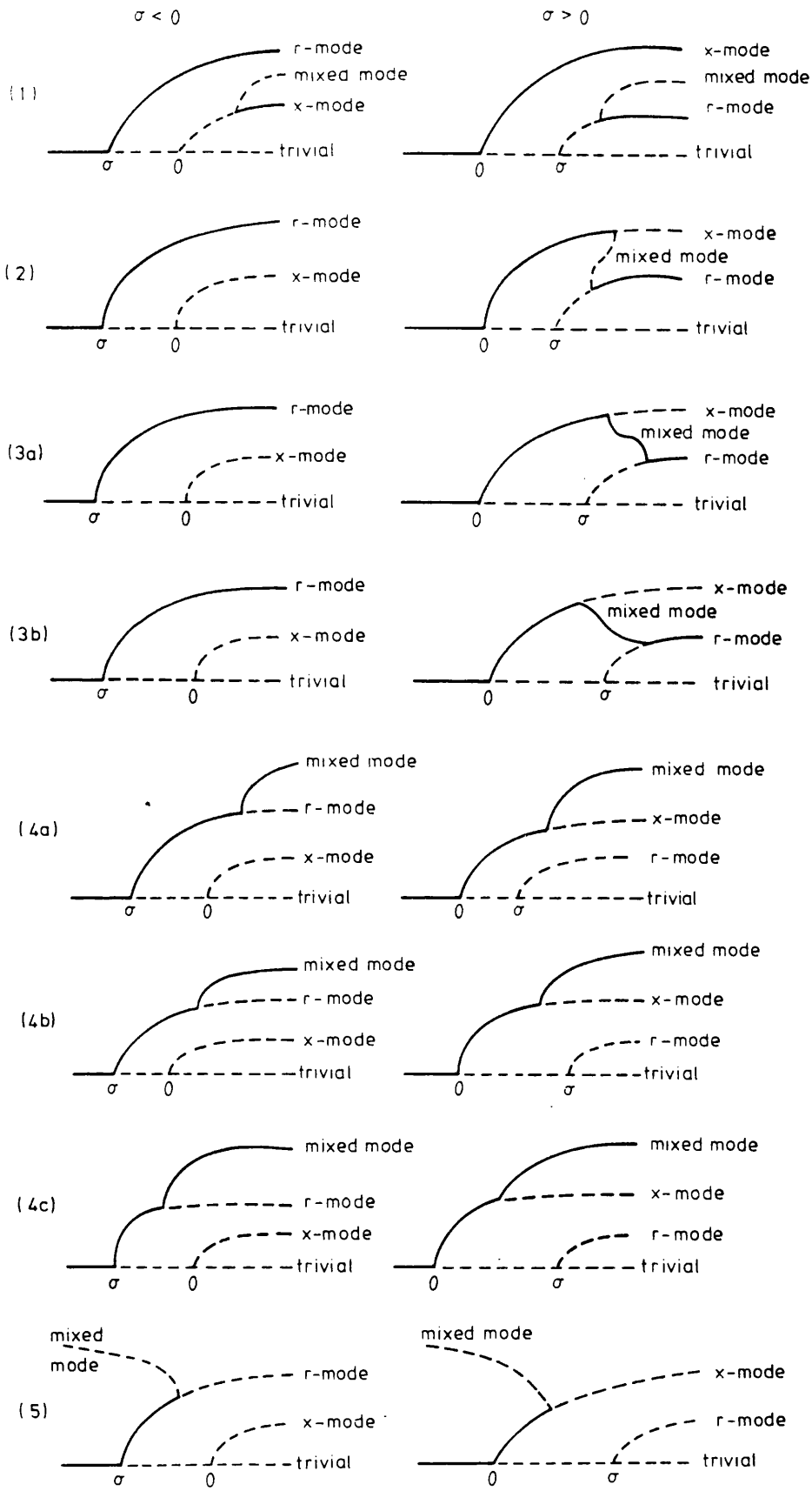

* Unstable solutions are indicated by dashed lines.

Figure 5.6 Perturbed Bifurcation Diagrams.
(Adapted from Golubitsky & Schaeffer [1985])

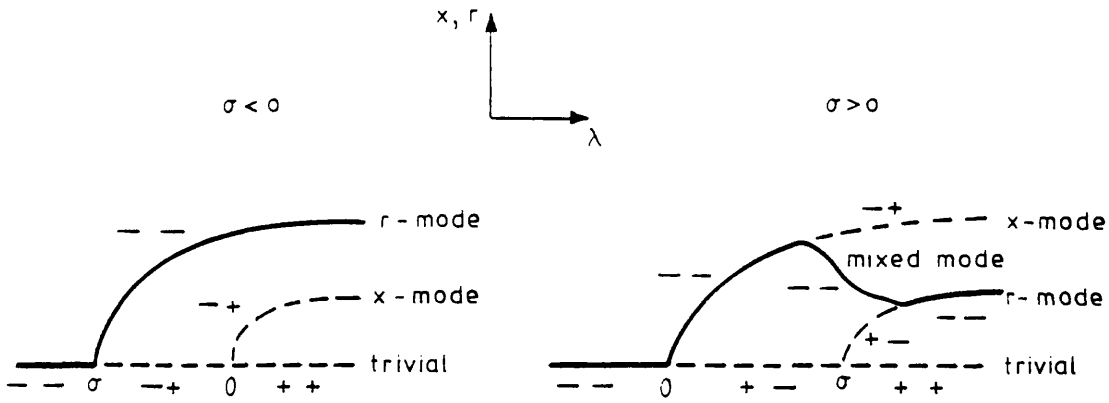

Figure 5.7 Stability Assignments in Region 3b.

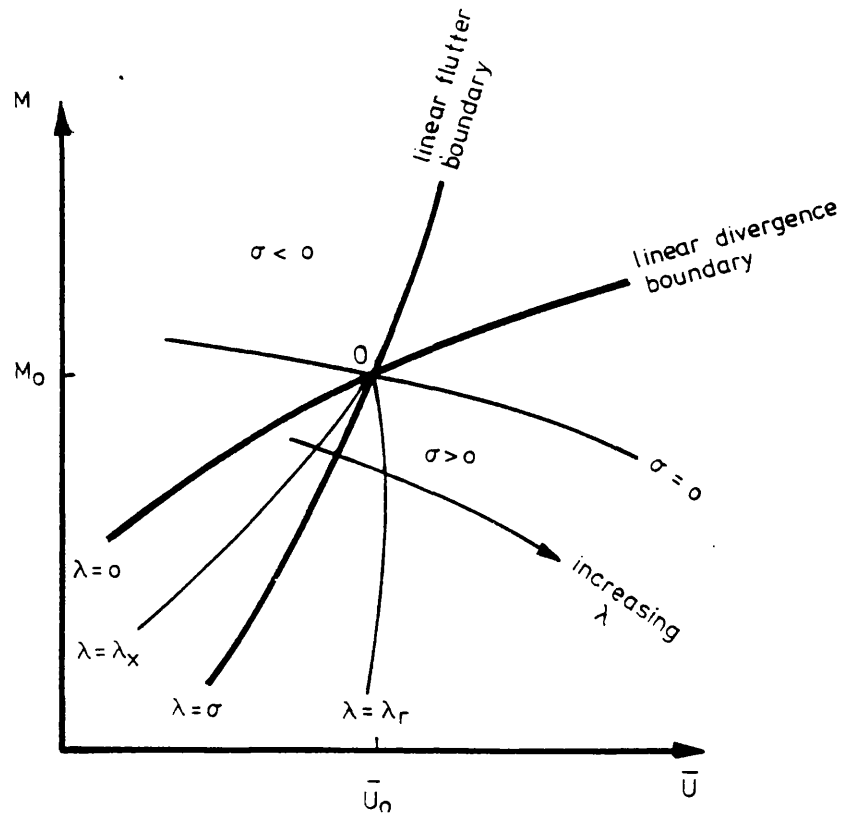

Figure 5.8 Hypothetical Bifurcation Sets in Physical Parameter Plane.

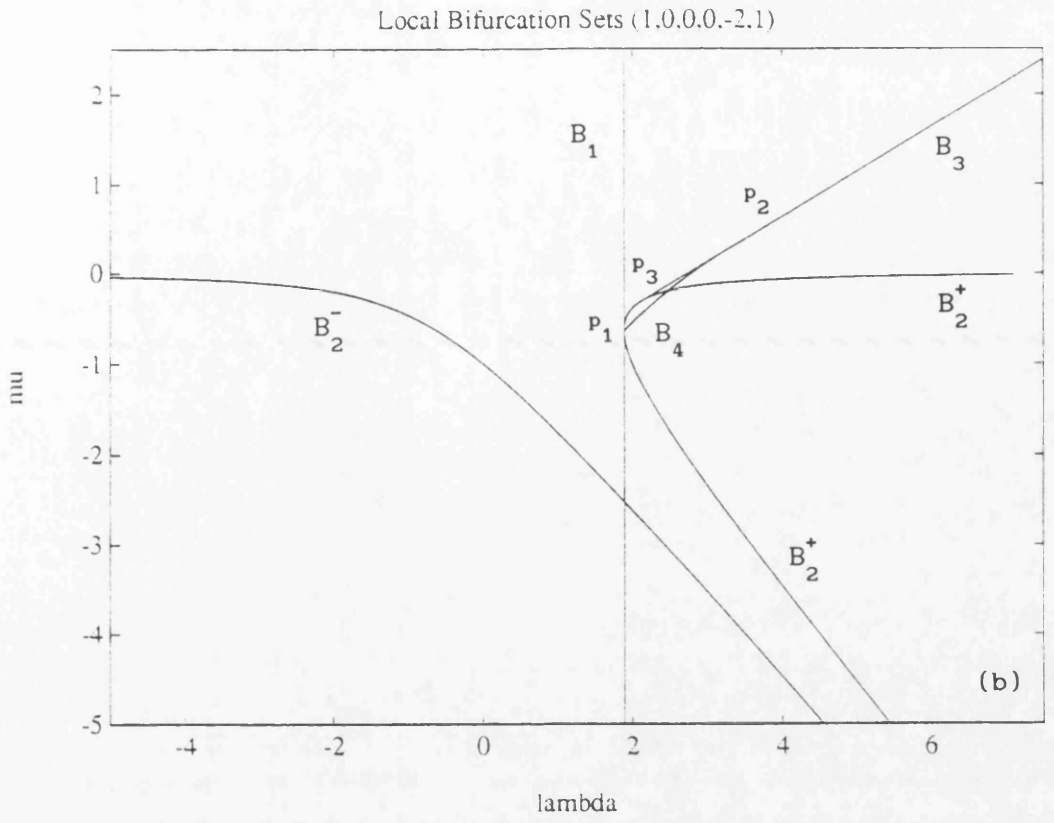

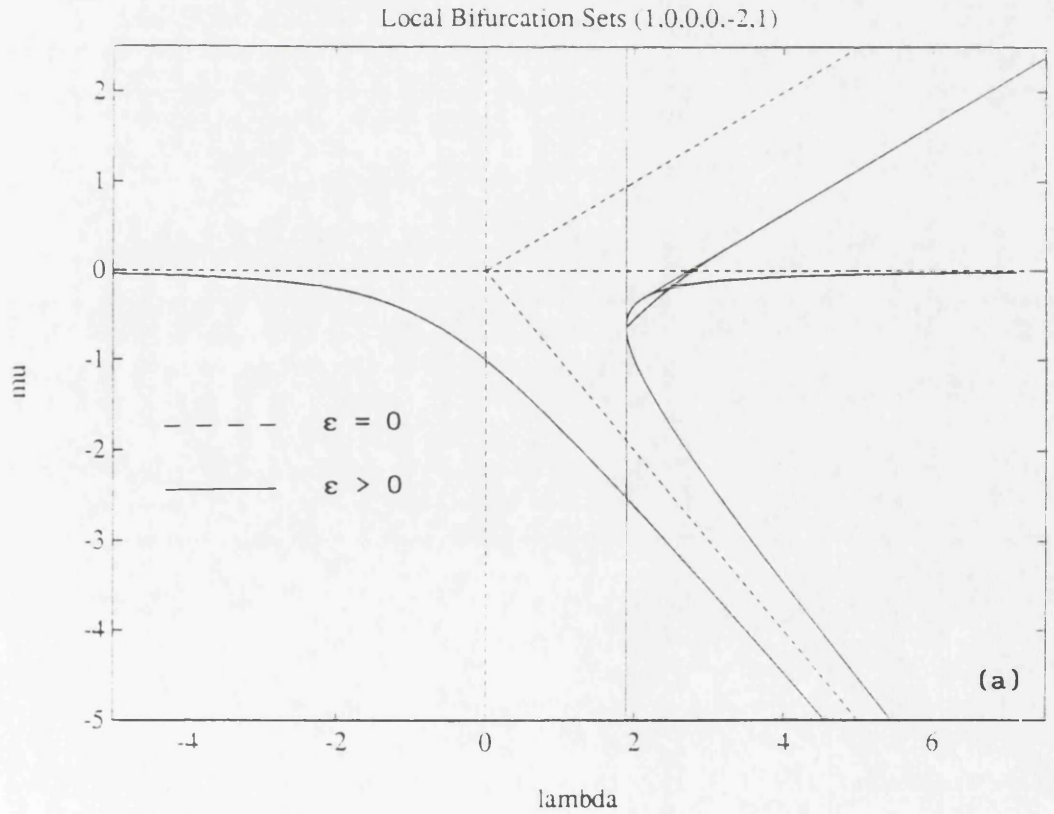

Figure 5.9 Local Bifurcation Sets ($\varepsilon > 0$).

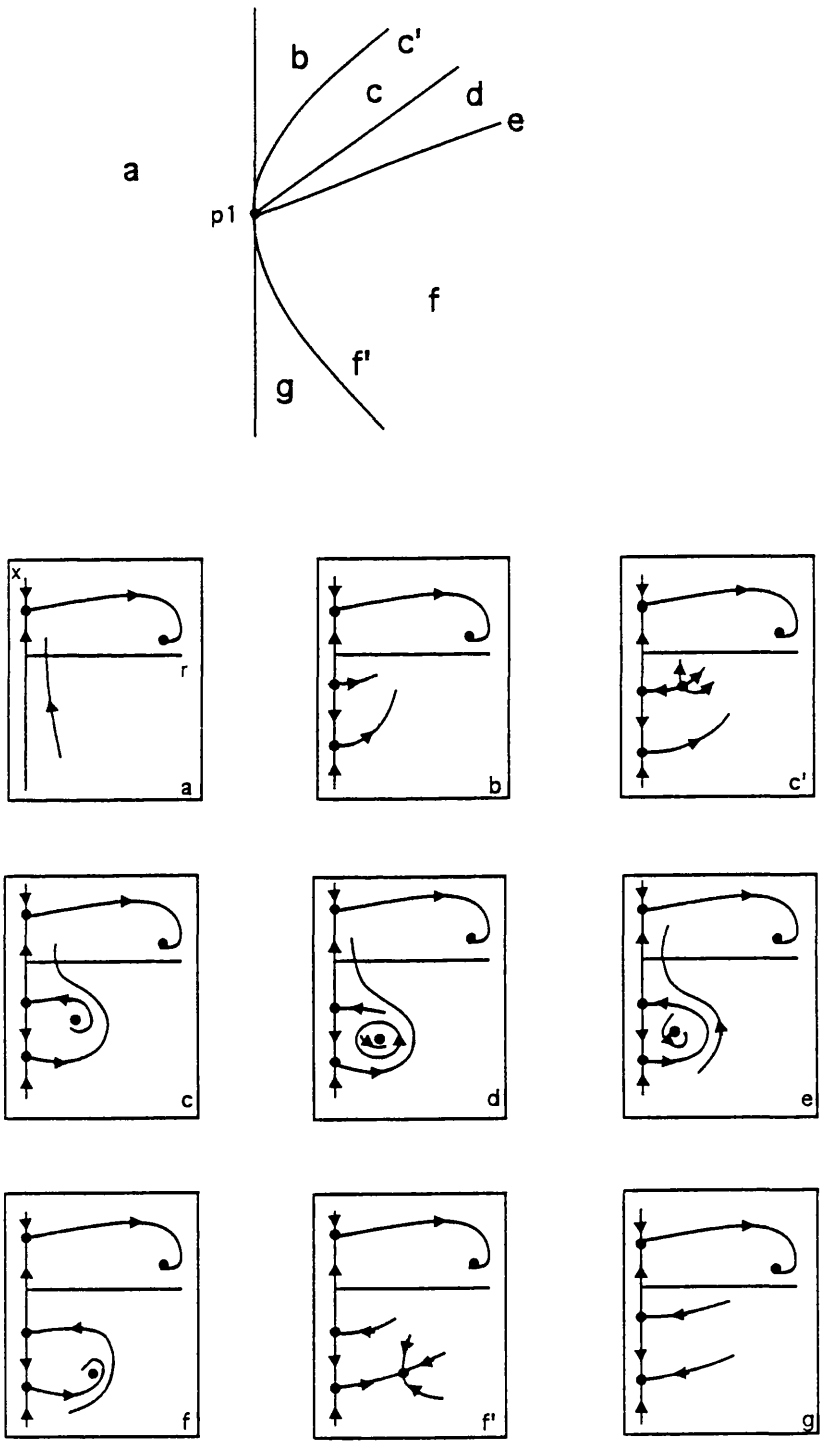

Figure 5.10 Phase Portraits Near the Codimension-Two Points.

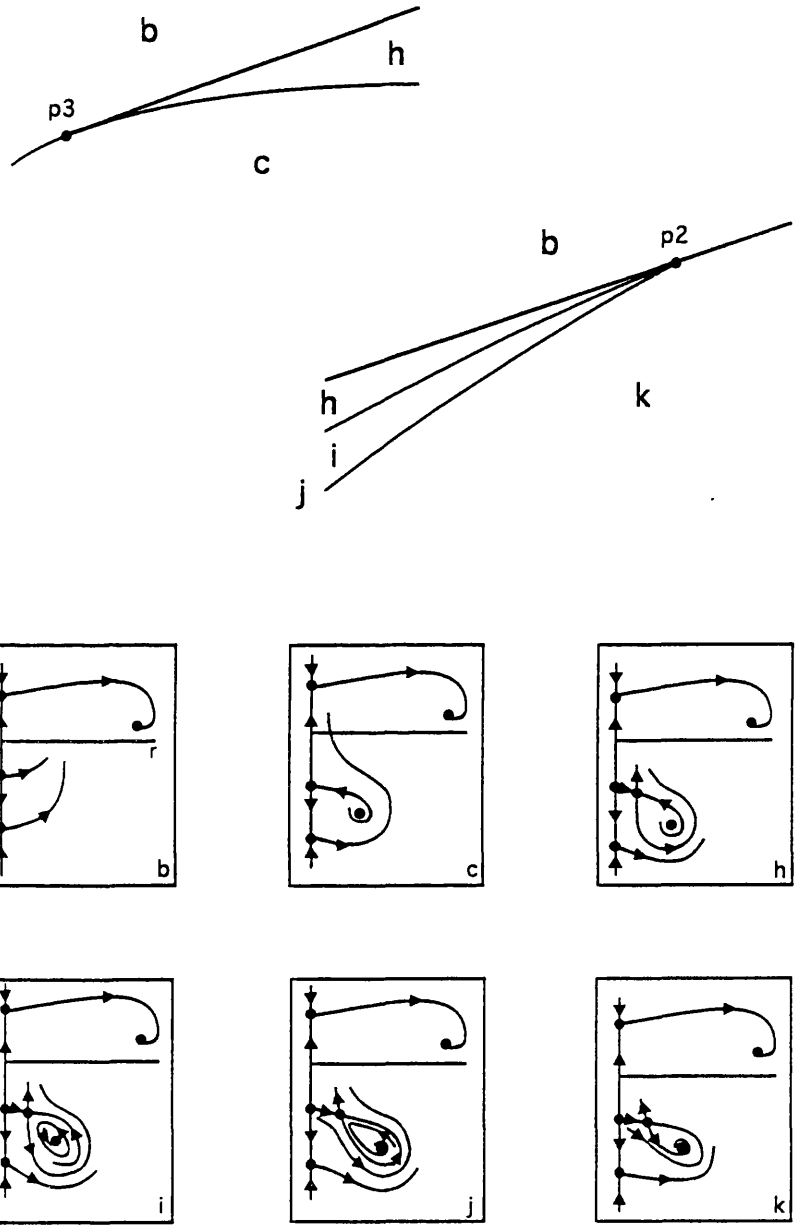

Figure 5.10 (Cont'd).

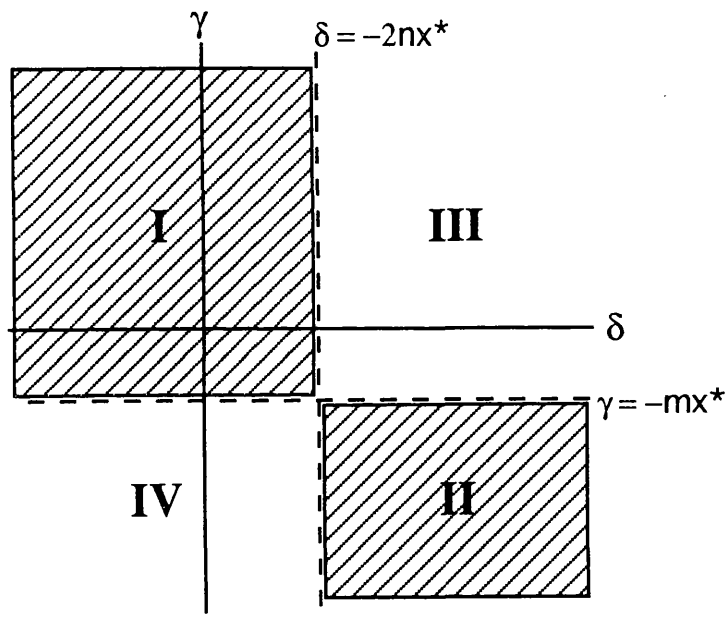

Figure 5.11 Feasible Saddle-Node/Hopf Partitions in (δ, γ) Space.

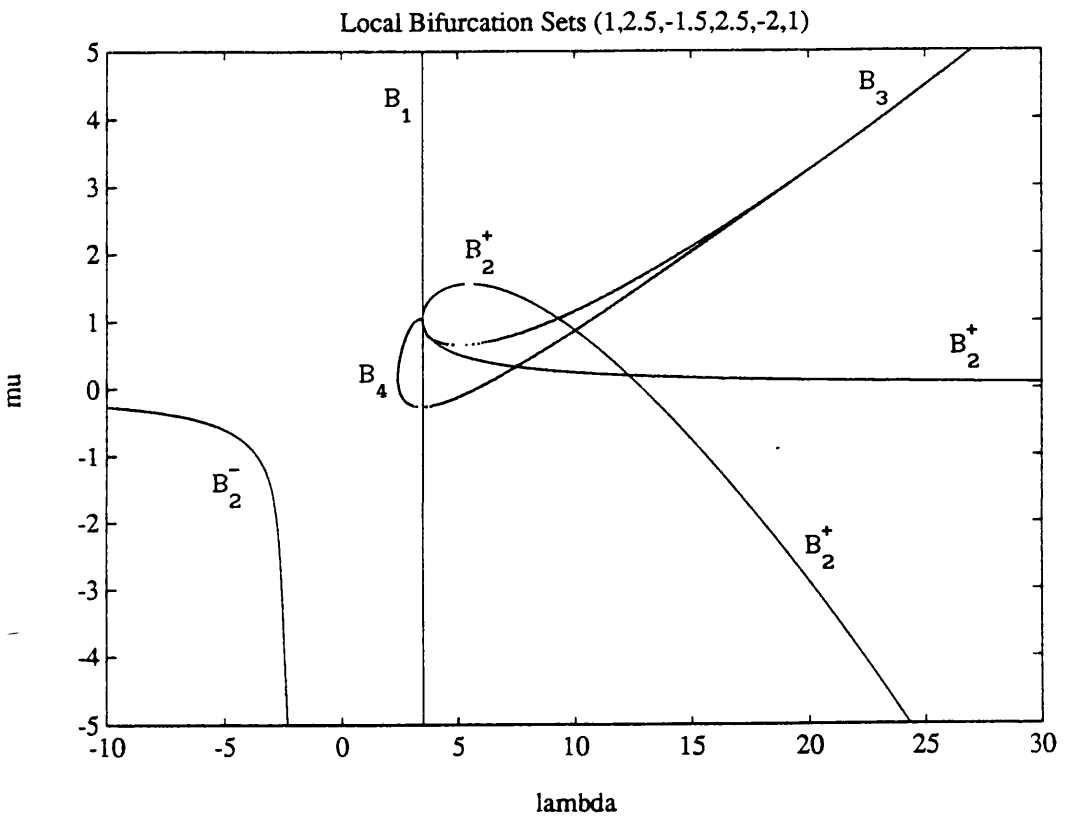

Figure 5.12 Region II Bifurcation Sets with Modified Sn/H Point.
($m < -1$, $n > 0$)

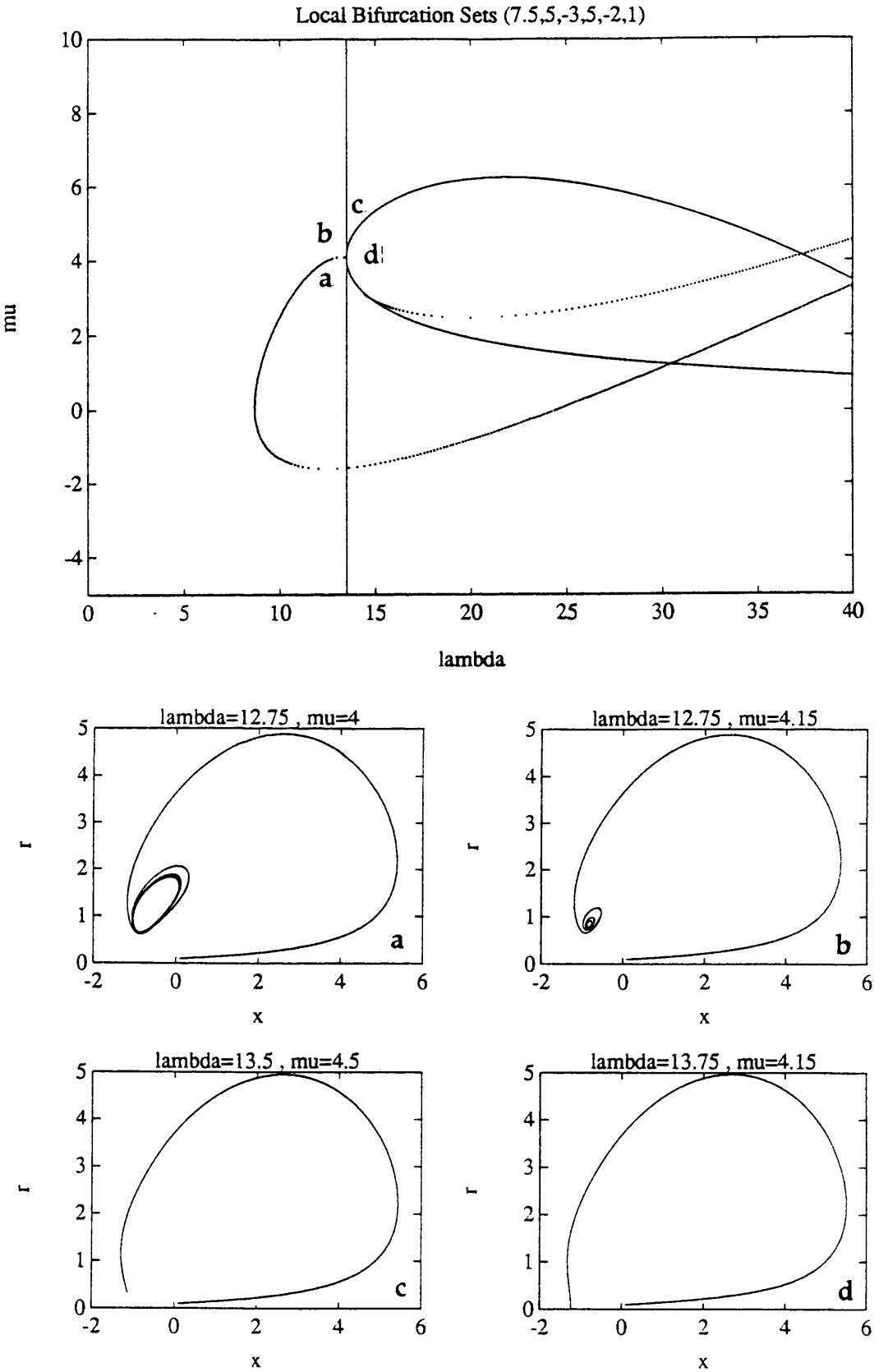

Figure 5.13 Global Phase Portraits Near Region II Sn/H Point.

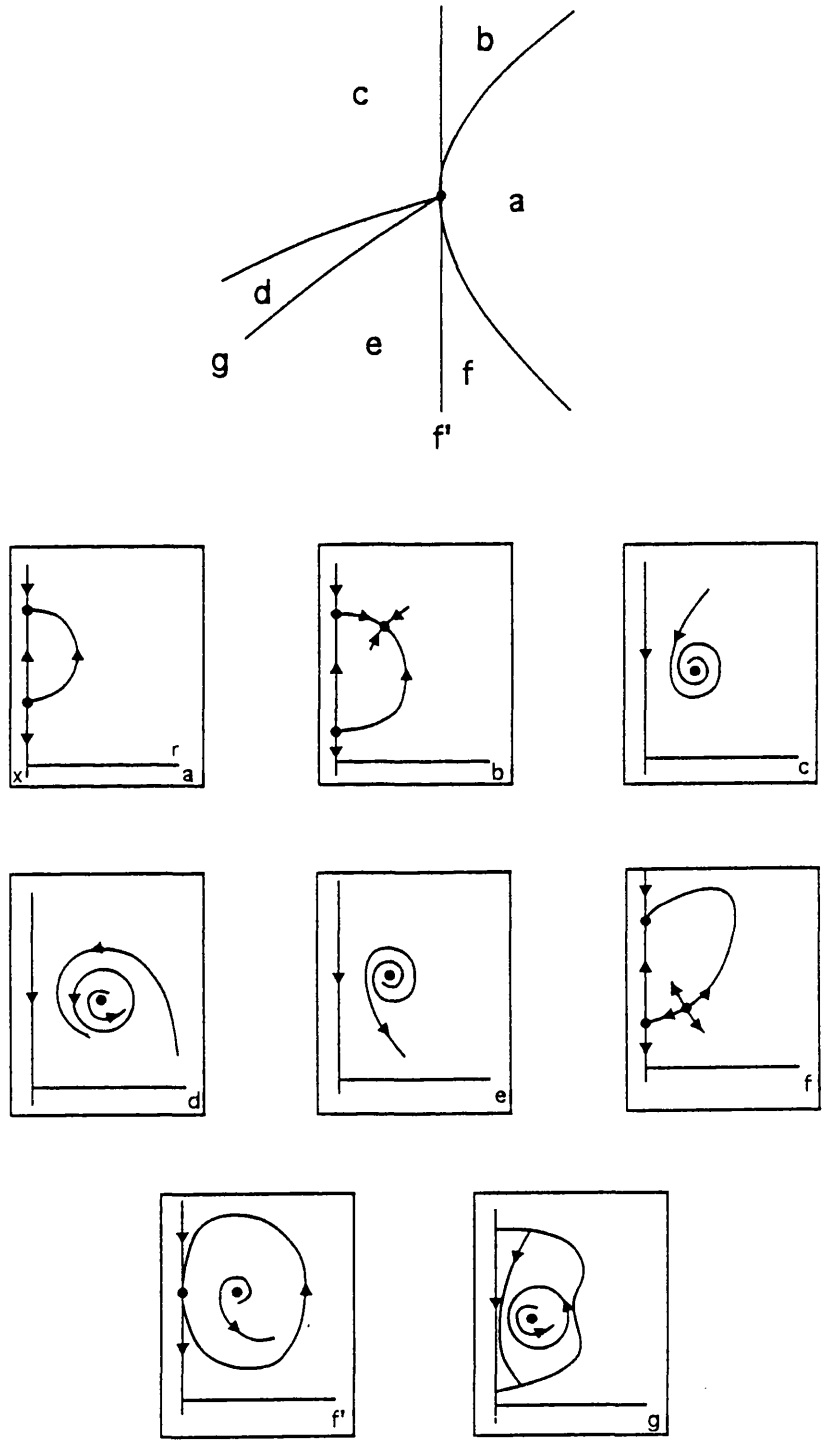

Figure 5.14 Local Phase Portraits Near Saddle-Node/Hopf Point.
(Adapted from Guckenheimer [1981])

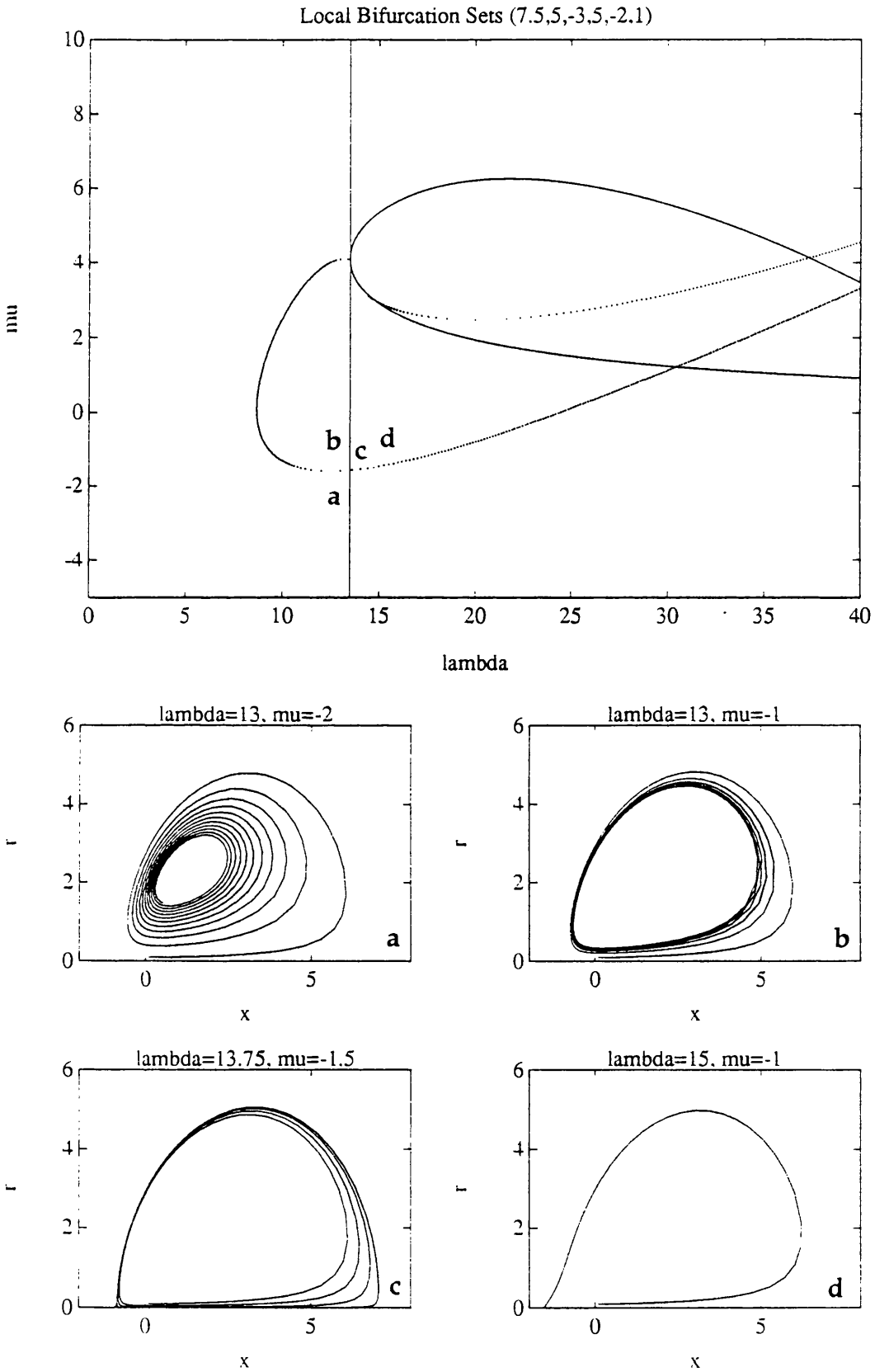

Figure 5.15 Global Phase Portraits Remote from Sn/H Point.

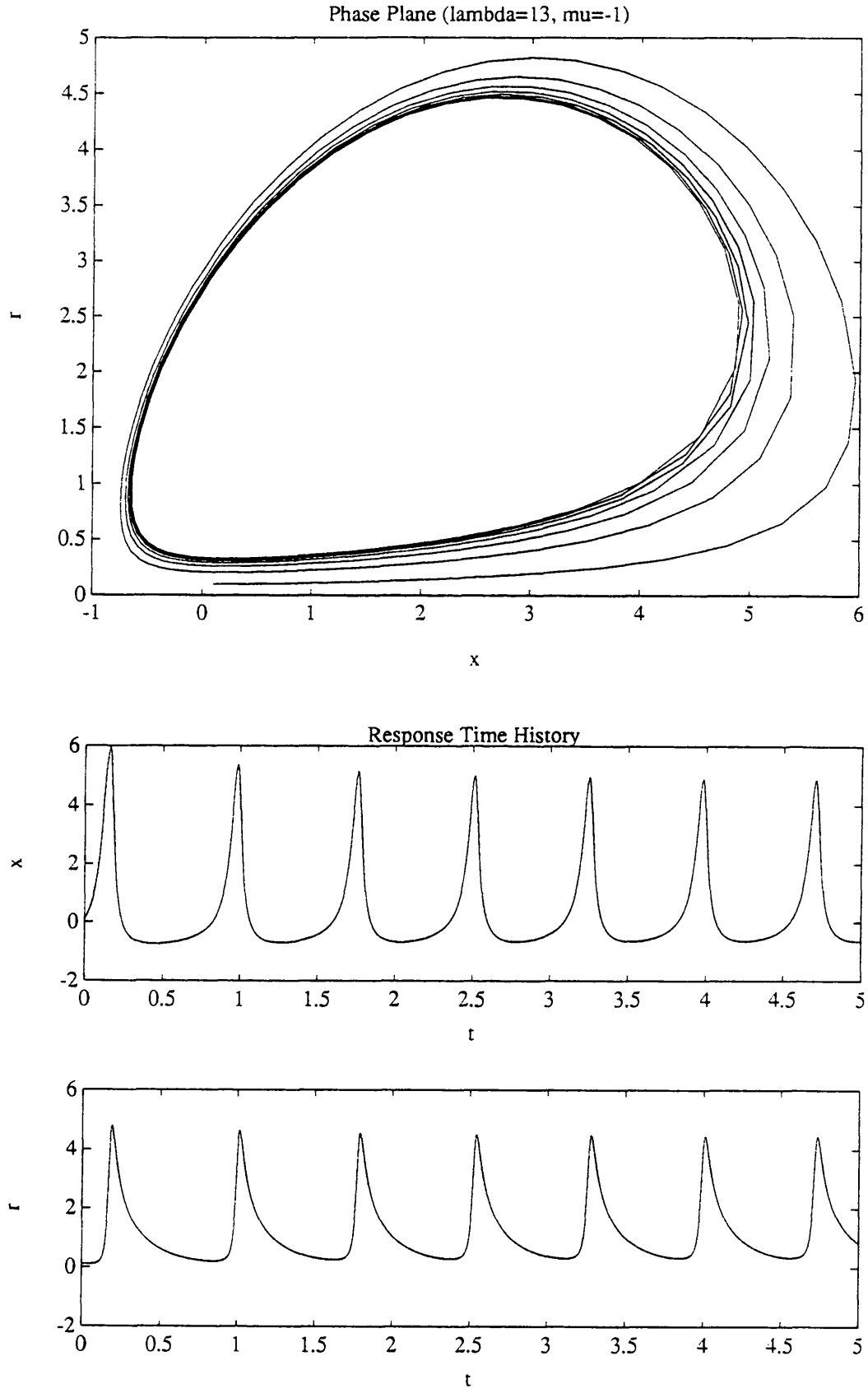

Figure 5.16 Intermittent Steady-State and Periodic Mode Interaction.

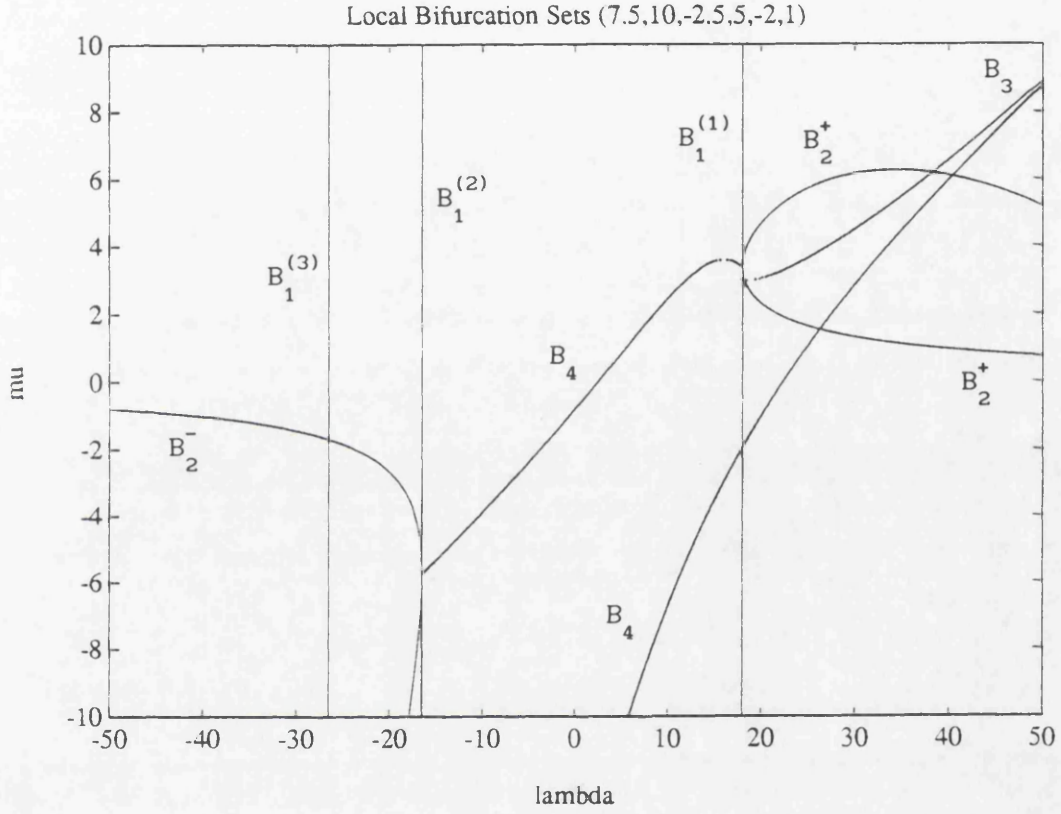

Figure 5.17 Local Bifurcation Sets ($\beta > 3\varepsilon^{1/3}$).